PROGESTERONE RECEPTOR TARGETS PLAY CRITICAL ROLES IN MAINTAINING PREGNANCY AND DISEASE PREVENTION

BY

ALISON NEFF

DISSERTATION

Submitted in partial fulfillment of the requirements
for the degree of Doctor of Philosophy in Molecular and Integrative Physiology
in the Graduate College of the
University of Illinois at Urbana-Champaign, 2019

Urbana, Illinois

Doctoral Committee:

Professor Milan Bagchi, Chair
Professor Indrani Bagchi
Associate Professor Eric Bolton
Associate Professor Lori Raetzman

ABSTRACT

The ovarian hormone progesterone influences many facets of uterine physiology through the transcriptional activity of progesterone receptor (PR). This body of work investigates the role of progesterone receptor targets heart and neural crest derivatives expressed 2 (HAND2) and insulin receptor substrate 2 (IRS2) in regulating uterine functions. Our lab has previously shown that the PR target HAND2 is a negative regulator of uterine epithelial proliferation and is hypermethylated and silenced in uteri from women diagnosed with endometrial hyperplasia and cancer. The study presented in chapter 2 demonstrates that exposure to the environmental toxicant bisphenol-A (BPA) causes increased methylation at the *Hand2* promoter and reduced HAND2 expression. BPA also stimulated expression of fibroblast growth factors (FGF), stromal derived factors that drive uterine epithelial proliferation. Increased expression of the pro-proliferative FGFs coupled with decreased expression of the anti-proliferative HAND2 led to aberrant epithelial proliferation. This is notable in the uterine glands, the site of origin for endometrial hyperplasia and cancer, suggesting that environmental BPA exposure poses as a risk factor for these uterine conditions.

We recently identified *IRS2* as a direct target of PR in human endometrial stromal cells. IRS2 serves as an adaptor molecule for insulin and IGF1 receptors (IR and IGF1R, respectively). The study presented in chapter 3 explores the function of IRS2 during stromal differentiation. We find that IRS2, acting downstream of IR, is critical for inducing the expression of decidual markers and the changes in cell morphology characteristic of stromal differentiation. We also show that IRS2 promotes expression and membrane localization of glucose transporters (GLUT), allowing for increased glucose movement into the cell to meet the metabolic demands of

differentiation. This work provides insight into the metabolic shifts in differentiating stromal cells and the hormone regulated factors that mediate it. These findings may also shed light on the mechanisms underlying the infertility associated with conditions presenting with peripheral insulin resistance, such as polycystic ovarian syndrome.

To my family and friends

TABLE OF CONTENTS

CHAPTER 1: Regulation of Uterine Function by the Ovarian Steroid Hormones Estrogen and Progesterone

INTRODUCTION

The uterus is a female reproductive organ composed of three distinct layers, a mucosal inner layer known as the endometrium, a muscular layer known as the myometrium, and a serosal layer known as the perimetrium. The endometrium can be further divided into an epithelial compartment made up of the epithelial cells lining the endometrial glands and uterine lumen and a stromal compartment composed of a population of fibroblast cells. These compartments work together to establish and maintain pregnancy. For successful pregnancy, the uterus must undergo a series of structural and functional changes early in gestation to promote invasion of the embryo into maternal tissue (implantation) and conversion of the maternal tissue into a secretory structure that will support the embryo (decidualization). These changes are driven by the coordinated actions of 17β-estradiol and progesterone (1, 2). Understanding how these hormones drive the process of implantation and decidualization will help us better understand the underlying causes of infertility.

BACKGROUND

Steroid hormone receptors regulate uterine biology

The endometrium undergoes dynamic changes throughout a woman's reproductive life. Many of these changes are driven by steroid hormones estrogen and progesterone. Estrogen and progesterone are synthesized from cholesterol in the ovary and can diffuse into a target cell to act on their cognate receptors. The estrogen receptors, ERα and ERβ, and the progesterone receptors,

PR-A and PR-B, are members of the nuclear receptor family of transcription factors. Hormone binding activates the receptor, promoting receptor dimerization and binding to specific genomic sites to activate or repress the expression of their target genes. Through the use of chromatin immunoprecipitation coupled to high throughput sequencing, genome-wide binding sites of ER and PR have been identified, representing consensus sequences GGTCAnnnTGACC and AGAACAnnnTGTTCT, respectively (3, 4). Many of these binding sites occur at distal enhancer regions, which then form complexes with the proximal promoter through a chromosomal looping event (5, 6).

The generation of mutant mouse models lacking functional ER or PR has provided great insight into the role of steroid hormone-regulated gene expression in the uterus during pregnancy. ERα is the predominant ER isoform that mediates critical uterine functions during the reproductive cycle and pregnancy. Its loss results in female infertility and insensitivity to the mitogenic effects of estrogen (7). Loss of ERβ, on the other hand, has no effect on uterine function but shows reduced fertility due to an ovarian defect (8). Generation of an epithelial-specific deletion of ERα also results in female infertility (9). Interestingly, loss of epithelial ERα does not prevent estrogen-induced epithelial cell proliferation, suggesting that ERα action in the stroma is critical for mediating this event in a paracrine manner. These findings are supported by tissue recombination experiments performed by Cunha et al, who demonstrated the interdependency between the endometrial epithelium and (10, 11).

PR knockout (PRKO) females are infertile due to an ovulation defect and uteri that are non-receptive to implanting embryos and fail to mount a decidual response during artificial decidualization (12). Uteri from PRKO mice are also hyperplastic, indicating that progesterone signaling is anti-proliferative. Mice lacking PR exclusively in the uterine epithelium are also

infertile (13). However, while one study showed that epithelial deletion of PR leads to persistent uterine epithelial proliferation, another group showed that epithelial PR is dispensable for the anti-proliferative effects of P on the uterine epithelium (13, 14). The findings of the later study are supported by tissue recombination experiments showing that uterine stromal PR is critical for suppressing estrogen induced uterine epithelial proliferation, while epithelial PR is dispensable (11). These data suggest epithelial proliferation is regulated by a paracrine mechanism involving stromal PR.

Implantation

The window of implantation represents a brief period of time where the uterus is receptive to the invading embryo. This state is achieved through the production of multiple signaling molecules produced in the epithelial and stromal compartments during the peri-implantation period that help prepare the maternal tissue for embryo attachment and invasion. Many of these factors are regulated by estrogen and progesterone. In humans, the 28 day uterine cycle is divided into 3 phases: menses, the proliferative phase, and the secretory phase (15). During menses, the endometrial lining is sloughed in the absence of pregnancy. During the proliferative phase, elevated ovarian estrogen drives endometrial proliferation to thicken the endometrial lining. The secretory phase begins after ovulation on day 14, and the hormonal profile shifts to elevated levels of progesterone and decreased estrogen produced from the ovaries. The window of implantation begins on cycle day 19 during the secretory phase, with implantation occurring 6-10 days after ovulation, when progesterone levels are elevated (16). In mice, the steroid hormone-regulated events leading to implantation are well defined. During days 1-2 of pregnancy (day 1 corresponds to the detection of a copulatory plug), estrogen is the

predominant hormone driving proliferation of the luminal and glandular epithelium. Estrogen stimulation of the uterine stroma drives production of insulin-like growth factor 1 (IGF1) and a subset of fibroblast growth factors that act in a paracrine fashion to drive epithelial proliferation (17, 18). By day 4 of pregnancy, with the rise of progesterone secreted from the newly formed corpora lutea, the uterine epithelium shifts from a proliferative to a differentiated state and becomes receptive to embryo attachment. The cessation of epithelial proliferation is requisite to achieve a receptive state; stromal factors like muscle segment homeobox genes MSX1/2 and heart and neural crest derivatives-expressed protein 2 (HAND2) are critical in suppressing epithelial proliferation (18, 19).

Development of a receptive uterus involves structural and functional remodeling of the uterine epithelium. During this process, the epithelial cells lose polarity through down-regulation of the cell-cell adhesion molecule E-cadherin, exhibit an inhibition of the cell surface glycoprotein mucin 1 (MUC1), and develop protrusions along the apical surface (20, 21, 22). As the uterus attains receptivity, the trophectoderm layer of the embryo can interact with the uterine luminal epithelium and begin invasion into the maternal tissue (1, 2). The process of implantation occurs in three stages; apposition, attachment, and invasion (2). Apposition represents the very first contact between the blastocyst and the maternal tissue. During the attachment phase, much stronger connections are made between the trophoblast cells of the blastocyst and the endometrial epithelium through receptor-ligand interactions, such as integrin αvβ3 on the surface of trophoblast cells interacting with its ligand osteopontin on the surface of endometrial epithelial cells (23). Once attached, the embryo begins the process of invasion, wherein trophoblast cells breach the epithelial layer and invade into the underlying stroma. The

invading trophoblast cells contact maternal spiral arteries and convert them to large, low resistance blood vessels to maintain a high rate of blood flow between mother and fetus (24).

Decidualization

During decidualization, the uterine stroma undergoes a process of extensive proliferation, differentiation, and vascularization to support the embryo during early pregnancy (1). In mice, this process is triggered by embryo implantation, whereas in humans, decidualization is initiated during the secretory phase of each uterine cycle, irrespective of the presence of a viable embryo (25). During decidualization, stromal cells undergo extensive morphological changes in the transformation to decidual cells. Undifferentiated stromal cells are fibroblastic with little cytoplasm and smaller elongated nuclei (25). Following transformation, decidual cells take on an epithelioid appearance with rounding of the nucleus, expansion of the cytoplasm, and accumulation of intracellular lipid and glycogen droplets (25). This transformation is driven by steroid hormones and the accumulation of cyclic adenosine monophosphate (cAMP) (25). Decidualization initiates in stromal cells underlying the luminal epithelium and surrounding terminal spiral arteries (1). In humans, this process prepares the endometrium for the implanting embryo, and in the event of pregnancy, decidualization will spread beyond the perivascular regions, throughout the entire endometrium (26). Decidual cells mediate multiple actions during early pregnancy, including production of growth factors and cytokines to support embryo development, promote vascular remodeling, and regulate trophoblast invasion (27, 28, 29). Factors produced by decidual cells are also critical for modulating the maternal immune response to ensure immunotolerance to the embryo (30). Several factors are produced in abundance by decidual cells, including prolactin (PRL) and IGF-1 binding protein-1 (IGFBP1) (25). PRL

production increases at day 22 of the uterine cycle and is involved in stimulating trophoblast growth and invasion, preventing immune rejection, and regulating water movement across the amnion (31, 32, 33). IGFBP1 is also produced during the secretory phase of the uterine cycle, and during early pregnancy regulates IGF1 signaling and trophoblast migration (34, 35, 36). These markers serve as useful tools to determine a successful decidual response.

Decidualization is necessary for successful pregnancy. In humans, in vitro decidualization of stromal cells from women experiencing recurrent pregnancy loss or from eutopic biopsies of women suffering from endometriosis show a blunted decidual response compared to cells from healthy patients (37, 38, 39). Successful decidualization is highly dependent on PR and the expression of PR targets (12). Transgenic mouse models have demonstrated that conditional deletion of progesterone responsive targets like CEBPβ, BMP2, IHH, and HAND2 showed impaired decidualization responses leading to infertility (40, 41, 42, 43). Chromatin immunoprecipitation coupled with high throughput sequencing (ChIP-seq) was performed to identify PR targets induced during decidualization (44, 45). This analysis revealed a role for PR in regulating the cell cycle, angiogenesis, lysosomal activity, cell death and apoptosis, and secretion of chemokines and cytokines, among others (44). Considerable work is needed to fully understand and appreciate how these PR-regulated factors work together to mediate decidualization.

Progesterone receptor targets within uterine stromal cells

The importance of functional PR signaling in the uterus is undeniable. PR is critical for successful pregnancy and dysregulation of PR signaling is linked to endometriosis, uterine fibroids, and endometrial cancer (46). ChIP-seq and gene expression analysis have identified

numerous PR target genes that orchestrate the molecular and biochemical changes required to maintain pregnancy (44, 45). Two of these factors have been highlighted below.

Heart and neural crest derivatives expressed 2 (HAND2)

PR signaling is associated with a shift from endometrial proliferation to endometrial differentiation. Using microarray-based profiling of progesterone responsive transcripts during the implantation window in the mouse identified *Hand2* as a P-regulated gene in the uterine stroma (47). HAND2 is a basic helix-loop-helix transcription factor found in distinct tissue types, including the neural crest, limb buds, in the developing and adult heart, myenteric and submucosal sympathetic ganglia, and adrenomedullary cells (48, 49, 50). It has also emerged as a critical factor in the uterine stroma that regulates epithelial function (18, 43).

HAND2 expression is induced by progesterone and is a direct target of PR (4, 18, 44, 45). During the peri-implantation period in mice, HAND2 expression is robustly induced in the stroma but is notably absent in the epithelium. Loss of HAND2 results in infertility due to a defect in implantation (18). *Hand2* knockout mice show persistent epithelial proliferation in the luminal epithelium as opposed to a quiescent epithelium in control animals. As this shift to quiescence is requisite for implantation, this indicates that HAND2 is critical for achieving a receptive state in the uterus. It has been demonstrated that uterine epithelial proliferation is controlled in a paracrine manner by estrogen and progesterone signaling in the uterine stroma (10, 11). HAND2 inhibits the expression of estrogen driven stromal fibroblast growth factors, *Fgf-1, -2, -9,* and *-18,* which act via FGFR on the luminal epithelial cell surface and induce epithelial proliferation via MAPK activation (18). Additionally, loss of HAND2 leads to persistent epithelial ESR1 activation and increased *Muc1* expression, indicative of a non-

receptive uterine lining. Together, these findings present a mechanism by which stromal expression of HAND2 inhibits epithelial proliferation to promote implantation.

The role of HAND2 during decidualization is less clear. Stromal expression of HAND2 persists well after implantation is complete, suggesting a role of HAND2 during decidualization (43). HAND2 itself is a transcription factor that binds consensus ebox motifs CATCTG in the DNA (51). It can interact with several other transcription factors, including GATA4, TWIST1, and E12 to regulate gene transcription (52, 53, 54). HAND2 ChIP-seq performed in mouse heart and limb buds provide insights into potential HAND2 targets in the uterus (55, 56). Interestingly, members of the FGF family, including FGF9, appear on both data sets as targets of HAND2 signaling. This suggests that HAND2 may directly target certain estrogen stimulated FGFs for transcriptional repression to promote uterine receptivity. A HAND2 ChIP-seq coupled with RNA-seq would be useful to help create a broader picture of target genes transcriptionally regulated by HAND2 during the decidualization process.

Uterine HAND2 is also important for maintaining uterine health, as dysregulation of HAND2 has been linked to endometrial cancer. HAND2 is the most commonly hypermethylated and silenced gene in endometrial hyperplasia and cancer (57). Loss of HAND2 expression correlated with lack of response to progestin treatment, further supporting that HAND2 is the primary mediator of the anti-proliferative effects of progesterone (57). This observation also suggests that HAND2 status can be used to help customize a treatment regimen for women diagnosed with endometrial cancer. In mice, conditional deletion of uterine HAND2 led to complex atypical hyperplasia and downregulation of the tumor suppressor PTEN, an early event in the progression of endometrial carcinogenesis (57). Endometrial cancer results from chronic estrogen exposure, coupled with an insufficient counterbalance by progesterone, which promotes

the hyperproliferation and transformation of cells (46). The aim of chapter 2 is to investigate how exposure to endocrine disrupting chemicals with estrogenic properties, like bisphenol A, can alter this balance between estrogen and progesterone signaling in the uterus, and the impact on the PR target HAND2.

Insulin receptor substrate 2 (IRS2)

IRS2 is a member of the IRS family of large docking proteins that function downstream of insulin and IGF1 receptor tyrosine kinases (58). IRS2 functions as an adaptor molecule bridging insulin (IR) and IGF-1 (IGF1R) receptor tyrosine kinases to downstream signaling proteins. Ligand binding induces dimerization and autophosphorylation of tyrosine residues on the intracellular subunits of the receptor dimers (58). The IRS2 protein contains a phosphotyrosine binding domain that binds the phosphorylated tyrosines on the activated receptor. This binding event prompts phosphorylation of multiple tyrosine residues on IRS2 by the activated receptor, and these residues can interact with the SH2 domains of downstream signaling proteins to activate PI3K/AKT and MAPK pathways. Activation of these signaling cascades regulates glucose influx, glycogen synthesis, and cell growth, proliferation, and differentiation (58). Global deletion of *Irs2* results in peripheral insulin resistance and a diabetic phenotype, demonstrating its critical role in the insulin signaling pathway (59). *Irs2* null mice also exhibit reduced fertility, although how IRS2 contributes to uterine function is unknown (60).

IRS2 acts as an adaptor molecule to IGF1R. It is well understood that estrogen-stimulated IGF1 produced in the uterine stroma acts on IGF1R in the uterine epithelium to mediate the proliferative effects of estrogen during the pre-implantation period (17, 61). However, despite the presence of IGF1R in the uterine stroma during the peri-implantation period, its function during decidualization is not well understood (62, 63). IRS2 also links insulin receptor (IR) to its

downstream signaling pathways. In the uterus, stromal IR expression is increased during the secretory phase of the uterine cycle, suggesting it plays a functional role in decidualization (64). In humans, insulin resistance is associated with a reduced rate of clinical pregnancies and increased risk of spontaneous miscarriage and recurrent pregnancy loss (65, 66, 67, 68). Interestingly, in vitro studies show that decidualization is reduced in the presence of added insulin (62, 69). In contrast, endometrial stromal cells isolated from women with polycystic ovarian syndrome (PCOS), a disease often associated with hyperinsulinemia and peripheral insulin resistance, showed impaired decidualization when differentiated in vitro (70). This suggests that insulin signaling is tightly regulated and perturbations can contribute to infertility.

IRS2 is a direct target of PR, and progesterone stimulation leads to transcriptional activation and increased expression (44, 45, 71). Additionally, siRNA mediated knockdown experiments suggest that IRS2 expression is required for decidualization in human endometrial stromal cells (HESC), although through what mechanism remains unclear (44). The aim of chapter 3 is to elucidate the mechanism by which IRS2 facilitates decidualization in primary HESC.

REFERENCES

1. Ramathal CY, BagchI IC, Taylor RN, Bagchi MK. Endometrial decidualization: of mice and men. *Semin Reprod Med*. 2010; 28(1): 17–26.
2. Cha J, Sun X, Dey SK. Mechanisms of implantation: strategies for successful pregnancy. *Nat Med*. 2012; 18(2): 1754–1767.
3. Hewitt SC, Li L, Grimm SA, Chen Y, Liu L, Li Y, Bushel PR, Fargo D, Korach KS. Research resource: whole-genome estrogen receptor α binding in mouse uterine tissue revealed by ChIP-seq. *Mol Endocrinol*. 2012; 26(5): 887–898.
4. Rubel CA, Lanz RB, Kommagani R, Franco HL, Lydon JP, DeMayo FJ. Research resource: Genome-wide profiling of progesterone receptor binding in the mouse uterus. *Mol Endocrinol*. 2012; 26(8): 1428–1442.
5. Pan YF, Wansa KD, Liu MH, Zhao B, Hong SZ, Tan PY, Lim KS, Bourque G, Liu ET, Cheung E. Regulation of estrogen receptor-mediated long range transcription via evolutionarily conserved distal response elements. *J Biol Chem*. 2008; 283(47): 32977–32988.

6. Li W, Notani D, Ma Q, Tanasa B, Nunez E, Chen AY, Merkurjev D, Zhang J, Ohgi K, Song X, Oh S, Kim HS, Glass CK, Rosenfeld MG. Functional roles of enhancer RNAs for oestrogen-dependent transcriptional activation. *Nature*. 2013; 498(7455): 516–520.
7. Hewitt SC, Korach KS. Oestrogen receptor knockout mice: roles for oestrogen receptors alpha and beta in reproductive tissues. *Reproduction*. 2003; 125(2): 143–149.
8. Krege JH, Hodgin JB, Couse JF, Enmark E, Warner M, Mahler JF, Sar M, Korach KS, Gustafsson JA, Smithies O. Generation and reproductive phenotypes of mice lacking estrogen receptor beta. *Proc Natl Acad Sci U S A*. 1998; 95(26): 15677–15682.
9. Winuthayanon W, Hewitt SC, Orvis GD, Behringer RR, Korach KS. Uterine epithelial estrogen receptor α is dispensable for proliferation but essential for complete biological and biochemical responses. *Proc Natl Acad Sci U S A*. 2010; 107(45): 19272–19277.
10. Cooke PS, Buchanan DL, Young P, Setiawan T, Brody J, Korach KS, Taylor J, Lubahn DB, Cunha GR. Stromal estrogen receptors mediate mitogenic effects of estradiol on uterine epithelium. *Proc Natl Acad Sci USA*. 1997; 94(12): 6535–6540.
11. Kurita T, Young P, Brody JR, Lydon JP, O'Malley BW, Cunha GR. Stromal progesterone receptors mediate the inhibitory effects of progesterone on estrogen-induced uterine epithelial cell deoxyribonucleic acid synthesis. *Endocrinology*. 1998; 139(11): 4708–4713.
12. Lydon JP, DeMayo FJ, Funk CR, Mani SK, Hughes AR, Montgomery CA, JR, Shyamala G, Conneely OM, O'Malley BW. Mice lacking progesterone receptor exhibit pleiotropic reproductive abnormalities. *Genes Dev*. 1995; 9(18): 2266–2278.
13. Franco HL, Rubel CA, Large MJ, Wetendorf M, Fernandez-Valdivia R, Jeong JW, Spencer TE, Behringer RR, Lydon JP, DeMayo FJ. Epithelial progesterone receptor exhibits pleiotropic roles in uterine development and function. *FASEB J*. 2012; 26(3): 1218–1227.
14. Mehta FF, Son J, Hewitt SC, Jang, E, Lydon JP, Korach KS, Chung S. Distinct functions and regulation of epithelial progesterone receptor in the mouse cervix, vagina, and uterus. *Oncotarget*.2016;7(14):17455-17467.
15. Hawkins SM, Matzuk MM. The menstrual cycle: basic biology. *Ann N Y Acad Sci*.2008;1135:10-18.
16. Blesa D, Ruiz-Alonso M, Simon C. Clinical management of endometrial receptivity. *Semin Reprod Med.* 2014; 32(5): 410-413.
17. Zhu L, Pollard JW. Estradiol-17beta regulates mouse uterine epithelial cell proliferation through insulin-like growth factor 1 signaling. *Proc Natl Acad Sci USA.* 2007; 104(40): 15847-15851.
18. Li Q, Kannan A, DeMayo FJ, Lydon JP, Cooke PS, Yamagishi H, Srivastava D, Bagchi MK, Bagchi IC. The antiproliferative action of progesterone in uterine epithelium is mediated by Hand2. *Science*. 2011; 331(6019): 912–916.
19. Nallasamy S, Li Q, Bagchi MK, Bagchi IC. Msx homeobox genes critically regulate embryo implantation by controlling paracrine signaling between uterine stroma and epithelium. *PLoS Genet.* 2012; 8(2): e1002500.
20. Thie M, Harrach-Ruprecht B, Sauer H, Fuchs P, Albers A, Denker HW. Cell adhesion to the apical pole of epithelium: a function of cell polarity. *Eur J Cell Biol.* 1995; 66(2): 180–191.

21. Surveyor GA, Gendler SJ, Pemberton L, Das SK, Chakraborty I, Julian J, Pimental RA, Wegner CC, Dey SK, Carson DD. Expression and steroid hormonal control of Muc-1 in the mouse uterus. *Endocrinology*. 1995; 136(8): 3639–3647.
22. Nikas G, Psychoyos A. Uterine pinopodes in peri-implantation human endometrium. Clinical relevance. *Ann N Y Acad Sci.* 1997; 816: 129–142.
23. Su RW, Fazleabas AT. Implantation and Establishment of Pregnancy in Human and Nonhuman Primates. *Adv Anat Embryol Cell Biol*. 2015; 216: 189-213.
24. Kim SM, Kim JS. A review of mechanisms of implantation. *Dev Reprod.* 2017; 21(4): 351-359.
25. Gellersen B, Brosens JJ. Cyclic decidualization of the human endometrium in reproductive health and failure. *Endocr Rev.* 2014; 35(6): 851-905.
26. Gellersen B, Brosens IA, Brosens JJ. Decidualization of the human endometrium: mechanisms, function, and clinical perspectives. *Semin Reprod Med.* 2007; 25(6): 445-453.
27. Dimitriadis E, Salamonsen LA, Robb L. Expression of interleukin-11 during the human menstrual cycle: coincidence with stromal cell decidualization and relationship to leukaemia inhibitory factor and prolactin. *Mol Hum Reprod.* 2000; 6(10):907-914.
28. Laws MJ, Taylor RN, Sidell N, DeMayo FJ, Lydon JP, Gutstein DE, Bagchi MK, Bagchi IC. Gap junction communication between uterine stromal cells plays a critical role in pregnancy-associated neovascularization and embryo survival. *Development*. 2008; 135(15): 2659-2668.
29. Gonzalez M, Neufeld J, Reimann K, Wittmann S, Samalecos A, Wolf A, Bamberger AM, Gellersen B. Expansion of human trophoblastic spheroids is promoted by decidualized endometrial stromal cells and enhanced by heparin-binding epidermal growth factor-like growth factor and interleukin-1 β. *Mol Hum Reprod*. 2011; 17(7): 421-433.
30. Erlebacher A. Immunology of the maternal-fetal interface. *Annu Rev Immunol*. 2013; 31: 387-411.
31. Maslar IA, Riddick DH. Prolactin production by human endometriu during the normal menstrual cycle. *Am J Obstet Gynecol*.1979;135(6):751-754.
32. Ben-Jonathan, LaPensee CR, LaPensee EW. What can we learn from rodents about prolactin in humans? *Endocr Rev*.2008;29(1):1-41.
33. Stefanoska I, Jovanovic KM, Vasilijc S, Cujic D, Vicovac L. Prolactin stimulates cell migration and invasion by human trophoblasts in vitro. *Placenta*.2013;34(9):775-783.
34. Rutanen EM, Koistinen R, Sjoberg J, Julkunen M, Wahlstrom T, Bohn H, Seppaia M. Synthesis of placental protein 12 by human endometrium. *Endocrinology*.1986;118(3):1067-1071.
35. Gleeson LM, Chakrabory C, McKinnon T, Lala PK. Insulin-like growth factor-binding protein 1 stimulates human trophoblast migration by signaling through alpha 5 beta 1 integrin via mitogen-activated protein Kinase pathway. *J Clin Endocrinol Metab*.2001;86(6):2484-2493.
36. Carter AM, Hills F, O'Gorman DB, Roberts CT, Sooranna SR, Watson CS, Westwood M. The insulin-like growth factor system in mammalian pregnancy-a workshop report. *Placenta*.2004;25:s53-s56.
37. Minici F, Tiberi F, Tropea A, Orlando M, Gangale MF, Romani F, Campo S, Bompiani A, Lanzone A, Apa R. Endometriosis and human infertility: a new investigation into the role of eutopic endometrium. *Human Reproduction*.2008;23(3):530-537.

38. Aghajanova L, Hamilton A, Kwintkiewicz J, Vo KC, Giudice LC. Steroidogenic enzyme and key decidualization marker dysregulation in endometrial stromal cells from women with versus without endometriosis. *Biol Reprod*.2009;80(1):105-114.
39. Salker M, Teklenburg G, Molokhia M, Lavery S, Trew S, Trew G, Aojanepong T, Mardon H, Lokugamage AU, Rai R, Landles C, Roelen BA, Quenby S, Kuijk EW, Kavelaars A, Heijnen CJ, Regan L, Macklon NS, Brosens JJ. Natural selection of human embryos: impaired decidualization of endometrium disables embryo-maternal interactions and causes recurrent pregnancy loss. *PLoS One*.2010;5(4):e10287.
40. Mantena SR, Kannan A, Cheon YP, Li Q, Johnson PF, Bagchi IC, Bagchi MK. C/EBPbeta is a critical mediator of steroid hormone-regulated cell proliferation and differentiation in the uterine epithelium and stroma. *Proc Natl Acad Sci U S A*. 2006; 103(6): 1870–1875.
41. Lee K, Jeong J, Kwak I, Yu CT, Lanske B, Soegiarto DW, Toftgard R, Tsai MJ, Tsai S, Lydon JP, DeMayo FJ. Indian hedgehog is a major mediator of progesterone signaling in the mouse uterus. *Nat Genet*. 2006;**38**(10):1204–1209.
42. Li Q, Kannan A, Wang W, DeMayo FJ, Taylor RN, Bagchi MK, Bagchi IC. Bone Morphogenetic Protein 2 Functions via a Conserved Signaling Pathway Involving Wnt4 to Regulate Uterine Decidualization in the Mouse and the Human. *J Biol Chem*. 2007;**282**(43):31725–31732.
43. Huyen DV, Bany BM. Evidence for a conserved function of heart and neural crest derivatives expressed transcript 2 in mouse and human decidualization. *Reproduction.* 2011; 142(2): 353–368.
44. Kaya HS, Hantak AM, Stubbs LJ, Taylor RN, Bagchi IC, Bagchi MK. Roles of progesterone receptor A and B isoforms during human endometrial decidualization. *Mol Endocrinol*. 2015: 29(6): 882-895.
45. Mazur EC, Vasquez YM, Li X, Kommagani R, Jiang L, Chen R, Lanz RB, Kovanci E, Gibbons WE, DeMayo FJ. Progesterone receptor transcriptome and cistrome in decidualized human endometrial stromal cells. *Endocrinology*. 2015; 156(6): 2239-2253.
46. Kim JJ, Kurita T, Bulun SE. Progesterone action in endometrial cancer, endometriosis, uterine fibroids, and breast cancer. *Endocrine Reviews*.2013;34(1):130-162.
47. Bagchi IC, Li Q, Cheon YP, Mantena SR, Kannan A, Bagchi MK. Use of the progesterone receptor antagonist RU 486 to identify novel progesterone receptor-regulated pathways in implantation. *Semin Reprod* Med. 2005; 23(1): 38–45.
48. Hollenberg SM, Sternglanz R, Cheng PF, Weintraub H. Identification of a new family of tissue-specific basic helix-loop-helix proteins with a two-hybrid system. *Mol Cell Biol.* 1995; 15(7): 3813–3822.
49. Firulli BA, Hadzic DB, McDaid JR, Firulli AB. The basic helix-loop-helix transcription factors dHAND and eHAND exhibit dimerization characteristics that suggest complex regulation of function. *J Biol Chem*. 2000; 275(43): 33567–33573.
50. Wu X, Howard MJ. Transcripts encoding HAND genes are differentially expressed and regulated by BMP4 and GDNF in developing avian gut. *Gene Expr*. 2002; 10(5-6): 279–293.
51. Dai YS, Cserjesi P. The basic helix-loop helix factor, HAND2, functions as a transcriptional activator by binding to E-boxes as a heterodimer. *J Biol Chem.* 2002; 277(15): 12604-12612.

52. Dai YS, Cserjesi P, Markham BE, Molkentin JD. The transcription factors GATA4 and dHAND physically interact to synergistically activate cardiac gene expression through a p300-dependent mechanism. *J Biol Chem.* 2002; 277(27): 24390-24398.

53. Thattaliyath BD, Firulli BA, Firulli AB. The basic-helix-loop-helix transcription factor HAND2 directly regulates transcription of the atrial naturetic peptide gene. *J Mol Cell Cardiol*. 2002; 34(10): 1335-1344.

54. Firulli BA, Redick BA, Conway SJ, Firulli AB. Mutations within helix I of Twist1 result in distinct limb defects and variation of DNA binding affinities. *J Biol Chem.* 2007; 282(37): 27536-27546.

55. Osterwalder M, Speziale D, Shoukry M, Mohan R, Ivanek R, Kholer M, Beisel C, Wen X, Scales SJ, Christoffels VM, Visel A, Lopez-Rios J, Zeller R. HAND2 targets define a network of transcriptional regulators that compartmentalize the early limb bud mesenchyme. *Dev Cell*. 2014; 31(3): 345-357.

56. Laurent F, Girdziusaite A, Gamart J, Barozzi I, Osterwalder M, Akiyama JA, Lincoln J, Lopez-Rios J, Visel A, Zuniga A, Zeller R. HAND2 target gene regulatory networks control atrioventricular canal and cardiac valve development. *Cell Rep.* 2017; 19(8): 1602-1613.

57. Jones A, Teschendorff AE, Li Q, Hayward JD, Kannan A, Mould T, West J, Zikan M, Cibula D, Fiegl H, Lee SH, Wik E, Hadwin R, Arora R, Lemech C, Turunen H, Pakarinen P, Jacobs IJ, Salvesen HB, Bagchi MK, Bagchi IC, Widschwendter M. Role of DNA methylation and epigenetic silencing of HAND2 in endometrial cancer development. *Plos* Med.2013;10(11): e1001551.

58. De Meyts P. The insulin receptor and its signal transduction network. *Endotext.* 2016.

59. Withers DJ, Gutierrez JS, Towery H, Burks DJ, Ren JM, Previs S, Zhang Y, Bernal D, Pons S, Shulman GI, Bonner-Weir S, White MF. Disruption of IRS-2 causes type 2 diabetes in mice. *Nature*.1998;391(6670):900-904.

60. Burks DJ, Font de Mora J, Schubert M, Withers DJ, Myers MG, Towery HH, Altamuro SL, Flint CL, White MF. IRS-2 pathways integrate female reproduction and energy homeostasis. *Nature*. 2000; 407(6802): 377-382.

61. Walker MP, Diaugustine RP, Zeringue E, Bunger MK, Schmitt M, Archer TK, Richards RG. An IGF1/insulin receptor substrate-1 pathway stimulates a mitotic kinase (cdk1) in the uterine epithelium during the proliferative response to estradiol. *J Endocrinol*. 2010; 207(2): 225–235.

62. Irwin JC, de las Fuentes L, Dsupin BA, Giudice LC. Insulin-like growth factor regulation of human endometrial stromal cell function: coordinate effects on insulin-like growth factor binding protein-1, cell proliferation and prolactin secretion. *Regul Pept*. 1993; 48(1-2): 165-177.

63. Ganeff C, Chatel G, Munaut C, Frankenne F, Foidart JM, Winkler R. The IGF system in in-vitro human decidualization. *Mol Hum Reprod*. 2009; 15(1): 27-38.

64. Mioni R, Mozzanega B, Granzotto M, Pierobon A, Zuliani L, Maffei P, Blandamura S, Grassi S, Sicolo N, Vettor R. Insulin receptor and glucose transporters mRNA expression throughout the menstrual cycle in human endometrium: a physiological and cyclical condition of tissue insulin resistance. *Gynecol Endocrinol*. 2012; 28(12): 1014-1018.

65. Craig LB, Ke RW, Kutteh WH. Increased prevalence of insulin resistance in women with a history of recurrent pregnancy loss. *Fertil Steril*.2002;78(3):487-490.

66. Tian L, Shen H, Lu Q, Norman RJ, Wang J. Insulin resistance increases the risk of spontaneous abortion after assisted reproduction technology treatment. *J Clin Endocrinol Metab*.2007;92(4):1430-1433.
67. Wang Y, Zhao H, Li Y, Zhang J, Tan J, Liu Y. Relationship between recurrent miscarriage and insulin resistance. *Gynecol Obstet Invest.*2011;72(4):245-251.
68. Chang EM, Han JE, Seok HH, Lee DR, Yoon TK, Lee WS. Insulin resistance does not affect early embryo development but lowers implantation rate in in vitro maturation-in vitro fertilization-embryo transfer cycle. *Clin Endocrinol (Oxf).* 2013; 79(1): 93-99.
69. Ujvari D, Jakson I, Babayeva S, Salamon D, Rethi B, Gidlöf S, Hirschberg AL. Dysregulation of In Vitro Decidualization of Human Endometrial Stromal Cells by Insulin via Transcriptional Inhibition of Forkhead Box Protein O1. *PLoS One*. 2017; 12(1): e0171004.
70. Piltonen TT, Chen JC, Khatun M, Kangasniemi M, Liakka A, Spitzer T, Tran N, Huddleston H, Irwin JC, Giudice LC. Endometrial stromal fibroblasts from women with polycystic ovary syndrome have impaired progesterone-mediated decidualization, aberrant cytokine profiles and promote enhanced immune cell migration in vitro. *Hum Reprod.* 2015; 30(5): 1203-15.
71. Vassen L, Wegrzyn W, Klein-Hitpass L. Human insulin receptor substrate-2 (IRS-2) is a primary progesterone response gene. *Mol Endocrinol.*1999;13(3):485-494.

CHAPTER 2: Chronic Exposure of Mice to Bisphenol-A Alters Uterine FGF Signaling and Leads to Aberrant Epithelial Proliferation

Published: Neff AM, Blanco SC, Flaws JA, Bagchi IC, Bagchi MK. Chronic Exposure of Mice to Bisphenol-A Alters Uterine FGF Signaling and Leads to Aberrant Epithelial Proliferation. *Endocrinology*. 2019; 60(5):1234-1246.

ABSTRACT

Uterine epithelial proliferation is regulated in a paracrine manner by a complex interplay between estrogen (E) and progesterone (P) signaling, in which E stimulates proliferation and P inhibits it. Perturbation of steroid hormone signaling within the uterine milieu could contribute to the development of endometrial hyperplasia and cancer. It is well established that bisphenol-A (BPA) is an endocrine disrupting chemical with weak estrogenic effects, although little is known about how it affects steroid hormone signaling in the adult uterus. Because BPA acts as a weak E, we hypothesized that chronic exposure to BPA would create an imbalance between E and P signaling and cause changes in the uterus, such as aberrant epithelial proliferation. Indeed, exposure to an environmentally relevant dose of BPA had a uterotrophic affect. BPA-treated mice showed increased proliferation, notably in the glandular epithelium, which is a site of origin for endometrial hyperplasia and cancer. Increased proliferation appeared to be mediated through a similar mechanism as E-induced proliferation, via activation of the fibroblast growth factor receptor pathway and phosphorylation of the ERK1/2 mitogen-activated protein kinases in the epithelium. Interestingly, BPA reduced expression of heart and neural crest derivatives expressed 2 (HAND2), a known mediator of the anti-proliferative effects of P. BPA also increased methylation of a CpG island in the Hand2 gene promoter, suggesting that BPA may promote epithelial proliferation through epigenetic silencing of anti-proliferative factors like HAND2. Collectively, these findings establish that chronic exposure to BPA impairs steroid hormone

signaling in the mouse uterus and may contribute to the pathogenesis of uterine hyperplasia and cancer.

INTRODUCTION

The endometrium is highly sensitive to stimulation by ovarian steroid hormones estrogen (E) and progesterone (P). These two hormones play critical roles both during the reproductive cycle and pregnancy to maintain normal uterine health. An imbalance in E and P signaling can lead to loss of pregnancy and a number of uterine pathologies, including endometrial hyperplasia and cancer. One of the physiological functions regulated by E and P is proliferation of the uterine epithelium. It is well established that E drives epithelial proliferation and P inhibits proliferation (1, 2). In the presence of E, uterine stromal cells produce a subset of fibroblast growth factors (FGFs) that act in a paracrine manner to activate FGF receptor (FGFR) signaling in the uterine epithelium, leading to subsequent proliferation through MAPK activation (3). When P is present, activation of its cognate receptor in the uterine stromal cells drives expression of heart and neural crest derivatives expressed 2 (HAND2), which inhibits the expression of these FGFs and acts as a mediator of the anti-proliferative actions of P (3). When HAND2 is lost from the uterus through conditional deletion, FGF levels remain elevated and uterine epithelial proliferation persists.

Unchecked endometrial proliferation is a common feature of endometrial hyperplasia and leads to an increased risk of endometrial cancer. Worldwide, endometrial cancer is the most common gynecological cancer, with an estimated 287,000 new cases developing annually (4). The majority of endometrial carcinomas are classified as endometrioid endometrial adenocarcinomas and originate in the epithelium lining the uterine glands (5). Women who are

nulliparous, obese, diabetic, or experiencing prolonged/unopposed exposure to E face an increased risk of developing endometrial cancer (5). Endometrial carcinomas are preceded by endometrial hyperplasia, a precursor lesion associated with abnormal proliferation. Endometrial hyperplasia results from chronic E exposure, coupled with an insufficient counterbalance by P, which promotes the hyperproliferation and transformation of cells (6). The findings of the Postmenopausal Estrogen/Progestin Interventions trial support these observations, showing that administration of E-only hormone replacement therapy increased incidence of endometrial hyperplasia, whereas administration of E+P showed rates of hyperplasia similar to placebo (7). Moreover, findings from the Women's Health Initiative show that combined E+P therapy in postmenopausal women decreased incidence of endometrial cancer compared with placebo (8). The findings of these trials highlight the importance of maintaining a proper balance of E and P for uterine health.

Endometrial hyperplasia is characterized by abnormal glandular proliferation resulting in an increase in the gland:stroma ratio and glandular remodeling, resulting in irregularities in gland shape and distribution throughout the endometrium (5, 9). Progestin therapy has been shown to be effective at regressing endometrial hyperplasia, demonstrating the importance of P as an anti-proliferative agent (10). These observations highlight the importance of maintaining a balance of pro-proliferative E and anti-proliferative P signaling in the uterus to maintain normal uterine health and function. Thus, it is important to determine if exposure to endocrine disrupting chemicals having estrogenic effects can disrupt this balance to promote endometrial hyperplasia and cancer.

Endocrine disruptors are both natural and manmade substances that interfere with or inhibit the body's normal endocrine function by mimicking endogenous hormones, interacting with the hormones' cognate receptor, and/or altering endogenous hormone synthesis. Perhaps one of the most pervasive endocrine disrupting chemicals is bisphenol-A (BPA), a component of polycarbonate plastics found in plastic food and drink containers, epoxy resins lining food cans, and thermal paper (11). Elevated serum or urine levels of BPA have been associated with several endocrine related diseases, including obesity, diabetes, polycystic ovarian syndrome, and thyroid dysfunction (12–15). Although it possesses a lower binding affinity to the estrogen receptor (ER) than estradiol itself, BPA has been shown to exhibit estrogenic effects (16–19). Because the uterus is highly sensitive to E stimulation, it is possible that estrogenic compounds such as BPA may adversely affect E-regulated processes involved in normal uterine cyclicity and pregnancy.

In rodent models, BPA has been shown to affect several reproductive parameters, including increased GnRH pulse frequency, reduced LH secretion, premature onset of puberty, and abnormal estrus cycle (20). Several animal studies have also demonstrated reduced fertility stemming from delayed embryo implantation and a decreased number of implantation sites in rodents exposed to BPA (21–24). Other studies have proposed a transgenerational effect of BPA on fertility, wherein pregnant dams dosed with BPA give rise to filial generations 1–3 exhibiting reduced fertility, including reduced number of pregnancies and reduced number of pregnancies carried to term (25, 26). These observations suggest BPA exposure in the mother causes changes in the daughters and granddaughters through an epigenetic mechanism. In women, elevated levels of BPA in serum or urine have been associated with lower antral follicle counts, implantation failure, and increased risk of miscarriage (27–29). It is clear based on the rodent studies and the human epidemiological studies that reproductive tissues are acutely sensitive to

the endocrine disrupting chemical BPA, and basic physiological processes, such as reproduction, are highly susceptible to BPA exposure.

Many studies have focused on the effects of BPA exposure during critical windows of development, such as during the perinatal period or during puberty, but relatively little is known about the consequences of BPA exposure during adulthood. Based on the endocrine disrupting nature of BPA, we hypothesized that BPA exposure would disrupt the balance of steroid hormone signaling in the adult uterus and lead to dysregulation of the molecular pathway controlling endometrial proliferation. We used an experimental model wherein reproductively mature cycling female mice were exposed for long durations to a concentration of BPA comparable to the level established by the US Environmental Protection Agency (EPA) as the safe level for human exposure. Moreover, we used oral administration to better mimic the route of human exposure to BPA. We found that chronic exposure to BPA induces uterine glandular proliferation through suppression of HAND2, a known mediator of the anti-proliferative effects of P.

MATERIALS AND METHODS

Animals and experimental protocol

C57BL6 mice were maintained in a University of Illinois–sponsored animal care facility and all procedures were approved by the University of Illinois Institutional Animal Care and Use Committee. Mice were housed in polysulfone cages containing corn cob bedding and fed Teklad 8664 rodent chow (Envigo) *ad libitum*. Water was provided *ad libitum* in glass bottles. For dosing experiments, reproductively mature (8-week-old) intact female mice were treated three

times per day (9:00 AM, 1:00 PM, and 5:00 PM) orally with BPA [60 µg/kg/d, cumulative, dissolved in ethanol, and suspended in tocopherol-stripped corn oil for 0.1% final ethanol concentration (Sigma)] or vehicle (tocopherol-stripped corn oil + 0.1% ethanol). Mice were fed these solutions by pipette and treatment continued for 60 days. At the end of the dosing period, vaginal cytology was used to determine stage of estrus, and animals were euthanized as they entered diestrus. Upon euthanization, uteri were collected, weighed, divided, and either fixed in 10% buffered formalin or flash frozen in liquid nitrogen for further analysis.

Immunohistochemistry

Formalin-fixed uterine segments were paraffin embedded and cross-sectioned to 5 µM thickness onto glass slides. Before staining, slides were deparaffinized in xylene and rehydrated in ethanol. Slides to be developed with chromagen were incubated in 0.3% hydrogen peroxide in methanol for 15 minutes at room temperature to quench endogenous peroxidase activity. Slides were subjected to antigen retrieval, blocked with normal donkey serum, and incubated overnight at 4°C with primary antibody diluted in immunohistochemistry block A solution (0.25% BSA, 0.3% Triton X-100, sterile PBS). Primary antibodies used are as follows: cytokeratin 8 (Hybridoma Bank; RRID: AB_531826) (30), Ki67 (BD Pharmingen; RRID: AB_393778) (31), phosphorylated FGFR substrate 2 (FRS2; R&D Systems; RRID: AB_2106234) (32), phosphorylated ERK1/2 (Santa Cruz; RRID: AB_653182) (33), PR (Dako; RRID: AB_2315192) (34), and HAND2 (Santa Cruz; RRID: AB_2115995) (35). The next day, slides were washed in PBS and incubated with either biotinylated or Cy3/Dylite conjugated secondary antibody (Jackson Immunoresearch Laboratories, Inc.; RRID: AB_2340788, RRID: AB_2340398, RRID: AB_2315777, RRID: AB_2307443, and RRID: AB_2340616) (36–40) diluted in PBS and 1% BSA for 1 hour at room temperature. Immunofluorescence stained slides were washed

and mounted with Prolong GOLD mounting medium (Promega) containing 4′,6-diamidino-2-phenylindole (DAPI). Biotinylated samples were incubated with streptavidin conjugated horseradish peroxidase (Invitrogen) for 30 minutes at room temperature. Samples were then stained with 3-amino-9-ethyl carbazole solution (Invitrogen) and counterstained with Mayer hematoxylin (Sigma). Slides were mounted with organic mounting medium before imaging. Imaging was performed using a Leica DM2500 light microscope (Leica Microsystems) fitted with a Qimaging Retiga 2000R camera (Teledyne Qimaging). Immunofluorescent images were captured on an Olympus BX51 fluorescence microscope (Olympus) fitted with an Olympus DP71 camera (Olympus). ImageJ software (National Institutes of Health) was used to perform post-imaging analysis.

Uterine stromal cell isolation

Uteri were isolated from intact, reproductively mature mice in diestrus, as determined by vaginal cytology. Uterine horns were cut open longitudinally and divided into 3 mm pieces. This tissue was incubated in a solution of Hanks buffered salt solution (HBSS) containing 25 g/L of pancreatin (Sigma-Aldrich) and 6 g/L of dispase (Gibco) at room temperature for 1 hour and then 37°C for 15 minutes. The tissue was then washed with HBSS supplemented with 10% FBS and then HBSS alone. Tissue was then incubated in HBSS containing 0.5 g/L of collagenase (Gibco) for 1 hour at 37°C. HBSS containing 10% FBS was added to stop digestion; stromal cells were dissociated by pipetting. Cell suspensions were then passed through a 70 µm mesh cell strainer (VWR) to remove tissue debris. Stromal cells were plated in DMEM/F12 culture media (Gibco) containing 2% charcoal–stripped calf serum (Gibco) and treated with 5 µM of BPA or ethanol as vehicle for 48 hours. In a subset of experiments, cells were plated and treated with 5 µM of BPA in the presence or absence of 10 µM ICI 182,780 (Sigma) for 48 hours. In

another subset of experiments, cells were plated and treated with ethanol vehicle or 10 μM *S*-adenosylmethionine (SAM; New England Biolabs) for 24 hours. To induce *Hand2* expression, 1 μM of P (Sigma) was added to the treatment and cells were cultured for an additional 12 hours. Cells were then washed in PBS and harvested in TRIZOL for further RNA isolation and gene expression analysis.

RNA isolation and real-time qPCR analysis

Frozen uteri were homogenized and RNA isolated using TRIZOL reagent (Life Technologies), according to the manufacturer's protocol. cDNA was prepared using the AffinityScript Multiple Temperature Reverse transcription, according to the manufacturer's protocol (Agilent Technologies). The cDNA was amplified to quantify gene expression by real-time PCR, using gene specific primers and Power SYBR Green PCR Master Mix (Applied Biosystems). The expression level of *36b4* was used as the internal control. For each treatment, the mean cycle threshold (Ct) and SD were calculated from individual Ct values obtained from three replicates of a sample. The normalized ΔCt in each sample was calculated as mean Ct of target gene subtracted by the mean Ct of internal control gene. ΔΔCt was then calculated as the difference between the ΔCt values of the vehicle and BPA treatment samples. The fold change of gene expression in each sample relative to a control was computed as $2^{-\Delta\Delta Ct}$. The mean fold induction and SEs were calculated from four independent experiments.

Methylation analysis

Methylation status was assessed using the EpiTect Methyl II PCR Assay (Qiagen). Briefly, genomic DNA was isolated from uteri of vehicle and BPA-treated mice using the DNeasy Blood and Tissue Kit (Qiagen), according to the manufacturer's protocol. In a subset of methylation analysis experiments, DNA was isolated from primary murine uterine stromal cells

that were treated with ethanol vehicle or SAM for 24 hours and then cotreated with P for 12 hours. Enzymatic treatment with the methyltransferase SssI and the methyl donor *S*-Adenosyl Methionine (New England Biolabs) was used to generate hypermethylated DNA as a positive control. Genomic DNA was then subjected to methyl-sensitive and methyl-dependent restriction enzyme digestion using the EpiTect II DNA Methylation Enzyme Kit (Qiagen). Methylation status of the isolated genomic DNA was assayed using the EpiTect Methyl II PCR Assay (Qiagen) with primer sets targeting two CpG islands in the mouse *Hand2* gene. Ct values obtained from the different restriction enzyme conditions were used to calculate the percentage of methylated and unmethylated input DNA, as described in the manufacturer's protocol. The mean percentage of methylated input DNA and SEs were calculated from four independent experiments.

Statistical Analysis

Statistical significance between control and BPA-treated samples/tissues was determined using the Student *t* test. Asterisks denote significance with a *P* value <0.05.

RESULTS

Chronic BPA treatment is uterotrophic and increases the gland:stroma ratio

To assess the risks of long-term exposure to the endocrine disruptor BPA in the uterus, we exposed reproductively mature cycling female mice three times a day orally to a cumulative dose of 60 µg/kg/d of BPA for 60 days. This concentration was chosen to reflect the reference dose established by the EPA and represents an estimate of the daily exposure likely to be without appreciable risk of deleterious effects (41). Oral route of administration was used to recapitulate the route of exposure in human populations. Uterine weight was measured upon euthanization,

normalized to body weight, and expressed as fold change compared to vehicle [Fig. 2.1(a)]. A substantial increase in uterine wet weight was observed following long-term exposure to BPA compared with uteri from vehicle (corn oil only)-treated animals, indicating that chronic exposure to BPA has a uterotrophic effect. We next used hematoxylin and eosin staining to look at general uterine morphology [Fig. 2.1(b)]. Uteri from BPA-treated animals appeared to have an increased number of uterine glands dispersed throughout the endometrium compared with vehicle-treated animals. To further investigate this observation, we subjected uterine sections to immunohistochemistry using cytokeratin 8 as an epithelial marker. Cytokeratin positive structures were counted and expressed relative to stromal area, as determined by ImageJ (National Institutes of Health). We found that exposure to BPA increased the uterine gland:stroma ratio compared with the vehicle as a control [Fig. 2.1(c)]. Because increased gland:stroma ratios are often observed in incidences of hyperplasia, we further investigated into uterine abnormalities following BPA exposure.

Changes in proliferation and glandular morphology following chronic BPA exposure

To determine if long-term exposure to BPA alters epithelial proliferation, we subjected uterine sections to immunohistochemistry using Ki67 as a marker for proliferation [Fig. 2.2(a)]. Indeed, we observed that uteri from mice exposed to BPA showed increased levels of proliferation, as indicated by $Ki67^{+}$ staining in brown. The staining was particularly pronounced in the luminal epithelium and the uterine glands of BPA-exposed animals compared with the vehicle-treated controls. Because aberrant proliferative activity in glandular epithelium is one of the hallmarks of endometrial hyperplasia, we further looked at the glandular morphology in uteri of vehicle and BPA-treated animals using cytokeratin 8 [Fig. 2.2(b)]. Uteri of BPA-exposed animals exhibited densely packed clusters of glands, as well as elongated, irregularly shaped

glands, compared with smaller, rounder, more evenly distributed glands found in uteri of vehicle-treated mice. These changes in proliferation, glandular architecture, and the gland:stroma ratio suggest that long-term BPA exposure may give rise to endometrial hyperplasia. We next determined the mechanism by which BPA alters endometrial proliferation.

BPA alters expression of the PR target HAND2

It is well established that endometrial proliferation is influenced by a balance of pro-proliferative E and anti-proliferative P signaling. Because we observed an increase in glandular proliferation following BPA exposure, we next wanted to investigate whether aspects of P signaling were impaired. We looked at expression of the progesterone receptor (PR) target HAND2, a stromal factor that has been shown to mediate the anti-proliferative effects of P (3). Gene expression analysis revealed that uterine *Hand2* expression is reduced following chronic BPA exposure compared with vehicle-treated animals [Fig. 2.3(a)]. In addition, HAND2 protein is robustly expressed in the subepithelial stroma of mice treated with vehicle, as indicated by immunohistochemistry [Fig. 2.3(b)]. In BPA-treated animals, HAND2 is also detected in the subepithelial stroma, but to a lesser extent than in vehicle-treated animals. Indeed, when we quantify the number of $HAND2^{+}$ stromal cells using ImageJ software, we see a substantial decrease in the number of $HAND2^{+}$ cells in the subepithelial stromal compartment of BPA-treated mice, compared with vehicle [Fig. 2.3(b)]. This indicates that BPA exposure leads to downregulation of the downstream mediator of PR, resulting in persistent epithelial proliferation.

We next determined whether PR expression itself is impaired in response to BPA exposure by using quantitative PCR (qPCR) [Fig. 2.3(c)]. Compared with vehicle, BPA-treated animals showed slightly higher expression of *PR*, although this was not statistically significant. Consistent with this RNA profile, we found that PR expression is maintained both in the

epithelium and the stroma following BPA exposure [Fig. 2.3(d)]. These data suggest that reduced HAND2 expression following BPA exposure is due to changes in PR transcriptional activity rather than reduced PR expression.

Chronic BPA exposure alters FGF signaling in the glandular epithelium

Previously, we have shown that a primary function of HAND2 is to regulate uterine epithelial proliferation by suppressing expression of paracrine acting FGFs in the uterine stroma (3). We next determined the consequences of BPA exposure on FGF levels by performing qPCR using uterine samples obtained from our BPA- or vehicle-exposed mice. We found that mice chronically exposed to BPA exhibited significantly increased uterine expression of *Fgf9* and *Fgf18* compared with vehicle-treated animals [Fig. 2.4(a)], indicating that reduced HAND2 expression corresponds with increased FGF production.

FGFs signal through membrane bound FGFR. Binding of the ligand to the receptor triggers receptor activation and subsequent phosphorylation of FRS2. Using this phosphorylation event as a readout of FGFR activation, we performed immunohistochemistry using an antibody specific for phosphorylated FRS2 (pFRS2) [Fig. 2.4(b)]. We found that FGFR activation was greatly increased in the glandular epithelium following chronic BPA exposure compared with vehicle-treated animals, as indicated by pFRS2 staining in red. FGFR activation can lead to increased proliferation, which is mediated through activation of the MAPK cascade. Indeed, we have previously shown that loss of MAPK activation can attenuate proliferation in the uterine epithelium (3). To determine if BPA exposure leads to increased MAPK activation, we performed immunohistochemistry using an antibody specific to phosphorylated ERK1/2 [Fig. 2.4(b)]. We found that phosphorylation and activation of ERK1/2 was robustly increased in the uterine glands of animals exposed to BPA compared with vehicle-treated animals, as indicated

by pERK1/2 staining in green. Together, these data establish a mechanism whereby BPA induces expression of FGFs that bind FGFR in the glandular epithelium, leading to downstream MAPK activation and increased proliferation.

To further investigate how BPA modulates *Fgf9* and *Fgf18* expression in the uterus, we used an *in vitro* system in which stromal cells were isolated from the uterus and placed into culture. These cells were then stimulated with 5 μM of BPA for 48 hours; the resulting RNA was subjected to gene expression analysis using primers specific to *Fgf9* and *Fgf18*. Indeed, cells exposed to BPA showed increased expression of *Fgf9* and *Fgf18* compared with vehicle-treated cells [Fig. 2.5(a)], indicating that BPA can drive expression of paracrine acting FGFs in stromal cells. These observations are in agreement with those seen *in vivo* [Fig. 2.4(a)]. We next investigated the nature of this regulation and the involvement of ER. Previous groups have shown that FGF expression is positively regulated by E (42, 43). To determine if BPA is promoting FGF production through ER, we treated uterine stromal cells *in vitro* with BPA in the presence or absence of ER antagonist ICI 182,780 [Fig. 2.5(b)]. We observe marked reduction in BPA stimulated *Fgf9* and *Fgf18*levels with inclusion of ICI 182,780, indicating that functional ER is required for BPA-mediated induction of FGFs.

BPA induces differential methylation at the *Hand2* promoter and increased expression of methylation related factors

Chronic BPA exposure reduces HAND2 expression, but does not alter the expression of PR, the upstream regulator of HAND2. This suggests that BPA may be interfering with the ability of PR to recognize and stably bind to its downstream targets as opposed to decreasing the levels of PR available to signal. Previous studies have shown that BPA exposure causes differential methylation of certain gene promoters, which can lead to changes in gene expression

from the affected promoters (44–47). To determine if BPA downregulates HAND2 in the uterus via hypermethylation and gene silencing, we looked at the methylation status of the *Hand2* promoter following chronic BPA exposure [Fig. 2.6(a)]. Our analysis focused on methylation within two different CpG islands proximal to the *Hand2* transcription start site [Fig. 2.6(a)]. We observed a substantial increase in DNA methylation in uterine samples following chronic BPA exposure at the first CpG island assayed, flanking the *Hand2*transcription start site. No differential methylation was observed in the second CpG island, coding for the 5′-UTR and exon1 of *Hand2*. MatInspector software by Genomatix was used to identify transcription factor binding sites within this first CpG island. We identified several potential transcription factor binding sites within this region, including response elements for Kruppel-like factors, signal transducer and activator of transcription, GATA binding proteins, and hypoxia inducible factors. Further investigation is needed to determine what regulatory elements in this region may be required for proper *Hand2* expression.

We next used our *in vitro* system to further investigate the link between methylation at the *Hand2* promoter and how this affects its expression. SAM is a methyl donor that supplies DNA methyltransferases with the methyl group for transfer to cytosine residues in DNA. We exposed uterine stromal cells to 10 μM of the methyl donor SAM and then stimulated *Hand2* expression with P. We observed increased DNA methylation at the CpG island 110765 flanking the *Hand2* transcription start site following treatment with P and SAM, compared with vehicle or P alone [Fig. 2.6(b)]. We saw no change in DNA methylation at CpG island 110766, consistent with our *in vivo* observations [Fig. 2.6(a)]. We next analyzed gene expression changes and observed increased *Hand2* expression following stimulation with P. This induction was blocked by treatment with SAM [Fig. 2.6(c)]. Moreover, expression of a DNA

methyltransferase, *Dnmt3b*, is unchanged, indicating that reduced gene expression in response to SAM is not a global effect. Together, these *in vitro* data suggest that increased methylation at the *Hand2* promoter can impair HAND2 expression.

DNA methylation and gene silencing are mediated by DNA methyltransferases and methylated DNA binding proteins. A growing body of literature suggests that BPA exposure modulates expression of these factors in a variety of tissue types (44–47). We observed increased uterine expression of several of these factors, including DNA methyltransferases *Dnmt1* and *Dnmt3b* and methylated DNA binding protein *Mbd2*, *in vivo* following chronic oral exposure to BPA [Fig. 2.7(a)]. We also observed increased *Dnmt1*, *Dnmt3b,* and *Mbd2* expression in primary uterine stromal cells treated with BPA *in vitro* [Fig. 2.7(b)]. Previous studies have shown *Dnmt* expression is induced by E acting through ER (48, 49). Inclusion of the ER antagonist ICI 182,780 to BPA-treated uterine stromal cells *in vitro* reduces the expression of *Dnmt1* and *Dnmt3b*, compared with BPA alone, suggesting that BPA acts via ER to upregulate *Dnmt* expression [Fig. 2.7(c)].

Based on these data, we propose a mechanism by which BPA exposure induces methylation at the *Hand2* promoter, which obstructs transcription factor binding and recruitment of transcription machinery and decreases *Hand2* expression. Reduced expression of HAND2 alleviates antagonism of FGF production, allowing for increased FGF stimulation of the uterine glandular epithelium and subsequent proliferation [Fig. 2.8].

DISCUSSION

BPA exposure in the general population is ubiquitous, and numerous biomonitoring studies have shown measurable BPA levels in serum and urine of children and adults all over the

world (11). These observations highlight the importance of understanding the adverse health effects associated with BPA exposure. A recent study demonstrated that a single oral exposure to 50 μg/kg led to BPA accumulation in the uteri of both cycling and pregnant rats and mice within an hour of exposure (50). Moreover, ~72% of the BPA recovered from uterine samples was in the aglycone form, which is capable of interacting with steroid receptors. In this study, we report that BPA has uterotrophic effects in the cycling mouse uterus [Fig. 2.1(a)]. This uterotrophic effect is consistent with observations made by other groups (51, 52). However, these studies used doses delivered via injection or continuous exposure via ALZET pump for short treatment periods and may not adequately represent the common oral route of exposure in humans. In the current study, we demonstrate that oral exposure to a lower concentration of BPA for a longer treatment period can also induce a uterotrophic response. Currently, the reference dose for BPA is 50 μg/kg/d, as established by the EPA. This represents an estimate of the daily exposure in humans likely to be without appreciable risk of deleterious effects. Our study establishes that BPA exposure comparable to what the EPA deems safe for human exposure can lead to undesirable uterine pathologies in mice.

Aberrant proliferation is a hallmark of hyperplasia, a condition characterized by an increase in cell number without changes to cell morphology. Hyperplasia is not cancer, but a pre-neoplastic lesion that can develop into cancer with further genetic mutations or environmental insults to the epigenome. Here we report that BPA exposure leads to aberrant proliferation of the uterine epithelium, as indicated by Ki67 staining [Fig. 2.2(a)]. Notably, proliferation was particularly robust in the epithelium of the uterine glands, which are the predominant site of origin for endometrial hyperplasia. A previous study demonstrated that gestational exposure to low doses of BPA (ng/kg/d) led to increased 5-bromo-2′-deoxyuridine incorporation and DNA

synthesis in the glandular epithelium of pups at 3 months of age (53). These findings support the observations made in this study; however, because a different dosing paradigm and age of exposure was used, different mechanisms may be at play compared with the current study. In addition to increased proliferation, we observed changes in uterine glandular architecture which are consistent with endometrial hyperplasia, including increased gland:stroma ratio [Fig. 2.1(c)], densely clustered glands, and enlarged, irregularly shaped glands [Fig. 2.2(b)]. Several rodent studies have shown that BPA exposure during the perinatal period increased incidence of uterine gland abnormalities later in life, including signs of cystic hyperplasia and squamous metaplasia (54, 55). Again, these data are consistent with our observations; however, our study also demonstrates that BPA exposure outside of the critical windows of development can have deleterious effects in the uterine glands, perhaps through an alternative mechanism. Another study reported changes in uterine architecture following BPA exposure in adults, including increased epithelial height and increased stromal and myometrial thickness (56). However, this study dosed mice acutely (4 days) and does not provide insight into the effects of chronic BPA exposure. Interestingly, Hiroi et al. examined serum BPA levels in women with endometrial hyperplasia and showed that BPA levels were reduced in patients with complex endometrial hyperplasia and endometrial cancer compared with healthy patients (57). The authors hypothesize that the reduced BPA levels may be a result of altered metabolism of BPA or that BPA exerts anti-estrogenic effects. Endocrine disrupting chemicals such as BPA have been shown to exhibit nonmonotonic dose responses, meaning that the dose response curve generated for a specific response resembles a “U” shape, showing a greater magnitude of response at lower and higher doses, and a lesser magnitude of response at intermediate doses (58). In light of this, perhaps the lower concentrations observed in women with endometrial hyperplasia and cancer

correspond with a greater response (*i.e.*, hyperplasia compared with healthy patients with higher serum BPA levels).

We report here that BPA causes aberrant *Fgf* production and FGFR activation in uterine tissue. The FGF family consists of 18 secreted proteins that serve as ligands to 4 membrane bound tyrosine kinase receptors (59). FGFs bind to membrane bound FGFRs and trigger receptor dimerization, activation, and autophosphorylation that recruits the adaptor protein FRS2. FRS2 is phosphorylated on several tyrosine residues that serve as docking sites for downstream signaling molecules that lead to activation of the MAPK pathway and the phosphatidylinositol 3-kinase/AKT pathway. FGF signaling orchestrates multiple biological responses, including cell proliferation, cell migration, and angiogenesis (60). In the uterus, FGFs produced in the stroma act in a paracrine fashion to induce proliferation of epithelial cells (3). In a previous study, using a delayed implantation model, we observed that pre-pubertal exposure to BPA leads to impaired implantation (24). This is accompanied by increased stromal FGF production, increased epithelial FGFR activation and MAPK activity, and persistent proliferation in the luminal epithelium that renders it unreceptive to blastocyst implantation. Similar to what is observed in the pregnant mouse uterus, here we show BPA increases *Fgf* production [Fig. 2.4(a) and 2.5(a)] and leads to FGFR activation and increased MAPK activity in the adult non-pregnant uterine glands, as indicated by pFRS2 and pERK1/2 staining [Fig. 2.4(b)]. Aberrant activation of this signaling pathway is likely a driver for epithelial proliferation, increased gland:stroma ratio, and changes in glandular morphology observed in BPA-treated mice. Aberrant FGF signaling has been previously observed in human endometrial cancer, where activating mutations in FGFR2 have been reported in 10% to 12% of primary uterine tumors (61, 62). Inhibition of FGFR2 expression or activity both resulted in decreased endometrial tumor cell survival and

transformation, indicating that excessive FGFR2 activation contributes to endometrial cancer progression (62). Pharmacological agents targeting FGF signaling are currently being explored for use in the treatment of endometrial cancers (63). Here, we show that BPA exposure leads to a robust increase in *Fgf9* expression and corresponding activation of FGFR in the glandular epithelium. FGF9 has a greater binding affinity for FGFR2 and FGFR3 than FGFR1 and 4 (64). We hypothesize that increased production of FGF9 in response to BPA exposure acts on FGFR2 in the glandular epithelial cells to promote proliferation. Further experiments are needed to determine which FGFR isoform is responsible for mediating the proliferative effects of FGF9 in the uterine glands.

In the current study, we show that chronic exposure to BPA increases methylation of a CpG island in the murine *Hand2* promoter and correlates with reduced uterine *Hand2* transcript levels compared with vehicle-treated animals [Fig. 2.6(a) and 2.3(a)]. This linkage between methylation at the *Hand2* promoter and reduced *Hand2* expression was also observed *in vitro* using the methyl donor SAM [Fig. 2.6(b-c)]. CpG islands represent short stretches of DNA that are rich in CpG dinucleotides. Many of these areas are associated with gene promoters, and CpGs in these regions are generally protected from methylation. In the incidence of cancer, global methylation analysis reveals that cancer genome in tissues such as breast, colon, and prostate tend to be hypomethylated in the intergenic and intronic regions relative to normal healthy tissue, whereas specific CpG islands tend to be concurrently hypermethylated with the incidence of cancer (65, 66). Other groups have shown that CpGs located within promoters of genes associated with tumor suppression, DNA repair, and hormone receptors are hypermethylated in tumor samples and cancer cell lines, and that demethylation of these regions with 5-aza-2′-deoxycytidine could restore gene expression (67–69). There is a growing body of

literature suggesting that BPA modifies gene expression through an epigenetic mechanism, including modulating CpG methylation at target gene promoters and regulatory regions that correlates with reduced gene expression (44–47, 70). A number of studies also show that exposure to BPA increases the expression of DNA methyltransferases in various tissues such as heart, liver, and testis, and suggest this may be a mechanism by which BPA mediates hypermethylation and gene silencing (44–47). Similarly, in our study in the uterus, we observed that BPA induces increased mRNA expression of *Dnmt1,* a maintenance methylase, *Dnmt3b,* a *de novo* methylase, as well as increased expression of *Mbd2*, a protein that binds methylated DNA and mediates transcriptional repression at methylated gene promoters [Fig. 2.7(a)]. We have further shown that, in regard to *Dnmt1* and *Dnmt3b,* this action is mediated through ER [Fig. 2.7(c)]. It is possible that elevated expression levels of these factors may be mediating the hypermethylation and transcriptional repression of *Hand2* in the uterus of BPA-treated mice.

Interestingly, we see that uterine PR expression appears to be unchanged between vehicle- and BPA-treated mice [Fig. 2.3(c-d)]. This is in contrast to our previous study showing the effects of BPA exposure during pregnancy, in which BPA reduced not only HAND2, but also PR expression (24). P, through the activation of PR, induces HAND2 expression in the uterine stroma. This suggests that during pregnancy, the reduction in HAND2 expression in response to BPA is due to reduced levels of PR. In the current study, our data indicate that in the non-pregnant uterus BPA is interfering with PR transcriptional activity by inhibiting its ability to interact with the target gene rather than through inhibition of PR expression itself.

HAND2 is a critical mediator of the anti-proliferative effects of P in the uterus (3). We have previously observed that BPA reduces HAND2 expression during early pregnancy (24). A

pervasive consequence of HAND2 loss is persistent epithelial proliferation, which would suggest that HAND2 may play a role in preventing uterine hyperplasia and cancer. Indeed, mice lacking uterine HAND2 exhibit signs of complex atypical hyperplasia in their uterine glands, including changes in glandular morphology and an increase in the gland:stoma ratio, compared with their age-matched controls (71). In humans, we have shown that *HAND2* is the most commonly hypermethylated and silenced gene in endometrial cancer (71).

Moreover, *HAND2* hypermethylation and silencing is observed in endometrial precancerous lesions, indicating that loss of HAND2 occurs early on in the progression of endometrial cancer. Interestingly, *HAND2* hypermethylation correlates with failure to respond to P therapies to treat endometrial cancer, indicating that HAND2 is the primary mediator of the anti-proliferative effects of P. With chronic BPA treatment in non-pregnant adult mice, we observed decreased HAND2 expression and increased glandular proliferation, suggesting that the repression of HAND2 plays a critical role in driving the hyperplastic effects of BPA in the uterus.

CONCLUSION

Our studies demonstrate that chronic oral exposure to a low concentration of BPA during adulthood impedes transcriptional activation of the anti-proliferative factor HAND2, likely through an epigenetic mechanism involving hypermethylation at the *Hand2* promoter. Reduction of HAND2 alleviates its repression of FGFs, increasing FGF levels and promoting FGF-induced epithelial proliferation in the uterine glands and altered glandular morphology. This is mediated through increased MAPK activity downstream of glandular FGFR activation. This study offers further insight into the endocrine disrupting nature of BPA and provides a potential mechanism by which BPA may influence endometrial hyperplasia and other uterine disorders.

FIGURES

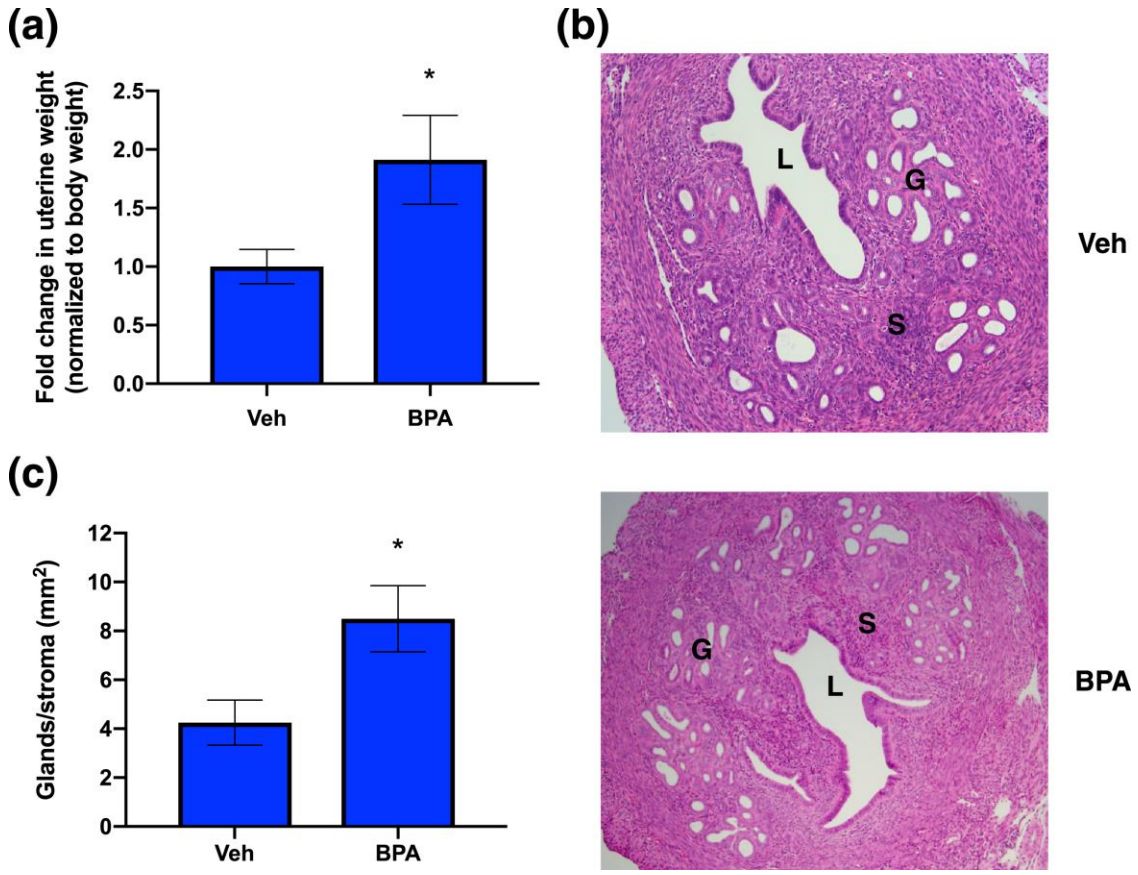

Figure 2.1 Chronic BPA treatment increases uterine weight and increases the gland:stroma ratio

(a) Reproductively mature female mice (8 wk of age) were treated three times per day with vehicle (corn oil) or BPA (cumulative dose of 60 µg/kg/d in corn oil) for 60 d. Animals were euthanized in diestrus, as determined by vaginal cytology. Uterine wet weight was measured on collection. Weights were normalized to animal body weight, and data are represented as the mean fold change ± SEM; **P* < 0.05. **(b)** Representative hematoxylin and eosin staining of uterine sections obtained from vehicle- and BPA-treated mice. (Magnification, ×10). **(c)** Uterine sections were subjected to immunohistochemistry and stained with cytokeratin 8 as an epithelial marker. Glands were counted and expressed relative to stromal area using ImageJ software. Data are represented as the mean ± SEM; **P* < 0.05. G, glands; L, lumen; S, stroma.

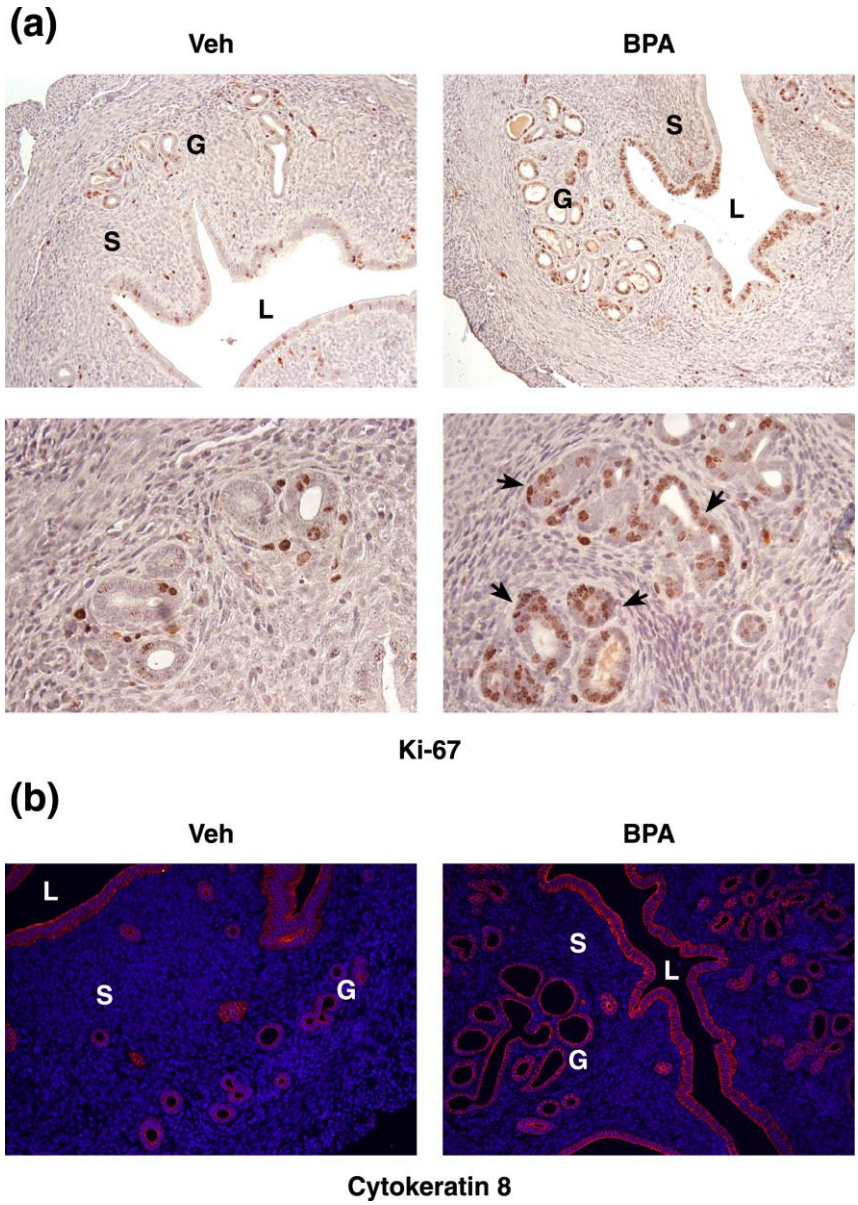

Figure 2.2 Changes in proliferation and glandular morphology following chronic BPA exposure

(a) Uterine sections obtained from vehicle- and BPA-treated (60 µg/kg/d for 60 d) mice were subjected to immunohistochemistry using Ki67 to indicate proliferating cells. Brown staining indicates $Ki67^{+}$ cells. Arrows highlight actively proliferating uterine glands. [Magnification, ×20 (top), ×40 (bottom).] **(b)** Cytokeratin 8 (red) staining of uterine sections obtained from vehicle- and BPA-treated mice. DAPI was used as a nuclear counterstain. (Magnification, ×20.) G, glands; L, lumen; S, stroma.

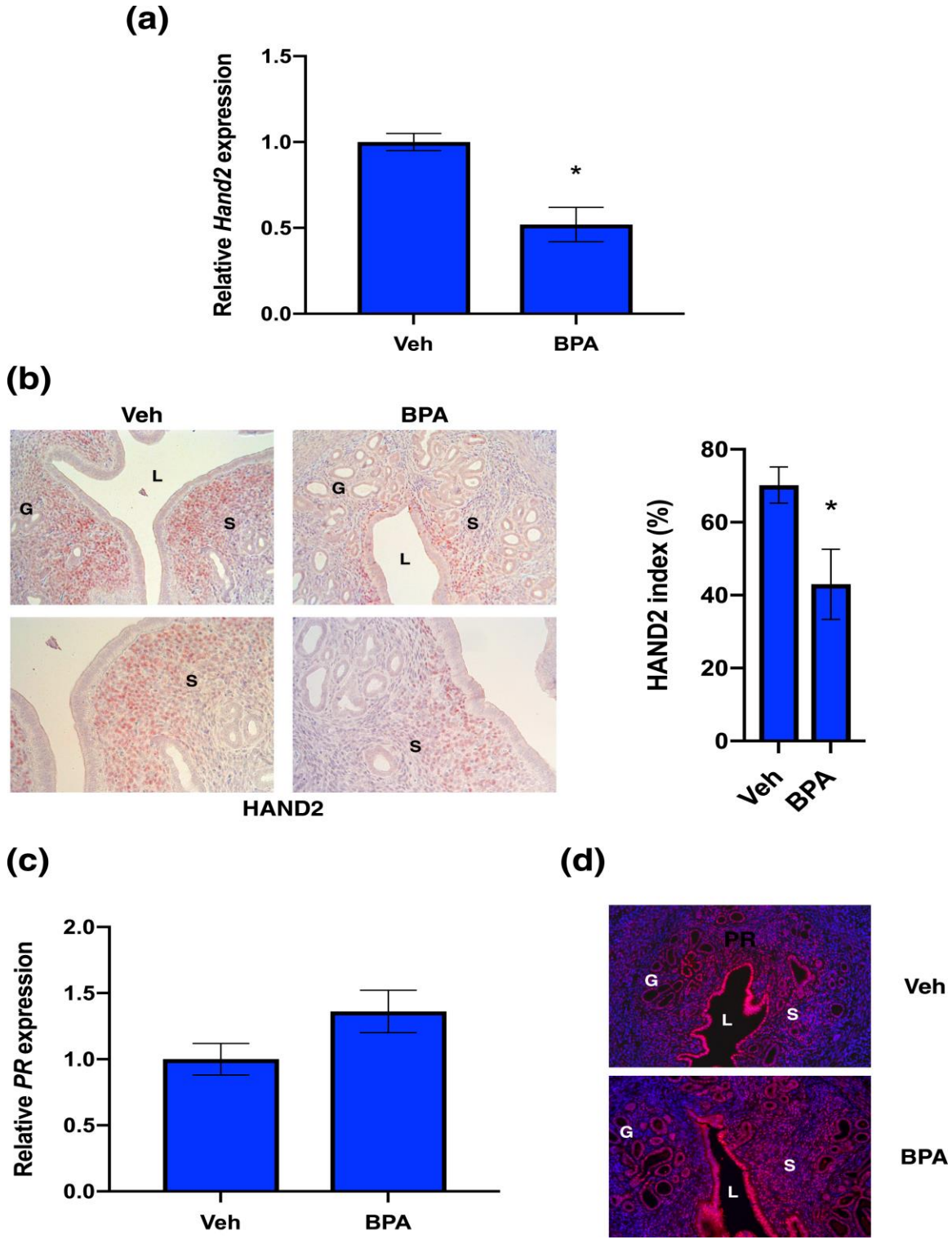

Figure 2.3 BPA alters expression of the PR target HAND2

Figure 2.3 continued: (a) RNA isolated from vehicle- and BPA-treated (60 μg/kg/d for 60 d) mice was subjected to qPCR using primers specific to *Hand2*. *36b4* was used for normalization. Data are represented as the mean fold induction ± SEM; **P* < 0.05. **(b)** Uterine sections obtained from vehicle- and BPA-treated mice were subjected to immunohistochemistry using an antibody specific for HAND2. HAND2 expression is indicated by the brown color. [Magnification, ×20 (top), ×40 (bottom)]. $HAND2^+$ cells were counted using ImageJ software and expressed as a percentage of total cells in the counting field. Data are represented as the mean percentage ± SEM; **P* < 0.05. **(c)** RNA isolated from vehicle- and BPA-treated mice was subjected to qPCR using primers specific to *PR*. *36b4* was used for normalization. Data are represented as the mean fold induction ± SEM. **(d)** Uterine sections obtained from vehicle- and BPA-treated mice were subjected to immunohistochemistry using an antibody specific for PR (red) and counterstained with DAPI (blue). (Magnification, ×20.) G, glands; L, lumen; S, stroma.

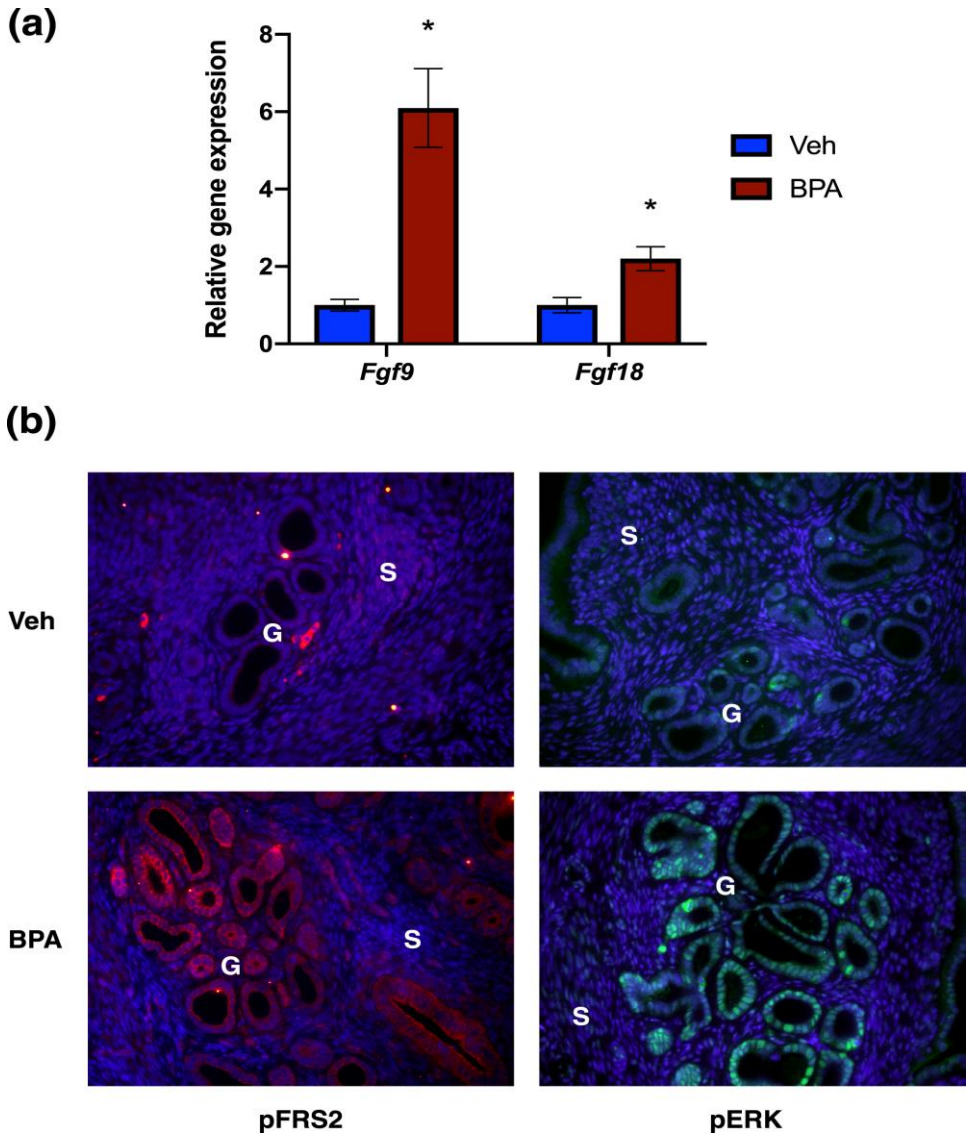

Figure 2.4 Chronic BPA exposure alters FGF signaling in the glandular epithelium
(a) RNA isolated from vehicle- and BPA-treated (60 µg/kg/d for 60d) mice was subjected to qPCR using primers specific to *Fgf9* and *Fgf18*. *36b4* was used for normalization. Data are represented as the mean fold induction ± SEM; **P* < 0.05. **(b)** Uterine sections obtained from vehicle- and BPA-treated mice were subjected to immunohistochemistry using an antibody specific to phosphorylated FRS2 (red, left) as an indicator of FGFR activation or phosphorylated ERK1/2 (green, right), and counterstained with DAPI (blue). (Magnification, ×40.) G, glands; S, stroma.

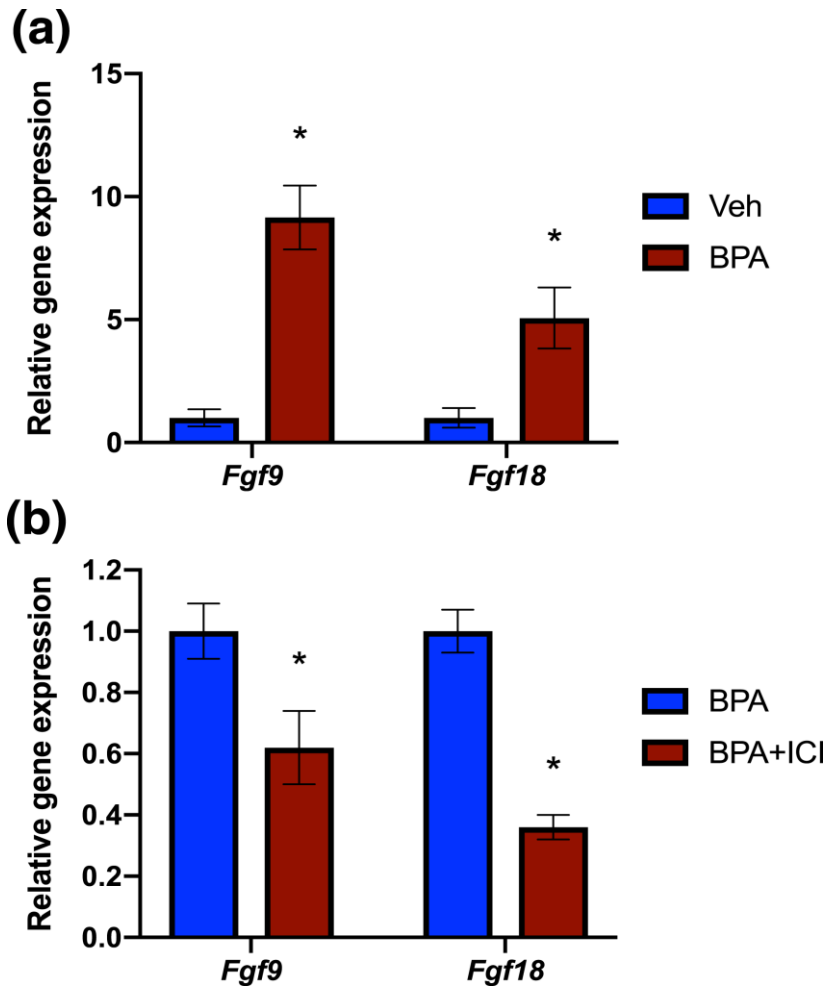

Figure 2.5 BPA induces FGF expression in vitro via estrogen receptor
(a) Primary murine uterine stromal cells were isolated and stimulated *in vitro* with vehicle (ethanol) or 5 µM BPA for 48 h. RNA was isolated and subjected to qPCR using primers specific to *Fgf9* and *Fgf18*. *36b4* was used for normalization. Data are represented as the mean fold induction ± SEM; **P* < 0.05. **(b)** Primary murine uterine stromal cells were isolated and stimulated *in vitro* with 5 µM BPA in the presence or absence of 10 µM ICI 182,780 for 48 h. RNA was isolated and subjected to qPCR using primers specific to *Fgf9* and *Fgf18*. *36b4* was used for normalization. Data are represented as the mean fold induction ± SEM; **P* < 0.05.

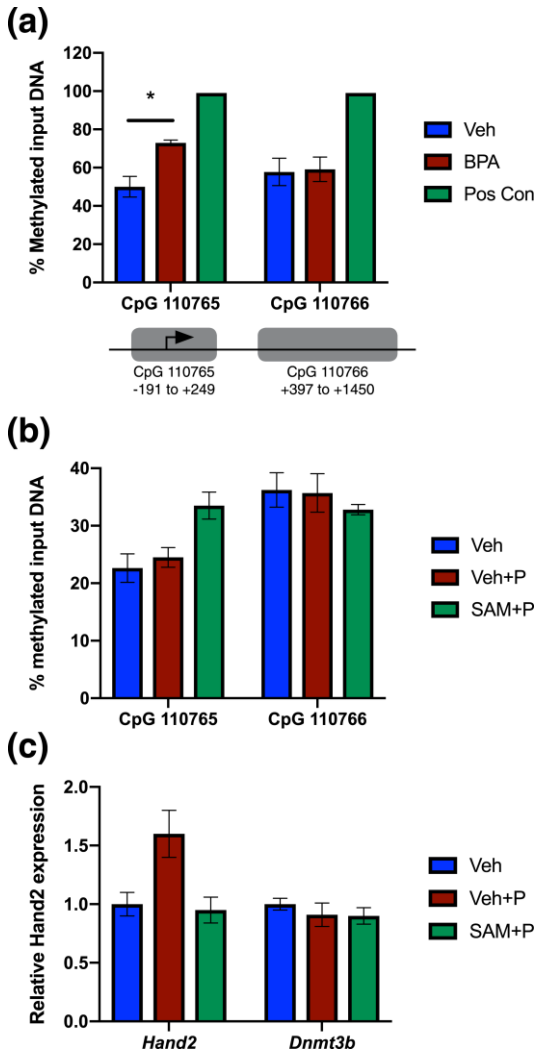

Figure 2.6 BPA induces differential methylation at the *Hand2* promoter
(a) Genomic DNA isolated from vehicle- and BPA-treated (60 µg/kg/d for 60 d) uteri was subjected to enzymatic digestion as described in "Materials and Methods"; SssI- and SAM-treated genomic DNA was used to generate hypermethylated DNA as a positive control. Digested DNA was subjected to qPCR using primers targeting the indicated *Hand2* CpG islands. Data are represented as the mean percent methylated input DNA ± SEM; **P* < 0.05. **(b)** Mouse uterine stromal cells were placed in culture and treated with 10 µM SAM or vehicle for 24 h. The treatment was supplemented with 1 µM of progesterone for 12 h to induce *Hand2* expression. Genomic DNA was isolated and subjected to enzymatic digestion as described in "Materials and Methods" and subjected to qPCR using primers targeting the *Hand2* CpG islands 110765 or 110766, shown in (a). Representative data are shown as mean percent methylated input DNA. **(c)** RNA isolated from mouse uterine stromal cells treated as described in (b) was subjected to qPCR using primers specific to *Hand2* and *Dnmt3b. 36b4* was used for normalization. Representative data are shown as mean fold induction.

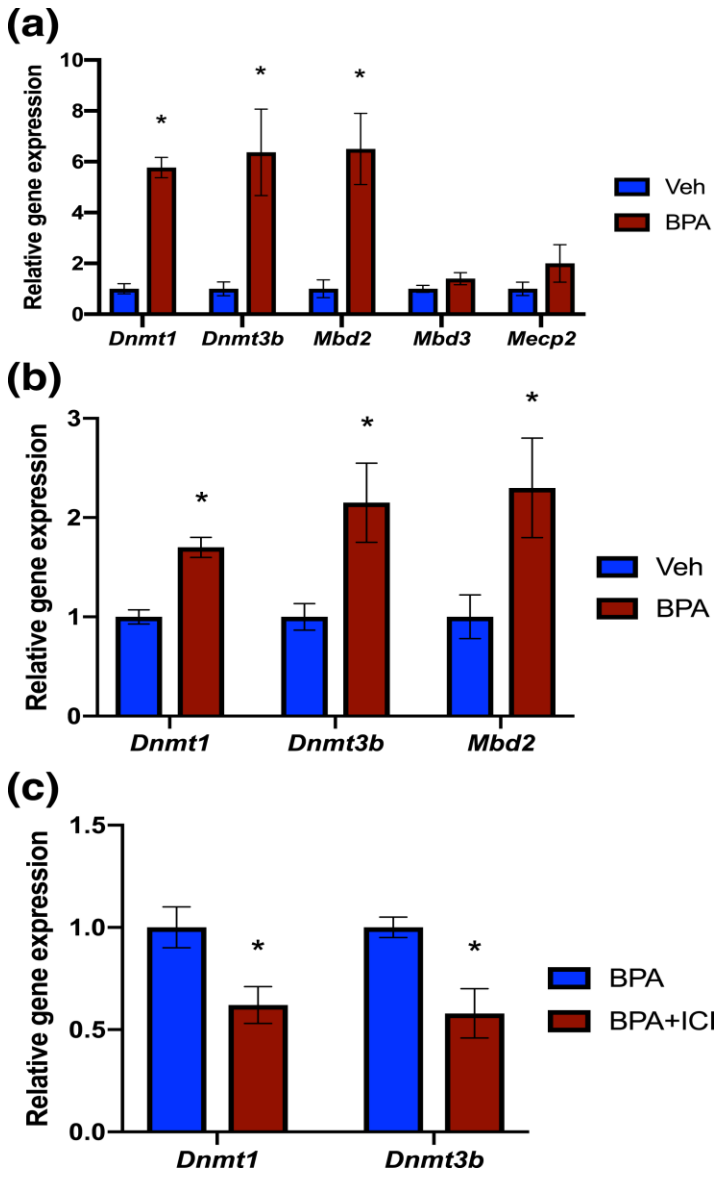

Figure 2.7 BPA induces expression of DNA methylation factors
(a) RNA isolated from vehicle- and BPA-treated mice was subjected to qPCR using primers specific to *Dnmt1*, *Dnmt3b*, *Mbd2*, *Mbd3, and Mecp2; 36b4*was used for normalization. **(b)** Primary murine uterine stromal cells were isolated and stimulated *in vitro* with vehicle (ethanol) or 5 μM BPA for 48 h. RNA was isolated and subjected to qPCR using primers specific to *Dnmt1*, *Dnmt3b*, and *Mbd2*. *36b4* was used for normalization. **(c)** Mouse uterine stromal cells were placed in culture and stimulated with 5 μM BPA in the presence or absence of 10 μM ICI 182,780 for 48 hours. RNA was isolated and subjected to qPCR using primers specific to *Dnmt1* and *Dnmt3b*; *36b4* was used for normalization. (a)–(c) Data are represented as the mean fold induction ± SEM; **P* < 0.05.

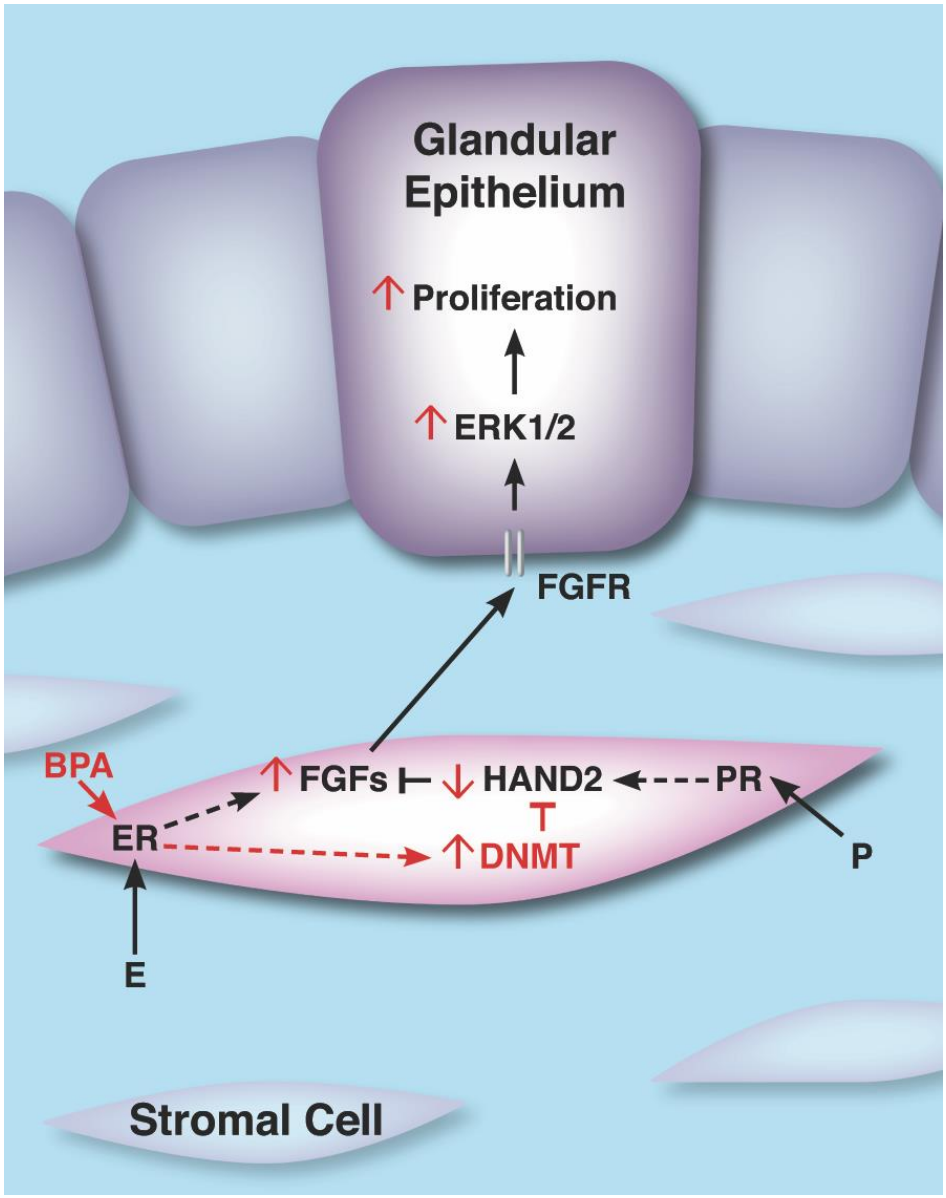

Figure 2.8 Proposed mechanism of BPA action in the mature murine uterus
BPA reduces stromal expression of the PR target HAND2, possibly through increased DNA methyltransferase expression and hypermethylation and gene silencing at the *Hand2* promoter. As HAND2 is a negative regulator of FGF production, loss of HAND2 allows enhanced FGF production which activates FGFR signaling in the epithelium and drives proliferation through MAPK activation.

ABBREVIATIONS

BPA, bisphenol-A; DAPI, 4′,6-diamidino-2-phenylindole; DNMT, DNA methyltransferase; E, estrogen; ER, estrogen receptor; ERK1/2, extracellular signal-regulated kinase 1/2; FGF, fibroblast growth factor; FGFR, FGF receptor; FRS2, FGFR substrate 2; HAND2, heart and neural crest derivatives expressed 2; MAPK, mitogen activated protein kinase; MBD, methylated DNA binding protein; P, progesterone; PR, progesterone receptor; SAM, S-adenosylmethionine

ACKNOWLEDGEMENTS

This work was supported by the National Institutes of Health grant R21 HD078983.

Alison Neff was supported by NIH T32ES007326. We thank Jason Neff for creating the figures.

REFERENCES

1. Martin L, Finn CA, Trinder G. Hypertrophy and hyperplasia in the mouse uterus after oestrogen treatment: an autoradiographic study. *J Endocrinol*.1973;56(1):133-144.
2. Pan H, Deng Y, Pollard JW. Progesterone blocks estrogen-induced DNA synthesis through the inhibition of replication licensing. *Proc Natl Acad Sci U S A*.2006;103(38):14021-14026.
3. Li Q, Kannan A, Demayo FJ, Lydon JP, Cooke PS, Yamagishi H, Srivastava D, Bagchi MK, Bagchi IC. The antiproliferative action of progesterone in uterine epithelium is mediated by Hand2. *Science*. 2011;331(6019):912–916.
4. Jemal A, Bray F, Center MM, Ferlay J, Ward E, Forman D. Global cancer statistics. *CA Cancer J Clin*.2011;61(2):69–90.
5. Trimble CL, Method M, Leitao M, Lu K, Ioffe O, Hampton M, Higgins R, Zaino R, Mutter GL. Management of endometrial precancers. *Obstet Gynecol.* 2012;120(5):1160-1175.
6. Kim JJ, Kurita T, Bulun S. Progesterone action in endometrial cancer, endometriosis, uterine fibroids, and breast cancer. *Endocr Rev.* 2013;34(1):130-162.
7. The Writing Group for the PEPI Trial. (1996) Effects of hormone replacement therapy on endometrial histology in postmenopausal women: The Postmenopausal Estrogen/Progestin Interventions (PEPI) Trial. *JAMA*. 1996 275(5):370-375.
8. Chlebowski RT, Anderson GL, Sarto GE, Haque R, Runowicz CD, Aragaki AK, Thomson CA, Howard BV, Wactawski-Wende J, Chen C, Rohan TE, Simon MS, Reed SD, Manson JE. Continuous Combined Estrogen Plus Progestin and Endometrial Cancer: The Women's Health Initiative Randomized Trial. *J Natl Cancer Inst*. 2015;108(3).doi:10.1093/jnci/djv350.

9. Sanderson PA, Critchley HO, Williams AR, Arends MJ, Saunders PT. New concepts for an old problem: the diagnosis of endometrial hyperplasia. *Hum Reprod Update*. 2017;23(2):232-254.
10. Chandra V, Kim JJ, Benbrook DM, Dwivedi A, Rajani R. Therapeutic options for management of endometrial hyperplasia. *J Gynecol Oncol*. 2016;27(1):e8.
11. Vandenberg LN, Chahoud I, Heindel JJ, Padmanabhan V, Paumgartten FJ, Schoenfelder G. Urinary, circulating, and tissue biomonitoring studies indicate widespread exposure to bisphenol A. *Environ Health Perspect*. 2010;118(8):1055-1070.
12. Trasande L, Attina TM, Blustein J. Association between urinary bisphenol A concentration and obesity prevalence in children and adolescents. *JAMA.* 2012;308(11):1113-1121.
13. Shankar A, Teppala S. Relationship between urinary bisphenol A levels and diabetes mellitus. *J Clin Endocrinol Metab*. 2011;96(12):3822-3826.
14. Kandaraki E, Chatzigeorgiou A, Livadas S, Palioura E, Economou F, Koutsilieris M, Palimeri S, Panidis D, Diamanti-Kandarakis E. Endocrine disruptors and polycystic ovary syndrome (PCOS): elevated serum levels of bisphenol A in women with PCOS. *J Clin Endocrinol Metab.* 2011;96(3):480-484.
15. Meeker JD, Ferguson KK. Relationship between urinary phthalate and bisphenol A concentrations and serum thyroid measures in U.S. adults and adolescents from the National Health and Nutrition Examination Survey (NHANES) 2007-2008. *Environ Health Perspect*. 2011;119(10):1396-1402.
16. Kuiper GG, Carlsson B, Grandien K, Enmark E, Häggblad J, Nilsson S, Gustafsson JA. Comparison of the ligand binding specificity and transcript tissue distribution of estrogen receptors alpha and beta. *Endocrinology*.1997;138(3):863-870.
17. vom Saal FS, Hughes C. An extensive new literature concerning low-dose effects of bisphenol A shows the need for a new risk assessment. *Environ Health Perspect*. 2005;113(8):926-933.
18. Singleton DW, Feng Y, Yang J, Puga A, Lee AV, Khan SA. Gene expression profiling reveals novel regulation by bisphenol-A in estrogen receptor-alpha-positive human cells. *Environ Res*. 2006;100(1):86-92.
19. Sekar TV, Foygel K, Massoud TF, Gambhir SS, Paulmurugan R. A transgenic mouse model expressing an ERα folding biosensor reveals the effects of Bisphenol A on estrogen receptor signaling. *Sci Rep*. 2016;6:34788.
20. Fernández M, Bianchi M, Lux-Lantos V, Libertun C. Neonatal exposure to bisphenol a alters reproductive parameters and gonadotropin releasing hormone signaling in female rats. *Environ Health Perspect.* 2009;117(5):757-762.
21. Berger RG, Foster WG, deCatanzaro D. Bisphenol-A exposure during the period of blastocyst implantation alters uterine morphology and perturbs measures of estrogen and progesterone receptor expression in mice. *Reprod Toxicol*. 2010;30(3):393-400.
22. Xiao S, Diao H, Smith MA, Song X, Ye X. Preimplantation exposure to bisphenol A (BPA) affects embryo transport, preimplantation embryo development and uterine receptivity in mice. *Reprod Toxicol*. 2011;32(4):434-441.
23. Pan X, Wang X, Sun Y, Dou Z, Li Z. Inhibitory effects of preimplantation exposure to bisphenol-A on blastocyst developmentand implantation. *Int J Clin Exp Med.* 2015;8(6):8720-8729.

24. Li Q, Davila J, Kannan A, Flaws JA, Bagchi MK, Bagchi IC. Chronic Exposure to Bisphenol A Affects Uterine Function During Early Pregnancy in Mice. *Endocrinology*. 2016;157(5):1764-1774.
25. Wang W, Hafner KS, Flaws JA. In utero bisphenol A exposure disrupts germ cell nest breakdown and reduces fertility with age in the mouse. *Toxicol Appl Pharmacol.* 2014; 276(2):157-64.
26. Ziv-Gal A, Wang W, Zhou C, Flaws JA. The effects of in utero bisphenol A exposure on reproductive capacity in several generations of mice. *Toxicol Appl Pharmacol*. 2015;284(3): 354-362.
27. Souter I, Smith KW, Dimitriadis I, Ehrlich S, Williams PL, Calafat AM, Hauser R. The association of bisphenol-A urinary concentrations with antral follicle counts and other measures of ovarian reserve in women undergoing infertility treatments. *Reprod Toxicol*.2013;42:224-231.
28. Ehrlich S, Williams PL, Missmer SA, Flaws JA, Berry KF, Calafat AM, Ye X, Petrozza JC, Wright D, Hauser R. Urinary bisphenol A concentrations and implantation failure among women undergoing in vitro fertilization. *Environ Health Perspect*. 2012;120(7):978-983.
29. Lathi RB, Liebert CA, Brookfield KF, Taylor JA, vom Saal FS, Fujimoto VY, Baker VL. Conjugated bisphenol A in maternal serum in relation to miscarriage risk. *Fertil Steril*. 2014;102(1):123-128.
30. RRID:AB_531826, https://scicrunch.org/resolver/AB_531826.
31. RRID:AB_393778, https://scicrunch.org/resolver/AB_393778.
32. RRID:AB_2106234, https://scicrunch.org/resolver/AB_2106234.
33. RRID:AB_653182, https://scicrunch.org/resolver/AB_653182.
34. RRID:AB_2315192, https://scicrunch.org/resolver/AB_2315192.
35. RRID:AB_2115995, https://scicrunch.org/resolver/AB_2115995.
36. RRID:AB_2340788, https://scicrunch.org/resolver/AB_2340788.
37. RRID:AB_2340398, https://scicrunch.org/resolver/AB_2340398
38. RRID:AB_2315777, https://scicrunch.org/resolver/AB_2315777.
39. RRID:AB_2307443, https://scicrunch.org/resolver/AB_2307443.
40. RRID:AB_2340616, https://scicrunch.org/resolver/AB_2340616.
41. U.S. Environmental Protection Agency National Center for Environmental Assessment. Bisphenol A; CASRN 80-05-7. *IRIS*. 2002
42. Tsai SJ, Wu MH, Chen HM, Chuang PC, Wing LY. Fibroblast growth factor-9 is an endometrial stromal growth factor. *Endocrinology*.2002;143(7):2715-2721.
43. Šućurović S, Nikolic T, Brosens JJ, Mulac-Jericevic B. Spatial and temporal analyses of FGF expression during early pregnancy. *Cell Physiol Biochem*.2017;42(6):2318-2329.
44. Doshi T, Mehta SS, Dighe V, Balasinor N, Vanage G. Hypermethylation of estrogen receptor promoter region in adult testis of rats exposed neonatally to bisphenol A. *Toxicology*. 2011; 289(3):74-82.
45. Patel BB, Raad M, Sebag IA, Chalifour LE. Lifelong Exposure to Bisphenol A Alters Cardiac Structure/Function, Protein Expression, and DNA Methylation in Adult Mice. Toxicol Sci. 2013;133(1):174–185.
46. Ma Y, Xia W, Wang DQ, Wan YJ, Xu B, Chen X, Li YY, Xu SQ. Hepatic DNA methylation modifications in early development of rats resulting from perinatal BPA

exposure contribute to insulin resistance in adulthood. *Diabetologia.* 2013;56(9):2059-2067.
47. Jiang Y, Xia W, Yang J, Zhu Y, Chang H, Liu J, Huo W, Xu B, Chen X, Li Y, Xu S. BPA-induced DNA hypermethylation of the master mitochondrial gene PGC-1α contributes to cardiomyopathy in male rats. *Toxicology*. 2015;329:21-31.
48. Cui M, Wen Z, Yang Z, Chen J, Wang F. Estrogen regulates DNA methyltransferase 3B expression in Ishikawa endometrial adenocarcinoma cells. *Mol Biol Rep*.2009;36(8):2201-2207.
49. Shi JF, Li XJ, Si XX, Li AD, Ding HJ, Han X, Sun YJ. ERα positively regulated DNMT1 expression by binding to the gene promoter region in human breast cancer MCF-7 cells. *Biochem Biophys Res Commun*.2012;427(1)47-53.
50. Pollock T, deCatanzaro D. Presence and bioavailability of bisphenol A in the uterus of rats and mice following single and repeated dietary administration at low doses. *Reprod Toxicol*. 2014;49:145-154.
51. Papaconstantinou AD, Fisher BR, Umbreit TH, Brown KM. Increases in mouse uterine heat shock protein levels are a sensitive and specific response to uterotrophic agents. *Environ Health Perspect*. 2002;110(12):1207-1212.
52. Markey CM, Michaelson CL, Veson EC, Sonnenschein C, Soto AM. The mouse uterotrophic assay: a reevaluation of its validity in assessing the estrogenicity of bisphenol A. *Environ Health Perspect*.2001;109(1):55-60.
53. Markey CM, Wadia PR, Rubin BS, Sonnenschein C, Soto AM. Long-term effects of fetal exposure to low doses of the xenoestrogen bisphenol-A in the female mouse genital tract. *Biol Reprod.* 2005;72(6):1344-1351.
54. Newbold RR, Jefferson WN, Padilla-Banks E. Long-term adverse effects of neonatal exposure to bisphenol A on the murine female reproductive tract. *Reprod Toxicol*.2007;24:253–8.
55. Vigezzi L, Bosquiazzo VL, Kass L, Ramos JG, Munoz-de-Toro M, Luque EH. Developmental exposure to bisphenol A alters the differentiation and functional response of the adult rat uterus to estrogen treatment. *Reprod Toxicol*. 2015;52:83-92.
56. Papaconstantinou AD, Umbreit TH, Fisher BR, Goering PL, Lappas NT, Brown KM. Bisphenol-A-induced increase in uterine weight and alterations in uterine morphology in ovariectomized B6C3F1 mice: role of estrogen receptor. *Toxicol Sci*.2000;56(2):332-339.
57. Hiroi H, Tsutsumi O, Takeuchi T, Momoeda M, Ikezuki Y, Okamura A, Yokota H, Taketani Y. Differences in serum bisphenol a concentrations in premenopausal normal women and women with endometrial hyperplasia. *Endocr J.* 2004;51(6):595-600.
58. Lagarde F, Beausoleil C, Belcher SM, Belzunces LP, Emond C, Guerbet M, Rousselle C. Non-monotonic dose-response relationships and endocrine disruptors: a qualitative method of assessment. *Environ Health*. 2015;14:13.
59. Ornitz DM, Itoh N. The fibroblast growth factor signaling pathway. *Wiley Interdiscip Rev Dev Biol.* 2015;4(3):215-266.
60. Wesche J, Haglund K, Haugsten EM. Fibroblast growth factors and their receptors in cancer. *Biochem J*. 2011;437(2):199-213.
61. Pollock PM, Gartside MG, Dejeza LC, Powell MA, Mallon MA, Davies H, Mohammadi M, Futreal PA, Stratton MR, Trent JM, Goodfellow PJ. Frequent activating FGFR2

mutations in endometrial carcinomas parallel germline mutations associated with craniosynostosis and skeletal dysplasia syndromes. *Oncogene*. 2007;25(50):7158-7162.
62. Dutt A, Salvesen HB, Chen TH, Ramos AH, Onofrio RC, Hatton C, Nicoletti R, Winckler W, Grewal R, Hanna M, Wyhs N, Ziaugra L, Richter DJ, Trovik J, Engelsen IB, Stefansson IM, Fennell T, Cibulskis K, Zody MC, Akslen LA, Gabriel S, Wong KK, Sellers WR, Meyerson M, Greulich H. Drug-sensitive FGFR2 mutations in endometrial carcinoma. *Proc Natl Acad Sci U S A.* 2008;105(25):8713-8717.
63. Lee PS, Secord AA. Targeting molecular pathways in endometrial cancer: a focus on the FGFR pathway. *Cancer Treat Rev*. 2014;40(4):507-512.
64. Hecht D, Zimmerman N, Bedford M, Avivi A, Yayon A. Identification of fibroblast growth factor 9 (FGF9) as a high affinity, heparin dependent ligand for FGF receptors 3 and 2 but not for FGF receptors 1 and 4. *Growth Factors*. 1995;12(3):223-233.
65. Wilson AS, Power BE, Molloy PL. DNA hypomethylation and human diseases. *Biochim Biophys Acta.* 2007;1775(1):138-162.
66. Sproul D, Meehan RR. Genomic insights into cancer-associated aberrant CpG island hypermethylation. *Brief Funct Genomics*. 2013;12(3):174-190.
67. Lopez-Serra L, Ballestar E, Fraga MF, Alaminos M, Setien F, Esteller M. A Profile of Methyl-CpG Binding Domain Protein Occupancy of Hypermethylated Promoter CpG Islands of Tumor Suppressor Genes in Human Cancer. *Cancer Res*. 2006;66(17):8342-8346.
68. Carter JA, Górecki DC, Mein CA, Ljungberg B, Hafizi S. CpG dinucleotide-specific hypermethylation of the TNS3 gene promoter in human renal cell carcinoma. *Epigenetics*. 2013;8(7):739-747.
69. Yang WT, Zheng PS. Promoter hypermethylation of KLF4 inactivates its tumor suppressor function in cervical carcinogenesis. *PLoS One*. 2014;9(2):e88827.
70. Zhang HQ, Zhang XF, Zhang LJ, Chao HH, Pan B, Feng YM, Li L, Sun XF, Shen W. Fetal exposure to bisphenol A affects the primordial follicle formation by inhibiting the meiotic progression of oocytes. *Mol Biol Rep*. 2012;39(5):5651-5657.
71. Jones A, Teschendorff AE, Li Q, Hayward JD, Kannan A, Mould T, West J, Zikan M, Cibula D, Fiegl H, Lee SH, Wik E, Hadwin R, Arora R, Lemech C, Turunen H, Pakarinen P, Jacobs IJ, Salvesen HB, Bagchi MK, Bagchi IC, Widschwendter M. Role of DNA methylation and epigenetic silencing of HAND2 in endometrial cancer development.*Plos Med.*2013;10(11):e1001551.doi:10.1371/journal.

CHAPTER 3: Insulin Signaling via Progesterone-dependent Insulin Receptor Substrate 2 is Critical for Human Endometrial Stromal Cell Decidualization

ABSTRACT

Decidualization, the process by which fibroblastic endometrial stromal cells proliferate and subsequently differentiate into secretory decidual cells, is a critical event during the establishment of pregnancy. It is dependent on the steroid hormone progesterone acting through the nuclear progesterone receptor (PR). Previously, we identified insulin receptor substrate 2 (IRS2) as a factor that is directly regulated by PR during decidualization. IRS2 is an adapter protein that functionally links receptor tyrosine kinases, such as insulin receptor (IR) and insulin-like growth factor 1 (IGF1) receptor (IGF1R), and their downstream effectors. During in vitro decidualization, IRS2 expression was induced within 24 hours of stimulation with estrogen, progesterone, and cAMP. siRNA-mediated down-regulation of *IRS2* transcripts in HESC resulted in attenuation of decidualization, indicating a critical role for IRS2 during this process. Further use of siRNAs targeted to *IR* or *IGF1R* transcripts showed that down-regulation of IR, but not IGF1R, led to impaired decidualization. siRNA-mediated knockdown of *IRS2* transcripts in HESC suppressed phosphorylation of both ERK1/2 and AKT, downstream effectors of insulin signaling, which mediate gene expression associated with decidualization and regulate glucose uptake. Indeed, loss of IRS2 resulted in reduced expression and membrane localization of glucose transporters GLUT1 and GLUT4, resulting in lowered glucose uptake during stromal decidualization. Collectively, these data suggest that the PR-regulated expression of IRS2 is necessary for proper insulin signaling controlling gene expression and glucose metabolism, which critically support the decidualization process to facilitate pregnancy. This study provides new insight into the mechanisms by which steroid hormone signaling intersects with insulin

signaling in the uterus during decidualization, which has important implications for pregnancy complications associated with insulin resistance and infertility.

INTRODUCTION

Infertility is a common issue faced by couples trying to conceive, and therefore it is critical to understand the events occurring during early pregnancy to help improve assisted reproductive technology. In women, the uterus prepares for pregnancy with each menstrual cycle. During the proliferative phase of the menstrual cycle, estrogen (E) produced by the ovaries drives proliferation of the endometrium. During the secretory phase, rising levels of progesterone (P) produced from the corpus luteum promote differentiation of the stromal cells, a process called decidualization. In humans, decidualization is critical to facilitate embryo implantation in the event of pregnancy, and impaired decidualization can lead to pregnancy loss.

During decidualization, under the direction of E and P, stromal cells undergo a transformation from spindle shaped fibroblasts to enlarged epithelioid-like decidual cells. Decidual cells produce and secrete factors to modulate the activities of uterine vascular endothelial cells, epithelial cells, and immune cells to help protect and nurture the embryo during early pregnancy (1, 2). Several rodent models have demonstrated that impaired decidualization often correlates with subfertility or infertility (3). Because this process is necessary for successful pregnancy, it is critical to understand what uterine factors are involved in driving decidualization.

Progesterone signaling though the progesterone receptor (PR) is essential for decidualization (4). PR is a member of the nuclear receptor superfamily of transcription factors and regulates gene expression upon hormone binding. To better understand the role of PR signaling in the uterus, our lab and another have performed ChIP-Seq to identify regions in the

human genome bound by PR during decidualization of primary human endometrial stromal cells (HESC) (5). These studies both identified insulin receptor substrate 2 (IRS2) as a direct target of PR during HESC decidualization. *IRS2* expression is induced in response to progesterone and can be reduced by siRNA-mediated knockdown of endogenous *PR* (5). The purpose of this study is to further elucidate the role of IRS2 during decidualization.

IRS2 is part of a family of large docking proteins called insulin receptor substrates (IRS) and serves as a cytoplasmic signaling molecule that mediates the downstream signaling of insulin and IGF1 receptor tyrosine kinases (RTK) (6). Phosphorylation of IRS2 by these RTKs activates two main pathways: the MAPK cascade to regulate transcriptional activity and the PI3K/AKT pathway to regulate glucose influx, glycogen synthesis, and transcriptional activity (7). Mice lacking IRS2 through global deletion of the *Irs2* gene exhibit peripheral insulin resistance and β-cell deficiency, culminating in a diabetic phenotype (8). *Irs2* null mice also showed reduced circulating steroid hormones and gonadotropins, ovarian defects, and severely reduced fertility, indicating an important role for IRS2 in reproductive function (9).

Based on insights gained from the rodent model, it is likely that IRS2 plays a critical role during human pregnancy as well, although little is known about the function of IRS2 in the uterus. Because the *Irs2*-null mouse exhibits symptoms of type 2 diabetes, we hypothesize that the PR target IRS2 facilitates decidualization by mediating local insulin signaling to promote glucose uptake to meet the increasing energy demands of the decidual cell. We found that loss of IRS2 impairs decidualization of HESC, decreases expression of glucose transporters, and reduces glucose uptake during in vitro decidualization. Our results offer insight into insulin receptor/IRS2 signaling in the uterus and implicate dysregulation of IRS2 as a contributing factor to early pregnancy loss.

MATERIALS AND METHODS

Primary human endometrial stromal cell culture

Endometrial samples from the early proliferative stage of the menstrual cycle were obtained by pipelle biopsy at Emory University and Wake Forest Medical Centers from fertile, regularly cycling women under anesthesia before laparoscopy as described previously (10). Donors displayed no signs of endometrial pathological conditions and provided written informed consent. The subjects ranged in age from 28 to 42 years and in parity from 1 to 2. Primary human endometrial stromal cell cultures (HESC) were isolated from the samples as described previously (10). HESC were cultured in DMEM/F-12 medium (Gibco) supplemented with 5% (v/v) fetal bovine serum (Atlanta Biologicals), 50 μg/mL penicillin, and 50 μg/mL streptomycin (Invitrogen). For in vitro decidualization, the cells were treated with a decidualization cocktail (DC) composed of 0.5 mM 8-bromo-adenosine-3′,5′-cyclic monophosphate (8-Br-cAMP) (Sigma-Aldrich), 1 μM progesterone (Sigma-Aldrich), and 10 nM 17β-estradiol (Sigma-Aldrich) in DMEM/F-12 medium (Invitrogen) supplemented with 2% (v/v) charcoal dextran–stripped fetal bovine serum (Atlanta Biologicals). In certain experiments, cells were pre-treated for 1 hour with 100nM MK2206 (ApexBio), 10μM U0126 (Promega), or 5μM rosiglitazone (Cayman Chemicals) before being co-treated with the respective compound and DC. The medium/decidualization cocktail/indicated compound was refreshed every 48 hours.

siRNA mediated knockdown

HESC were transfected with siRNA targeting *IRS2*, *IR,* or *IGF1R* transcripts (Dharmacon) or control scrambled siRNA (Dharmacon) following the manufacturer's protocol (Transfectin; Bio-Rad Laboratories). In brief, a final concentration of 50 nM siRNA was mixed with Transfectin lipid reagent to transfect the cells. Cells were incubated with siRNA for 24

hours and then the media was replaced with DC to induce decidualization. Cells were stimulated with DC for 24-72h with media refreshed every 48h.

RNA isolation and real time PCR analysis

Total RNA was extracted from cultured HESC using TRIzol (Invitrogen) according to the manufacturer's instructions. Total RNA was converted to cDNA using the AffinityScript Multiple Temperature Reverse Transcriptase kit (Agilent), following the manufacturer's instructions. cDNA was subjected to quantitative PCR analysis using Power Sybr Green PCR master mix (Applied Biosystems) and gene-specific primers (IDT Integrated DNA Technologies). *36B4* was used as the reference gene. For a given sample, threshold cycle (C_t) and SD were calculated as an average of individual C_t values from 3 replicates. The normalized mean C_t (ΔC_t) was calculated by subtracting the mean C_t of the reference gene *36B4* from the mean C_t of a target gene. The $\Delta\Delta C_t$ was then calculated for each gene as a difference in ΔC_t values between the control and the experimental sample. Fold change in gene expression was then computed as $2^{-\Delta\Delta C_t}$. The mean fold induction and SEM were calculated from 3-5 independent experiments.

Western blot analysis

Primary HESC were subjected to different treatments conditions as described in the figure legends. Whole-cell extracts were prepared using RIPA lysis buffer containing Complete Protease Inhibitor Cocktail (Roche) and HALT Phosphatase Inhibitor Cocktail (Thermo Fisher). Membrane associated proteins were isolated using Mem-PER Plus Membrane Protein Extraction kit (Pierce) per manufacturer's instruction. Equal amounts of proteins were analyzed by SDS-PAGE and transferred to polyvinylidene difluoride membrane (Amersham) and the specific proteins were detected by Western blotting using antibodies against IRS2 (Abcam), calnexin

(Santa Cruz; RRID:AB_2243890) (11), IGFBP1 (Santa Cruz; RRID:AB_2123081) (12), BMP2 (Proteintech; RRID:AB_10641999) (13), WNT4 (Proteintech; RRID:AB_2215428) (14), HAND2 (Millipore), AKT (Santa Cruz; RRID:AB_671714) (15), phosphorylated AKT (Santa Cruz; RRID:AB_2225021) (16), ERK1/2 (Santa Cruz; RRID:AB_2650548) (17), phosphorylated ERK1/2 (Santa Cruz; RRID:AB_2141287) (18), GLUT1 (Abcam; RRID:AB_10903230) (19), GLUT4 (EMD Millipore; RRID:AB_1587080) (20), Integrin β3 (Santa Cruz; RRID:AB_647490) (21), HSP90 (Santa Cruz; RRID:AB_2121235) (22). Membranes were incubated overnight at 4°C with primary antibodies diluted in 5% milk buffer. Next day, membranes were washed with PBST and incubated for 1h at room temperature with an appropriate IgG HRP-linked secondary antibody (Cell Signaling Technology; RRID:AB_330924; RRID:AB_2099233) (23, 24) diluted in 5% milk buffer. Membranes were washed, incubated with SuperSignal® West Femto Maximum Sensitivity Substrate (Pierce), and imaged using the iBright chemiluminescent imaging system (Thermo Fisher Scientific). Image J software (NIH) was used to perform densitometry analysis.

Immunocytochemistry

HESC were plated in chamber slides (Cell Treat) and treated as indicated in the figure legend. Cells were fixed with 3.7% formaldehyde and permeabilized with 0.1-0.25% Trixton-X (Sigma-Aldrich) in PBS. Following blocking with 5% normal donkey serum (Jackson Laboratories) and 1% BSA (Jackson Laboratories) in PBS, cells were incubated at 4°C overnight with primary antibodies targeting Ki67 (BD Pharmingen; RRID:AB_393778) (25), phosphorylated AKT (16), and phosphorylated ERK1/2 (18). Next day, cells were washed with PBS and then incubated with the appropriate Cy3 conjugated secondary antibody (Jackson Laboratories; AB_2315777; RRID:AB_2307443) (26, 27). For some experiments, F-actin

filaments were stained using Alexa Fluor 488 Phalloidin (Thermo Fisher; RRID:AB_2315147) (28). Cells were mounted with Prolong GOLD mounting medium (Promega) containing 4′,6-diamidino-2-phenylindole nuclear counterstain. Imaging was performed using an Olympus BX51 microscope fitted with an Olympus DP71 camera (Olympus). ImageJ software was used to perform post-imaging analysis.

Glucose uptake assay

HESC were subjected to siRNA knockdown, as indicated above. These cells were stimulated for 72h with DC, with media replacement every 48h. Cells were then washed 3 times with PBS and incubated in fresh glucose free DMEM supplemented with 2% CD-FBS containing 50μM of a fluorescently labeled glucose analog 2-NBDG (Cayman Chemicals) and DC for 1h. Cells were then washed 3 times with PBS. 2-NBDG uptake was detected with fluorescent filters designed to detect fluorescein (excitation/emission = 485/535 nm). Cells were then lysed and protein concentration was measured by BCA assay (Pierce). 2-NBDG uptake was normalized to total protein.

Statistical analysis

Statistical analysis was performed using 3-5 independent samples. Statistical significance was determined using the Students *t* test. Asterisks denotes significance with a *P* value of <0.05.

RESULTS

Insulin receptor substrate 2 is required for human stromal cell decidualization

Previously, we showed that IRS2 is a direct target of PR during stromal cell decidualization (5). To establish the pattern of IRS2 expression, HESC were treated with

decidualization cocktail (E+P+cAMP; DC). IRS2 expression was induced within 24 hours of treatment with DC both at the mRNA and protein level and remained elevated through the 6-day treatment period [Fig. 3.1(a-b)]. To determine the role of IRS2 during decidualization, we performed siRNA mediated knockdown as indicated in the materials and methods, followed by 72h stimulation with DC. Using this knockdown strategy, we observed approximately 80% reduction of *IRS2* (siIRS2) at the mRNA level and reduced levels of IRS2 protein to an undetectable concentration, relative to a scrambled siRNA control (siCtrl) [Fig. 3.1(c-d)]. We next looked at expression of factors that are induced during decidualization. Loss of IRS2 led to significantly reduced expression of decidualization markers *IGFBP1, BMP2, WNT4,* and *HAND2* in HESC following 72 hours of stimulation with DC [Fig. 3.2(a)]. *PRL* expression was not significantly altered from control with IRS2 knockdown. Moreover, we observed reduced protein expression of IGFBP1, BMP2, WNT4, and HAND2 in whole cell lysates with loss of IRS2 compared to control cells, as indicated by western blot [Fig. 3.2(b)].

Successful stromal decidualization results in changes in cell morphology, shifting from a spindly fibroblast cell to a rounded decidual cell. We examined the impact of IRS2 knockdown on cell morphology by immunocytochemistry, using phalloidin and DAPI to stain actin filaments and nuclei, respectively. Upon stimulation with DC, control cells underwent transformation to rounded decidual cells, while cells lacking IRS2 retained much of their fibroblastic shape, indicating that decidualization was impaired [Fig. 3.2(c)].

Another key characteristic of in vitro decidualization is the cessation of stromal proliferation with the introduction of cAMP, a key component of our DC treatment. Following siRNA knockdown, we treated cells with either E and P or the DC containing cAMP for 24 hours. Proliferation was assessed using an antibody targeting Ki67, a proliferative marker, and

Ki67 positive cells were quantified by ImageJ analysis. No difference in proliferation was detected between the siCtrl and siIRS2 cells in either the proliferative (E and P) or decidualization (DC) culture conditions [Fig. 3.2(d)], suggesting that IRS2 does not play a critical role in regulating HESC proliferation. Taken together, these data demonstrate that loss of IRS2 attenuates the gene expression and morphological changes associated with decidualization. These results establish IRS2 as a critical mediator of progesterone action during endometrial stromal cell decidualization.

IRS2 acts downstream of the insulin receptor to regulate decidualization

In various cell types, IRS2 is reported to act as an adaptor molecule for both the insulin receptor (IR) and IGF1 receptor (IGF1R). Expression of both of these tyrosine kinase receptors was induced in HESC in response to DC [Fig. 3.3(a)]. To elucidate the role of IGF1R/IRS2 and IR/IRS2 signaling during decidualization, we performed siRNA mediated knockdown using siRNA targeting *IGF1R* or *IR* transcripts. Loss of IGF1R did not affect the expression of decidualization markers *IGFBP1, BMP2, WNT4, HAND2,* or *PRL* [Fig. 3.3(b)]. siRNA mediated loss of IR, however, significantly reduced expression of *IGFBP1, BMP2, WNT4,* and *HAND2,* but not *PRL* [Fig. 3.3(c)]. This pattern of gene expression is similar to that observed with knockdown of IRS2 [Fig. 3.2(a)].

The culture conditions used in our in vitro decidualization experiments contain 0.04 ng/ml of insulin, so we next wanted to see if increasing IR activation through increased concentrations of the ligand in the culture medium can enhance decidualization. At 0.1 ng/ml, the lowest concentration of insulin utilized, *IGFBP1* expression was increased compared to DC alone [Fig. 3.3(d)]. At higher concentrations, we observed reduced expression of *IGFBP1* and *WNT4* compared to DC alone. Interestingly, we also saw reduced expression of *IR* itself,

suggesting that excess ligand caused downregulation of the receptor and had similar effects on gene expression as those observed with siRNA mediated knockdown of *IR*. We next treated cells with rosiglitazone, an anti-diabetic drug that enhances peripheral insulin sensitivity and glucose uptake. Addition of rosiglitazone to the culture media significantly increased expression of decidualization markers *WNT4*, *BMP2*, and *IGFPB1* compared to DC alone [Fig. 3.3(e)]. Rosiglitazone also enhanced the DC stimulated expression of *IRS2*. Together, these data suggest that IRS2 acts as part of the IR signaling pathway during stromal decidualization and that this pathway is sensitive to hyperinsulinemia.

Loss of IRS2 reduces PI3K/AKT and MAPK activation in HESC during decidualization

IR activation in insulin target tissues such as liver, muscle, and fat leads to recruitment and phosphorylation of IRS2, which in turn mediates the downstream activation of MAPK and/or PI3K/AKT to mediate changes in gene expression and regulate glucose transport into the cell (6). Loss of IRS2 in HESC stimulated for 24 hours with DC reduced the phosphorylation of both AKT and ERK1/2, as determined by western blot [Fig. 3.4(a)] and immunofluorescence [Fig. 3.4(b)]. To determine if PI3K/AKT and/or MAPK activation are required for decidualization, we used pharmacological inhibitors MK2206 and U0126 to inhibit AKT and ERK1/2 phosphorylation, respectively. Similar to what we observed with either IR or IRS2 knockdown, co-treatment with DC and either MK2206 or U0126 had no effect on *PRL* expression [Fig. 3.4(c)]. However, *IGFBP1* and *WNT4* expression were both reduced in response to either MK2206 or U0126. Together, these data suggest that both MAPK and PI3K/AKT mediate the downstream effects of IRS2 activation to control stromal decidualization.

IRS2 regulates GLUT transporter expression and localization during HESC decidualization

Because IR/IRS2 signaling is important for glucose uptake and utilization, we wanted to explore how these functions are altered with loss of IRS2 during decidualization. We first looked at the RNA and protein expression pattern of glucose transporters in HESC stimulated with DC. GLUT1 mRNA [Fig. 3.5(a)] and protein [Fig. 3.5(b)] expression increased within 24 hours of DC stimulation and remained elevated throughout the treatment period. GLUT4 mRNA [Fig. 3.5(a)] and protein [Fig. 3.5(b)] expression was also modestly increased in response to DC. This indicates that glucose transporters are induced during decidualization and likely facilitate glucose transport into the cell to meet the energy demands of decidualization.

To examine how IRS2 affects GLUT expression, we performed siRNA mediated knockdown of *IRS2* and stimulated the cells with DC. Both GLUT1 and GLUT4 mRNA and protein levels were decreased with loss of IRS2 compared to control cells, as indicated by gene expression analysis [Fig. 3.5(c)] and western blot using whole cell lysates [Fig. 3.5(d)], respectively. To observe how GLUT localization is influenced by IRS2, we isolated membrane and cytoplasmic protein fractions and measured expression by western blot. With loss of IRS2, we observed reduced expression of GLUT1 in the cytoplasmic fraction [Fig. 3.6(a)]. Interestingly, we also saw reduced expression of GLUT1 and GLUT4 in the membrane protein fraction [Fig. 3.6(a)]. Similar observations were made using immunofluorescence. Following knockdown and treatment with DC, we stained cells with either GLUT1 or GLUT4 (red) and used phalloidin to stain F-actin filaments to visualize the outer boundaries of the cells (green). We observed membrane expression of GLUT1 and GLUT4 in our control cells following stimulation with DC [Fig. 3.6(b)], as indicated by the yellow color representing overlap between

the respective GLUT and F-actin; this was less apparent with loss of IRS2. Taken together, these data demonstrate that IRS2 is necessary for proper GLUT expression and membrane localization during decidualization.

Signaling via IRS2 controls glucose uptake during HESC decidualization

Since glucose movement into the cell is controlled by glucose transporters, we next investigated changes in glucose uptake with loss of IRS2. Following knockdown, cells were treated for 72 hours with DC and then exposed to the fluorescently labeled glucose analogue 2-NBDG, as described in the materials and methods. We found that siIRS2 cells exhibited reduced 2-NBDG uptake compared to siCtrl cells, suggesting that glucose uptake is impaired with loss of IRS2 [Fig. 3.7(a)]. To better understand the effects of glucose availability on decidualization, we stimulated HESCs with DC in the presence of reduced concentrations of glucose in the media. We observed a decreased expression of *IGFBP1* and *WNT4* with reduced glucose concentrations compared to our normal treatment media [Fig. 3.7(b)], suggesting that reduced glucose availability impairs decidualization.

Collectively, these data suggest that insulin signaling via IRS2 plays a critical role in decidualization by regulating GLUT transporter expression and membrane localization to promote glucose uptake by endometrial stromal cells to meet the energy demands of the decidualization process.

DISCUSSION

Little is known about the function of insulin signaling in the uterus. The aim of this study was to better understand how IRS2, a mediator of insulin signaling, impacts decidualization, the process of endometrial stromal differentiation that is required for maintenance of pregnancy.

Previously, we identified *IRS2* as a direct target of PR signaling in primary HESC and showed PR occupancy at two regions (-88kb and -307Kb) upstream of the *IRS2* transcription start site in HESC during decidualization (5). Indeed, we see that IRS2 is induced in HESC with the introduction of a decidualization cocktail containing estrogen, progesterone, and cAMP (DC) [Fig. 3.1(a-b)]. Stromal cells undergo several changes during their transformation to decidual cells, including cessation of proliferation, changes in gene expression (including induction of decidual markers IGFPB1, PRL, and WNT4), and a morphological shift from a fibroblastic cell type to an epithelioid cell type. We found that loss of IRS2 via siRNA mediated knockdown blunted the expression of decidual markers [Fig. 3.2(a-b)] and led to retention of a fibroblastic cell shape characteristic of undifferentiated HESC [Fig. 3.2(c)], indicating that IRS2 function is essential for decidualization.

IRS2 functions as an adaptor molecule bridging receptor tyrosine kinases like insulin receptor (IR) to downstream signaling proteins. In the uterus, IR expression has been detected in the stroma of human endometrial tissue biopsies taken in the secretory phase of the menstrual cycle and stromal cells decidualized in vitro, although its role is unclear (29, 30, 31). Findings from previous in vitro studies are somewhat contradictory as to whether insulin signaling promotes or impairs decidualization (32, 32, 34). Our present study establishes a clear requirement for IR expression in stromal decidualization [Fig. 3.3(c)]. Consistent with this finding, stimulation of HESC with increasing concentrations of insulin, which resulted in reduced *IR* expression, impaired decidualization [Fig. 3.3(d)]. IR downregulation in response to hyperinsulinemic conditions has been demonstrated both in vitro and in vivo and is a contributing factor of insulin resistance (6). Moreover, epidemiological studies suggest a link between insulin resistance and an increased risk of spontaneous miscarriage and recurrent

pregnancy loss (35, 36). In light of these observations, it appears that insulin signaling is tightly regulated in the uterus, and its dysregulation during early pregnancy may be a contributing factor towards infertility in women presenting with peripheral insulin resistance.

Signaling through IR/IRS2 leads to downstream activation of PI3K/AKT and MAPK pathways to regulate glucose influx, glycogen synthesis, and gene expression to control cell growth, proliferation, and differentiation in target tissues (6). In the present study, loss of IRS2 during decidualization led to reduced MAPK and PI3K/AKT activation [Fig. 3.4(a-b)]. Our studies using pharmacological inhibition of ERK activation confirms earlier observations indicating a role for MAPK signaling in mediating decidualization [Fig. 3.4(c)] (37). The role of PI3K/AKT activity during decidualization is less clear. Immunohistochemical analysis of human tissue samples indicated that phosphorylated AKT in the stroma is low in the proliferative and early secretory phase of the uterine cycle, but increases in late secretory phase and in decidual tissues (38). Other groups have demonstrated that AKT phosphorylation decreases during in vitro stromal decidualization (39, 40). Reduced PI3K/AKT activity is necessary for increased nuclear accumulation and transcriptional activity of FOXO1, which can regulate gene expression of decidual markers (41). However, AKT also plays a critical role in glucose metabolism through its regulation and localization of glucose transporters as well as increasing glycogen synthesis through inhibition of glycogen synthase kinase (42). Increased glucose uptake and formation of intracellular glycogen stores occur during decidualization, suggesting that some level of AKT activation is required to mediate these functions. Our studies indicated that phosphorylation-dependent AKT activation is impaired in the absence of IRS2 function, leading to inhibition of at least certain of the decidualization-associated factors, such as WNT4 [Fig. 3.4(a-c)]. In light of these observations, AKT activity during decidualization is more nuanced and may involve a fine

balance in phosphorylation/activation to support both its downstream transcriptional and metabolic effects.

One of the major functions of insulin signaling is to promote movement of glucose from the blood into the cell through integral membrane transporters called glucose transporters (GLUT). The facilitative GLUT transporter family is comprised of 14 GLUT protein family members with varying kinetics, regulatory properties, and tissue expression patterns (43). The presence of several GLUT family members was reported in the endometrium, but the most abundant is GLUT1 (44). GLUT1 is robustly expressed in the stroma during the secretory phase of the uterine cycle and in the decidua (31, 46). We observed an increased stromal GLUT1 expression induced by progesterone, estrogen, and cAMP, which reflects its pattern of expression during the secretory phase [Fig. 3.5(a-b)]. Reduced stromal expression of GLUT1 has been observed in women suffering from idiopathic infertility compared to those whose infertility is independent of endometrial function, such as tubal occlusion or male infertility (45). Our study finds that IRS2 is necessary for GLUT1 expression during decidualization [Fig. 3.5(c-d)]. While the insertion of GLUT1 into the cell membrane is not considered to be an insulin dependent process, insulin, as well as MAPK and PI3K/AKT activity, have been shown to stimulate GLUT1 expression in muscle, liver, fat, and mesangial cells (46, 47, 48, 49, 50). Disruption of IR signaling through loss of IRS2 impairs GLUT1 production and decreases the reserve of GLUT1 transporters, leading to its decreased presence at the membrane [Fig. 3.6(a-b)].

In contrast to GLUT1, less is known about uterine GLUT4. Tissue analysis studies report GLUT4 is weakly expressed in uterine stromal cells (51). GLUT4 is considered insulin dependent in that insulin stimulates GLUT4 insertion at the cell membrane. Consistent with this, loss of IRS2 reduced the accumulation of GLUT4 in the cell membrane [Fig. 3.6(a-b)]. Although

its expression during decidualization is less robust than that of GLUT1, perturbations in the temporal distribution of GLUT4 likely contribute to the overall reduction of glucose uptake observed with loss of IRS2.

The increase in stromal GLUT expression suggests a functional relevance of increased glucose usage during decidualization. Indeed, previous reports indicated that glucose uptake is increased in endometrial stromal cells undergoing in vitro decidualization (33, 44). As shown in Fig. 3.7(b), culturing HESC in reduced glucose impaired decidualization. IRS2 clearly supports increased glucose flux into HESC [Fig. 3.7(a)], although other signaling mediators are likely to be involved. Once in the stromal cell, glucose is shuttled through several metabolic pathways, including glycolysis to provide energy in the form of ATP and the pentose phosphate pathway to aid in cholesterol, fatty acid, and nucleotide synthesis (52, 53). Future work is needed to establish how IRS2 acts in concert with other insulin receptor signaling components to impact the shuttling of glucose during decidualization of HESC.

Several endocrine conditions associated with insulin resistance have been linked to pregnancy complications. Polycystic ovarian syndrome (PCOS) is a condition characterized by hyperandrogenism and hyperinsulinemia that can reflect insulin resistance in peripheral tissues. A retrospective study performed among PCOS patients suggests that those with accompanying insulin resistance have an increased risk of miscarriage than patients who do not exhibit insulin resistance (54). Metformin is a common treatment for PCOS and other manifestations of type 2 diabetes to improve insulin sensitivity and alleviate hyperinsulinemia. PCOS patients who continued taking metformin during their pregnancy showed a reduced rate of early pregnancy loss compared to PCOS patients that stopped taking the drug upon determination of pregnancy (55, 56). Gestational diabetes mellitus (GDM), a condition manifesting towards the end of the

second trimester, is also characterized by maternal insulin resistance and insufficient production of insulin to overcome this resistance. Analysis of post-partum placental tissues from women who presented with GDM showed reduced expression of glucose transporters and components of the insulin signal transduction pathway compared to control tissue from healthy pregnant women (57). Interestingly, Ayaz et al., 2014 observed a link between the IRS2 G1057D polymorphism, which has diminished capacity to associate with downstream signaling molecules, and increased risk for developing GDM, suggesting that impaired signaling through IRS2 may contribute to the manifestation of GDM (58, 59).

CONCLUSION

Our study establishes a critical role for the PR target IRS2 in mediating IR signaling during HESC decidualization [Fig. 3.8]. IRS2 acts downstream of the IR and is required for MAPK activation that is critical for decidualization-specific gene expression. IRS2 also controls activation of AKT and expression of glucose transporters, thereby modulating cellular glucose uptake that meets the energy demands of the decidualization process. This study provides insight into the regulation of glucose metabolism in the uterus by the concerted actions of steroid hormone progesterone and insulin and it increases our understanding of the underlying mechanisms of infertility and pregnancy complications associated with insulin resistance.

FIGURES

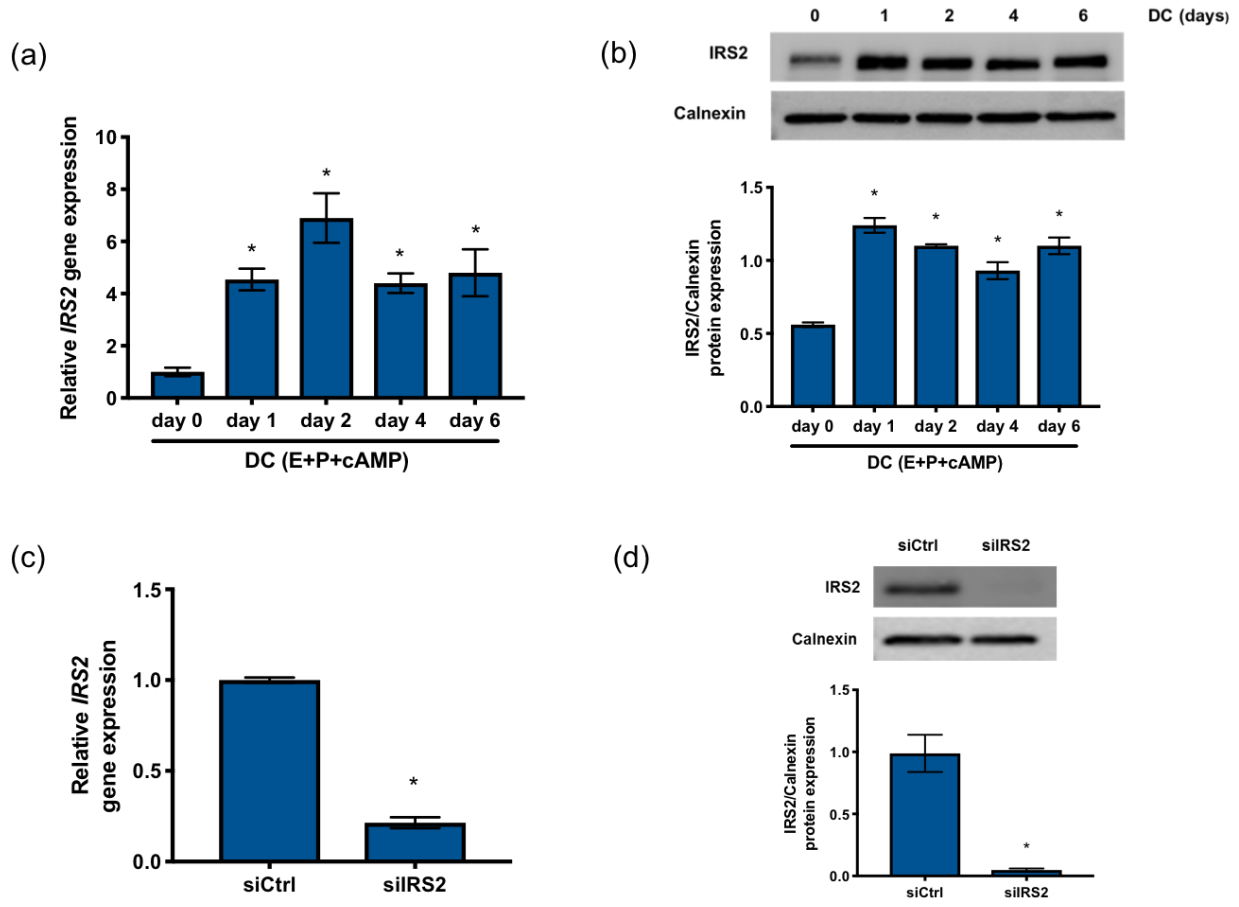

Figure 3.1 IRS2 is expressed in HESC during decidualization
IRS2 mRNA (**a)** and protein (**b**) expression was observed in HESC treated with DC (E+P+cAMP) for 0-6 days. (**a**) Gene expression analysis was performed using primers specific for *IRS2*. *36B4* was used for normalization. Data are represented as the mean fold induction ± SEM. *, P<.05 relative to day 0. (**b**) Whole cell lysates were analyzed by western blot and probed with antibody specific to IRS2. Calnexin is provided as a loading control. Densitometry analysis is provided (below). (**c**) Following siRNA mediated knockdown of *IRS2* and stimulation with DC for 72h, gene expression analysis was performed using primers specific to *IRS2*. *36B4* was used for normalization. Data are represented as the mean fold induction ± SEM. *, P<.05 relative to siCtrl. (**d**) Following knockdown and stimulation with DC for 72h, IRS2 expression was determined by western blot. Calnexin is provided as a loading control. Densitometry analysis is provided (below).

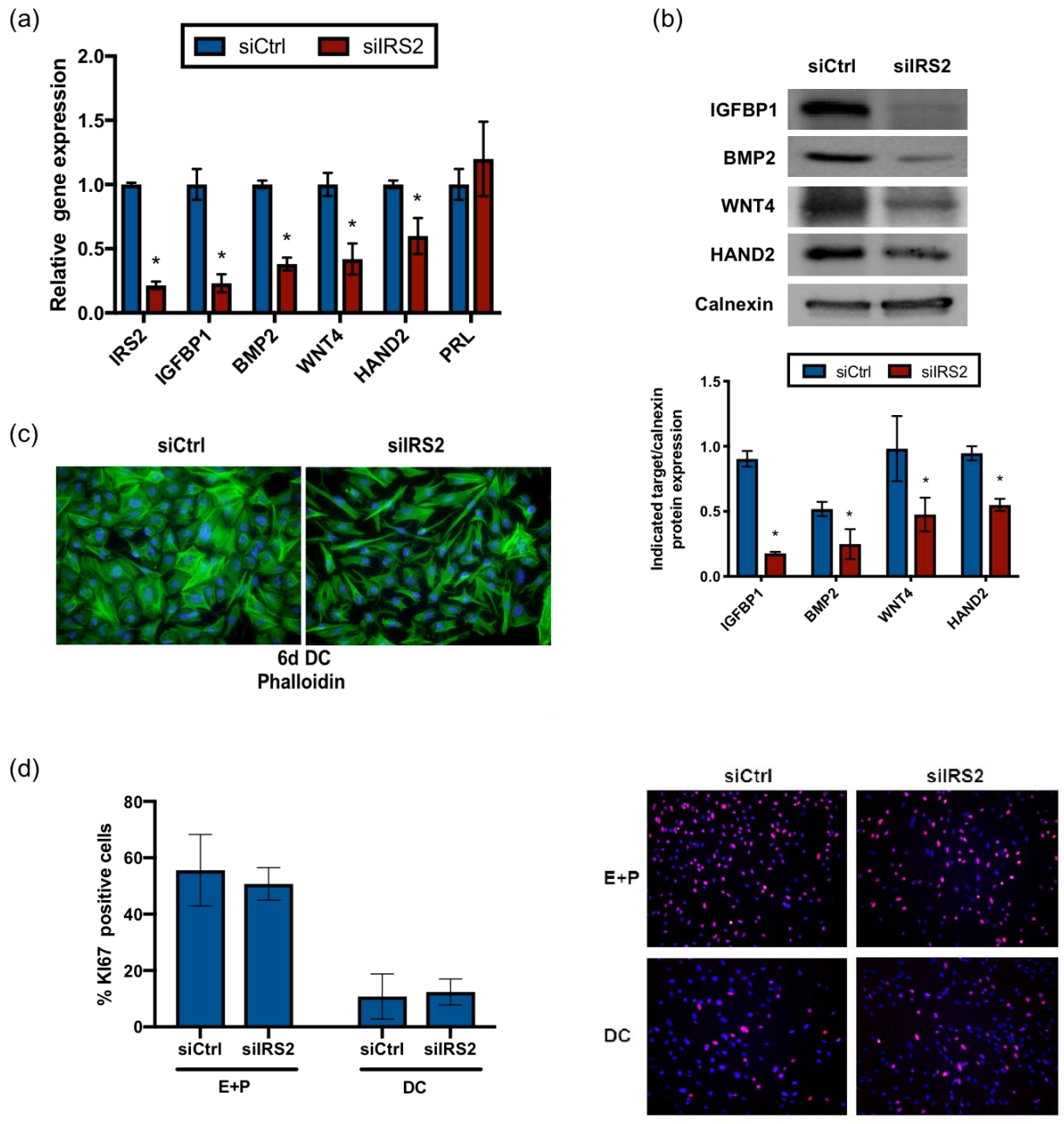

Figure 3.2 IRS2 is required for human stromal cell decidualization
(**a**) Gene expression analysis was performed following IRS2 knockdown and 72h stimulation with DC using primers specific for *IGFBP1*, *BMP2*, *WNT4*, *HAND2*, and *PRL*. *36B4* was used for normalization. Data are represented as the mean fold induction ± SEM. *, P<.05 relative to siCtrl. (**b**) Following knockdown and stimulation with DC for 72h, IGFBP1, BMP2, WNT4, and HAND2 expression was determined by western blot. Calnexin is provided as a loading control. Densitometry analysis is provided (below). (**c**) IRS2 knockdown was performed and cells were stimulated for 6 days with DC and stained with phalloidin to bind actin filaments. DAPI was used as a nuclear stain. Images provided are x40 magnification. (**d**) IRS2 knockdown was performed and cells were exposed for 24h of proliferative (E+P) and differentiating

Figure 3.2 continued: (DC; E+P+cAMP) conditions. Immunofluorescent staining of Ki67 was performed and DAPI was used as a nuclear stain. Ki67 positive cells were counted using ImageJ and expressed as a percentage of total cells. Representative panels are shown; x20 magnification.

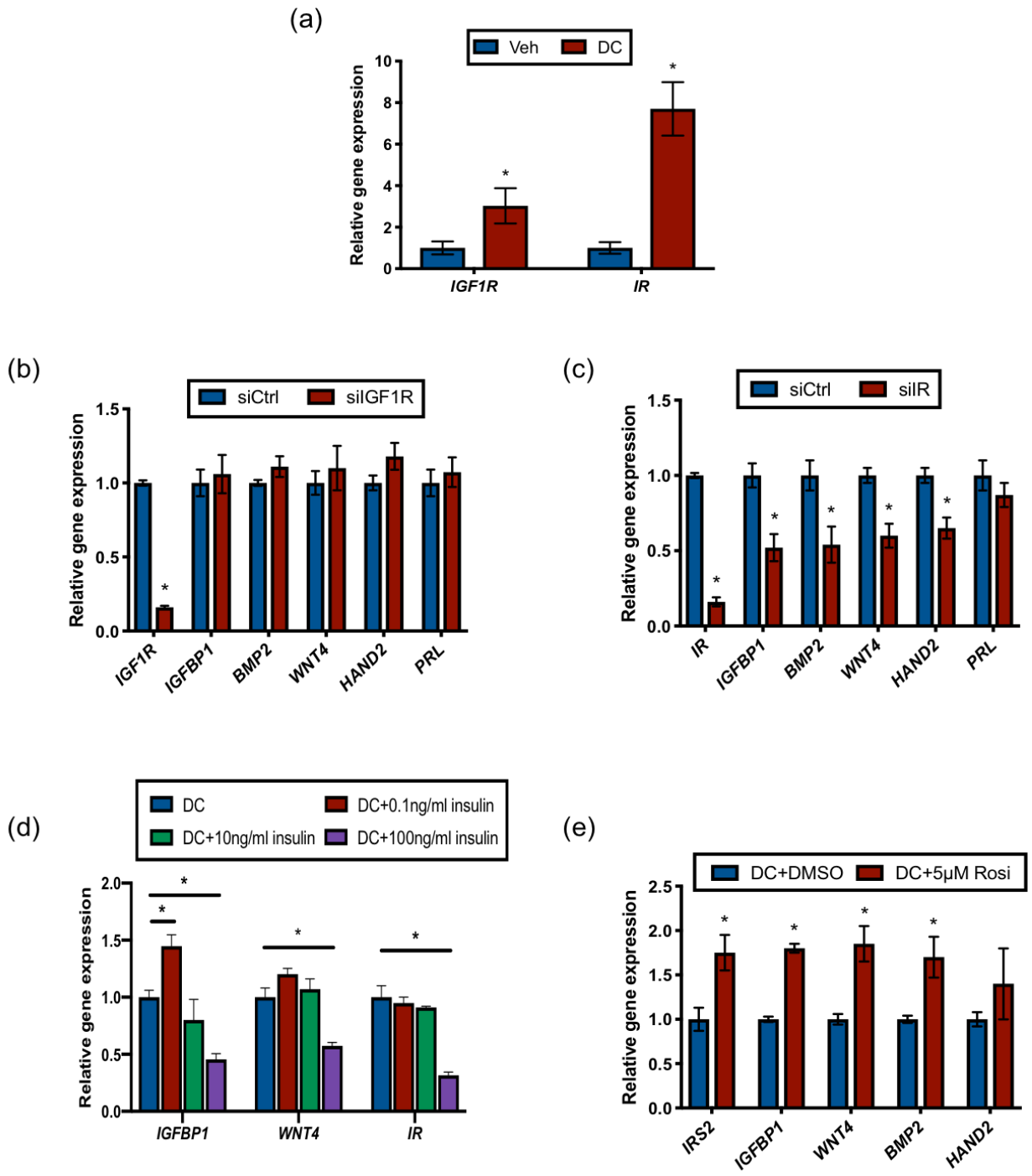

Figure 3.3 IRS2 acts downstream of the insulin receptor (IR) to regulate decidualization
(**a**) Gene expression analysis was performed with RNA isolated from HESC treated with vehicle (ethanol) or DC for 72h using primers specific to *IGF1R* and *IR*. *36B4* was used for normalization. Data are represented as the mean fold induction ± SEM. *, P<.05 relative to vehicle. Following siRNA mediated knockdown of *IGF1R* (**b**) or *IR* (**c**) and stimulation with DC for 72h, gene expression analysis was performed using primers for *IGFBP1, BMP2, WNT4, HAND2,* and *PRL*. *36B4* was used for normalization. Data are represented as the mean fold

Figure 3.3 continued: induction ± SEM. *, P<.05 relative to siCtrl. (**d**) HESC were co-stimulated with DC and the indicated concentration of insulin for 72 hours. Gene expression analysis was performed using primers for *IGFBP1, WNT4,* and *IR. 36B4* was used for normalization. Data are represented as the mean fold induction ± SEM. *, P<.05 relative to DC alone. (**e**) Gene expression analysis was performed with RNA isolated from HESC treated with DC with or without 5μM rosiglitazone (Rosi) for 72h using primers specific to *IGFBP1, BMP2, WNT4, HAND2,* and *IRS2. 36B4* was used for normalization. Data are represented as the mean fold induction ± SEM. *, P<.05 relative to DC alone.

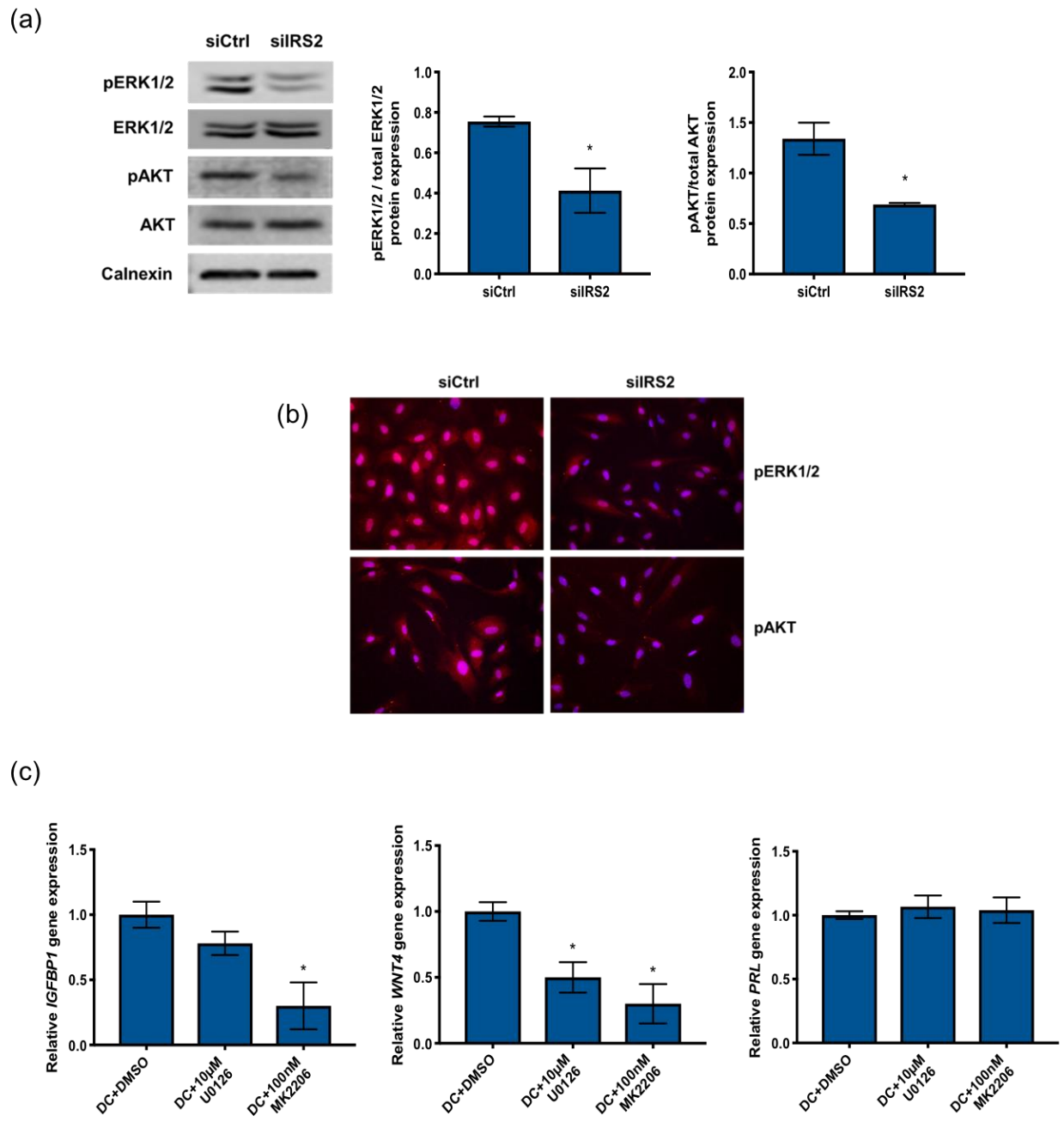

Figure 3.4 Loss of IRS2 reduces PI3K/AKT and MAPK activation in HESC during decidualization

Following siRNA mediated knockdown of *IRS2* and 24h stimulation with DC, protein expression was investigated by western blot (**a**) and immunofluorescence (**b**). (**a**) Whole cell lysates were analyzed by western blot and probed with antibodies specific for phosphorylated and total ERK1/2 and phosphorylated and total AKT. Calnexin was used as a loading control. Densitometry analysis is provided (right). (**b**) Immunofluorescent staining using antibodies specific for phosphorylated ERK1/2 and phosphorylated AKT. DAPI was used as a nuclear stain. Images provided are x40 magnification. (**c**) Gene expression analysis was performed with RNA

Figure 3.4 continued: isolated from HESC treated with DC and DMSO or either 10μM U0126 or 100nM MK2206 for 72h using primers specific for *IGFBP1, WNT4,* and *PRL*. *36B4* was used for normalization. Data are represented as the mean fold induction ± SEM. *, P<.05 relative to DC+DMSO.

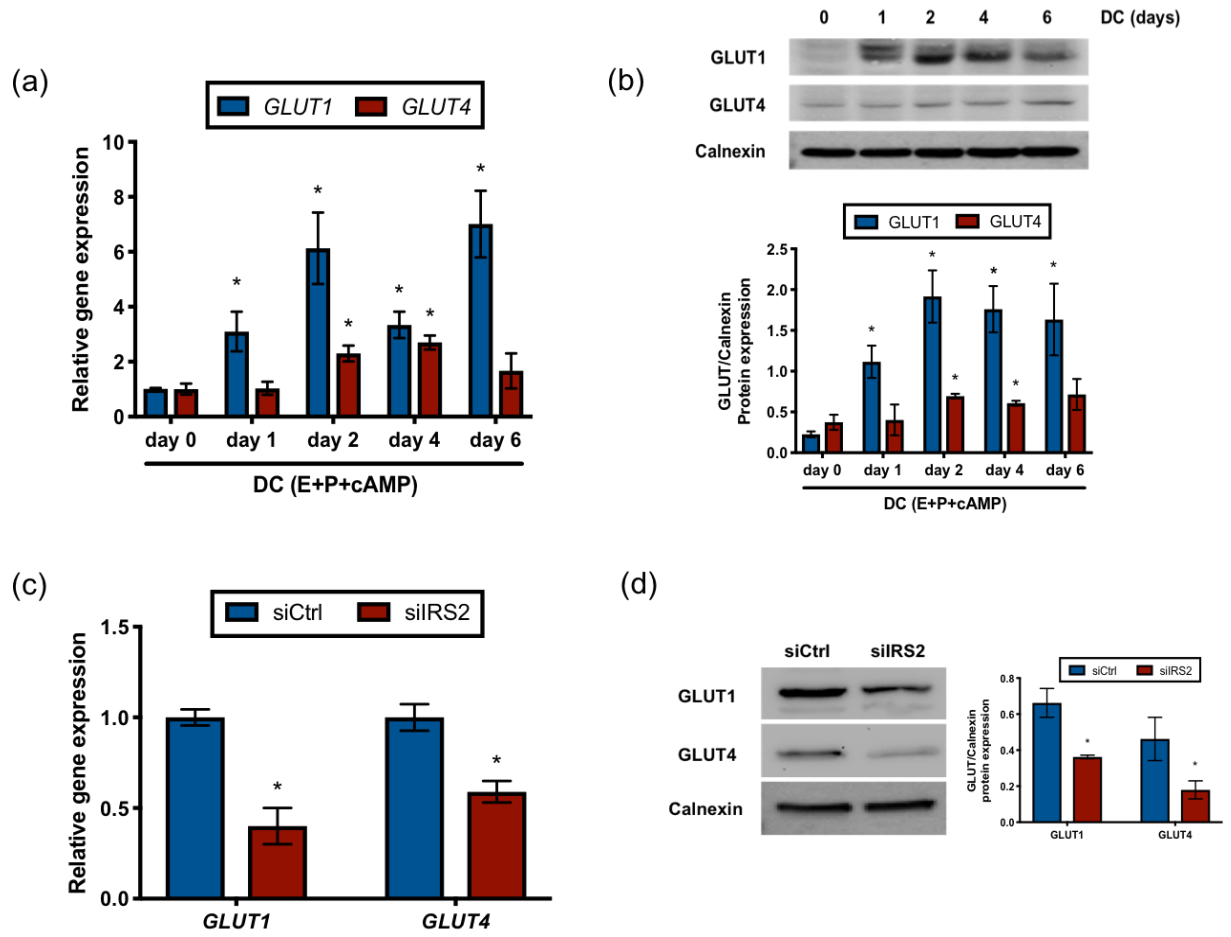

Figure 3.5 IRS2 regulates GLUT transporter expression during decidualization
GLUT mRNA (**a**) and protein (**b**) expression was observed in HESC treated with DC for 0-6 days. (**a**) Gene expression analysis was performed using primers specific for *GLUT1* and *GLUT4*. *36B4* was used for normalization. Data are represented as the mean fold induction ± SEM. *, P<.05 relative to day 0. (**b**) Whole cell lysates were analyzed by western blot and probed with antibodies specific to GLUT1 and GLUT4. Calnexin is provided as a loading control. Densitometry analysis is provided (below). GLUT mRNA (**c**) and protein (**d**) expression was observed in HESC stimulated for 72h with DC following siRNA mediated knockdown of *IRS2*. (**c**) Gene expression analysis was performed using primers specific for *GLUT1* and *GLUT4*. *36B4* was used for normalization. Data are represented as the mean fold induction ± SEM. *, P<.05 relative to siCtrl. (**d**) Whole cell lysates were analyzed by western blot and probed with antibodies specific for GLUT1 and GLUT4. Calnexin is provided as a loading control. Densitometry analysis is provided (right).

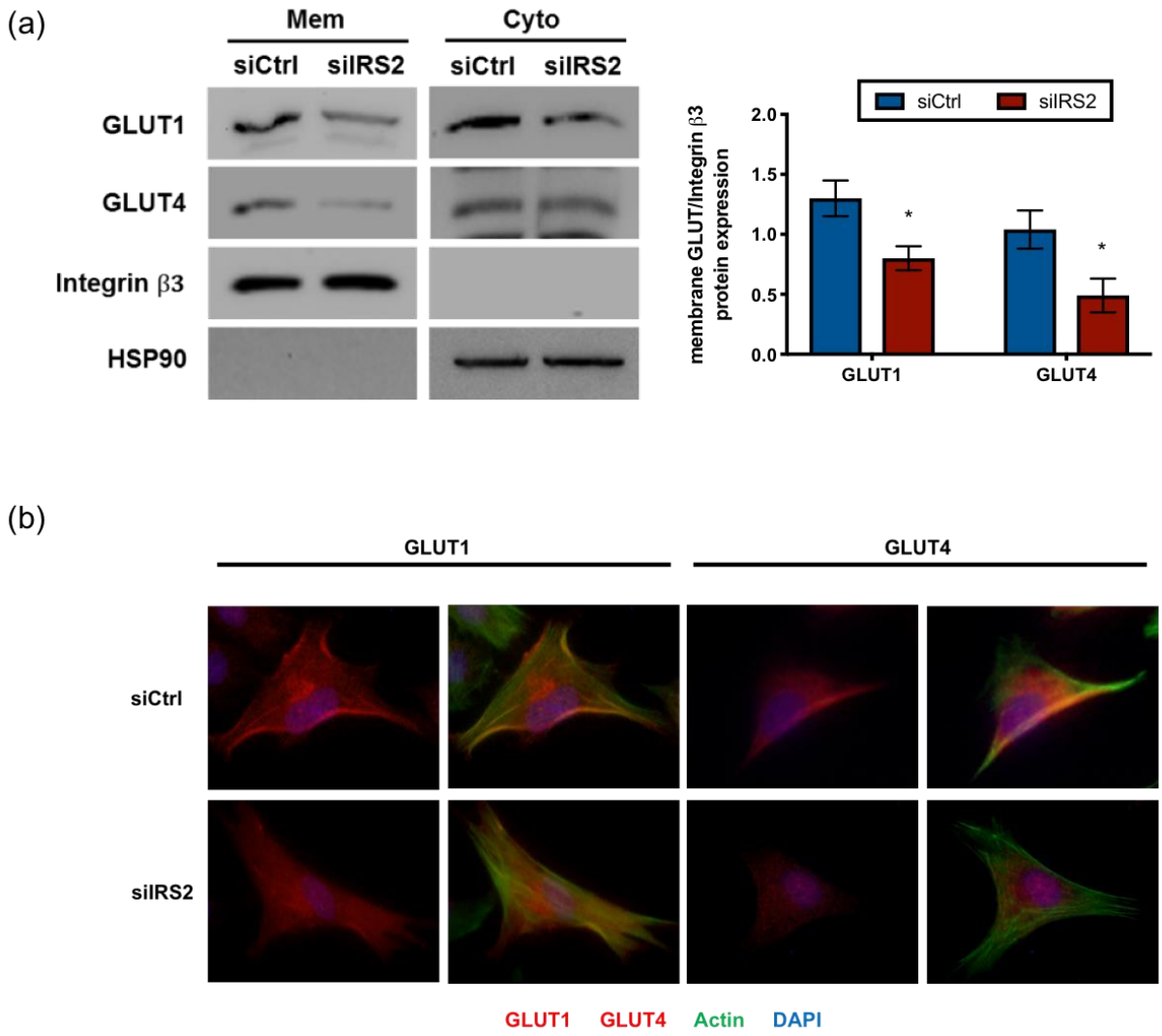

Figure 3.6 IRS2 promotes membrane localization of GLUTs during decidualization
HESC were treated for 72h with DC following siRNA mediated knockdown of *IRS2*. Membrane associated GLUT expression was observed using western blot (**a**) and immunofluorescence (**b**). (**a**) Membrane associated and cytoplasmic protein fractions were isolated as described in materials and methods. These fractions were subjected to western blot and probed with antibodies for GLUT1 and GLUT4. Integrin β3 and HSP90 were used as fraction-specific controls. Densitometry of membrane fraction is provided (right). (**b**) Immunofluorescent staining using antibodies specific for GLUT1 and GLUT4. DAPI was used as a nuclear stain and phalloidin was used to stain actin filaments.

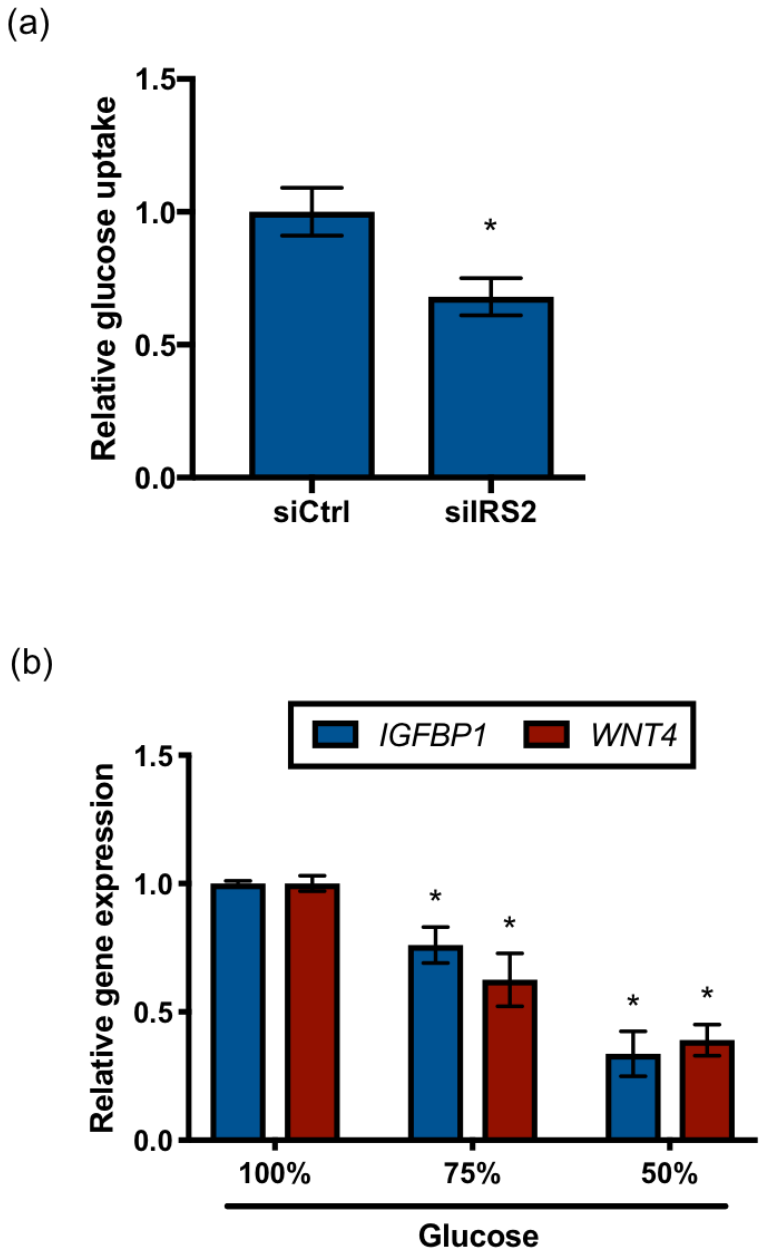

Figure 3.7 Loss of IRS2 reduces glucose uptake by HESC undergoing decidualization
(**a**) HESC were treated for 72h with DC following siRNA mediated knockdown of *IRS2*. Cells were switched to a glucose free medium for 1h prior to addition of 50μM of 2-NBDG for 1h. Cells were washed and 2-NBDG incorporation was measured and normalized to total protein. Data are represented as the mean fold glucose uptake ± SEM. *, P<.05 relative to siCtrl. **(b)** HESC were stimulated with DC in the presence of full (100%; 17.5mM) or reduced (75 and 50%; 13 and 8.75mM, respectively) glucose concentrations in the culture media for 72h. Gene expression analysis was performed using primers specific for *IGFBP1* and *WNT4*. *36B4* was used for normalization. Data are represented as the mean fold induction ± SEM. *, P<.05 relative to DC in full glucose concentration of the culture media.

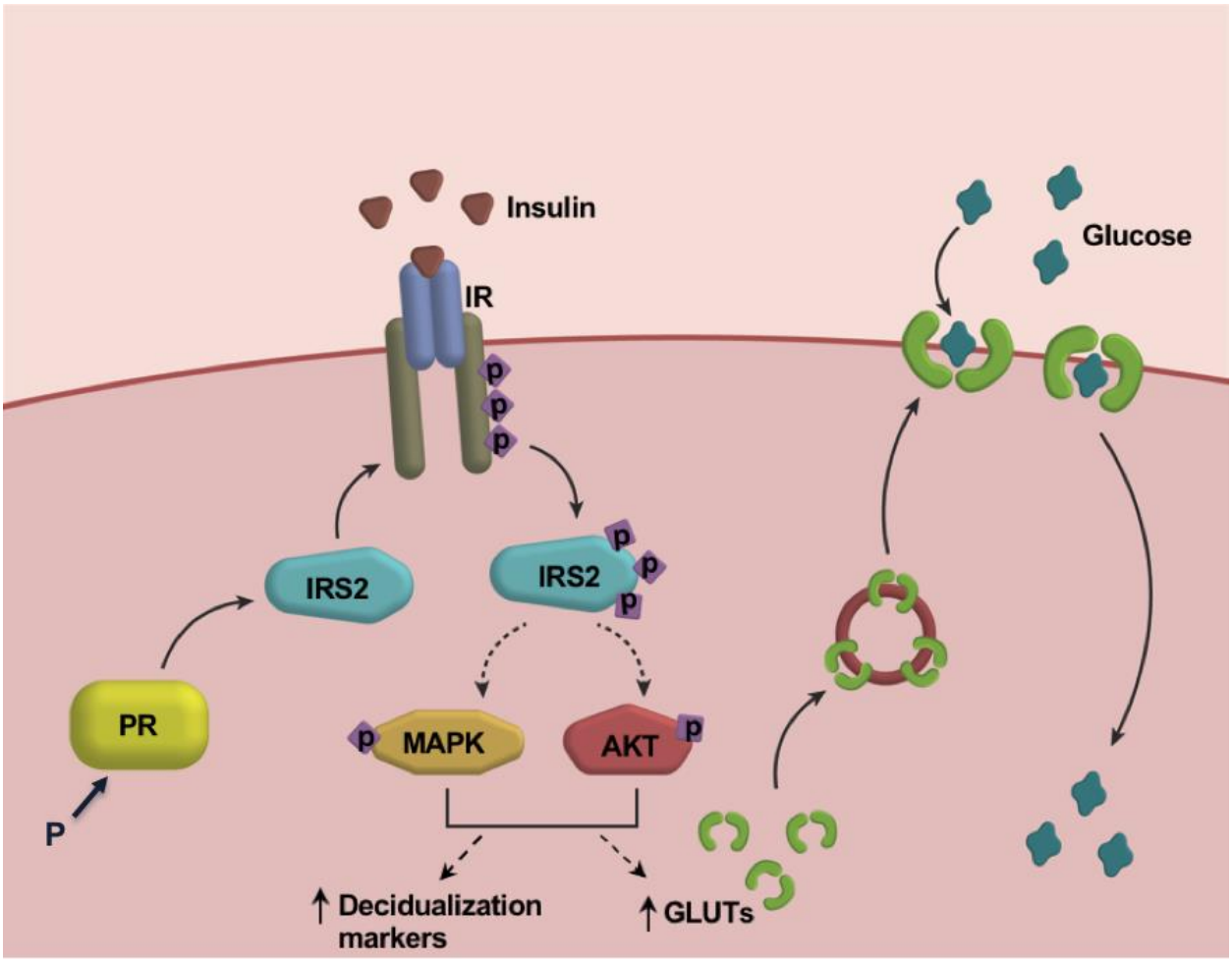

Figure 3.8 Potential mechanism by which the PR target IRS2 promotes decidualization
During decidualization, PR induces IRS2 expression. IRS2 acts as an adaptor to insulin receptor, leading to downstream activation of MAPK and PI3K/AKT pathways, and increased expression of decidualization markers and glucose transporters. These GLUTs transport glucose into the cell to meet the increased metabolic demands of HESC decidualization, a critical step during pregnancy.

ABBREVIATIONS

BMP2, bone morphogenetic protein 2; E, estrogen; ERK, extracellular-signal regulated kinase; DC, differentiation cocktail; GDM, gestational diabetes mellitus; GLUT, glucose transporter; HAND2, heart and neural crest derivatives expressed 2; HESC, human endometrial stromal cells; IGF1, insulin like growth factor 1; IGF1R, IGF1 receptor; IGFBP1, insulin like growth factor binding protein 1; IR, insulin receptor; IRS2, insulin receptor substrate 2; MAPK, mitogen activated protein kinase; PCOS, polycystic ovarian syndrome; PI3K/AKT, phosphoinositide 3-kinase/AKT; P, progesterone; PR, progesterone receptor; PRL, prolactin; RTK, receptor tyrosine kinase; WNT4, wingless-type MMTV integration site family, member 4

ACKNOWLEDGEMENTS

This work was supported by the National Institutes of Health grant R21 HD078983. Alison Neff was supported by NIH T32ES007326. We thank Shreya Singh for her assistance in data collection and Jason Neff for creating the figures.

REFERENCES

1. Ramathal CY, Bagchi IC, Taylor RN, Bagchi MK. Endometrial decidualization: of mice and men. *Semin Reprod Med*.2010;28(1):17-26.
2. Zhu H, Hou CC, Luo LF, Hu YJ, Yang WX. Endometrial stromal cells and decidualized stromal cells: origins, transformation and functions. *Gene*.2014;551(1):1-14.
3. Cha J, Sun X, Dey SK. Mechanism of implantation: strategies for successful pregnancy. *Nat Med*.2012;18(12):1754-1767.
4. Lydon JP, DeMayo FJ, Funk CR, Mani SK, Hughes AR, Montgomery CA Jr, Shyamala G, Conneely OM, O'Malley BW. Mice lacking progesterone receptor exhibit pleiotropic reproductive abnormalities. *Genes Dev*.1995;9(18):2266-2278.
5. Kaya HS, Hantak AM, Stubbs LJ, Taylor RN, Bagchi IC, Bagchi MK. Roles of progesterone receptor A and B isoforms during human endometrial decidualization. *Mol Endocrinol*.2015:29(6):882-895.
6. De Meyts P. The insulin receptor and its signal transduction network. *Endotext.2016.*
7. White MF. IRS2 integrates insulin/IGF1 signaling with metabolism, neurodegeneration and longevity. *Diabetes Obes Metab.*2014;16:4-15.
8. Withers DJ, Gutierrez JS, Towery H, Burks DJ, Ren JM, Previs S, Zhang Y, Bernal D, Pons S, Shulman GI, Bonner-Weir S, White MF. Disruption of IRS-2 causes type 2 diabetes in mice. *Nature.*1998;391(6670):900-904.

9. Burks DJ, Font de Mora J, Schubert M, Withers DJ, Myers MG, Towery HH, Altamuro SL, Flint CL, White MF. IRS-2 pathways integrate female reproduction and energy homeostasis. *Nature*.2000;407(6802):377-382.
10. Ryan IP, Schriock ED, Taylor RN. Isolation, characterization, and comparison of human endometrial and endometriosis cells in vitro. *J Clin Endocrinol Metab.*1994;78(3):642-649.
11. RRID:AB_2243890, https://scicrunch.RRID:AB_2243890.
12. RRID:AB_2123081, https://scicrunch.org/resolver/RRID:AB_2123081.
13. RRID:AB_10641999, https://scicrunch.org/resolver/RRID:AB_10641999.
14. RRID:AB_2215428, https://scicrunch.org/resolver/RRID:AB_2215428.
15. RRID:AB_671714, https://scicrunch.org/resolver/RRID:AB_671714.
16. RRID:AB_2225021, https://scicrunch.org/resolver/RRID:AB_2225021.
17. RRID:AB_2650548, https://scicrunch.org/resolver/RRID:AB_2650548.
18. RRID:AB_2141287, https://scicrunch.org/resolver/RRID:AB_2141287.
19. RRID:AB_10903230, https://scicrunch.org/resolver/RRID:AB_10903230.
20. RRID:AB_1587080, https://scicrunch.org/resolver/RRID:AB_1587080.
21. RRID:AB_647490, https://scicrunch.org/resolver/RRID:AB_647490.
22. RRID:AB_2121235, https://scicrunch.org/resolver/RRID:AB_2121235.
23. RRID:AB_330924, https://scicrunch.org/resolver/RRID:AB_330924.
24. RRID:AB_2099233, https://scicrunch.org/resolver/RRID:AB_2099233.
25. RRID:AB_393778, https://scicrunch.org/resolver/RRID:AB_393778.
26. RRID:AB_2315777, https://scicrunch.org/resolver/RRID:AB_2315777.
27. RRID:AB_2307443, https://scicrunch.org/resolver/RRID:AB_2307443.
28. RRID:AB_2315147, https://scicrunch.org/resolver/RRID:AB_2315147.
29. Ganeff C, Chatel G, Munaut C, Frankenne F, Foidart JM, Winkler R. The IGF system in in-vitro human decidualization. *Mol Hum Reprod*.2009;15(1):27-38.
30. Mioni R, Mozzanega B, Granzotto M, Pierobon A, Zuliani L, Maffei P, Blandamura S, Grassi S, Sicolo N, Vettor R. Insulin receptor and glucose transporters mRNA expression throughout the menstrual cycle in human endometrium: a physiological and cyclical condition of tissue insulin resistance. *Gynecol Endocrinol*.2012;28(12):1014-1018.
31. Flannery CA, Saleh FL, Choe GH, Selen DJ, Kodaman PH, Kliman HJ, Wood TL, Taylor HS. Differential expression of IR-A, IR-B and IGF1R in endometrial physiology and distinct signature in adenocarcinoma. *J Clin Endocrinol Metab*.2016;101(7):2883-2891.
32. Lathi RB Hess AP, Tulac S, Nayak NR, Conti M, Giudice LC. Dose-dependent insulin regulation of insulin-like growth factor binding protein-1 in human endometrial stromal cells is mediated by distinct signaling pathways. *J Clin Endocrinol Metab*.2005;90(3):1599-1606.
33. Tamura I, Ohkawa Y, Sato T, Suyama M, Jozaki K, Okada M, Lee L, Maekawa R, Asada H, Sato S, Yamagata Y, Tamura H, Sugino N. Genome-wide analysis of histone modifications in human endometrial stromal cells. *Mol Endocrinol*.2014;28(10):1656-1669.
34. Ujvari D, Jakson I, Babayeva S, Salamon D, Rethi B, Gidlöf S, Hirschberg AL. Dysregulation of In Vitro Decidualization of Human Endometrial Stromal Cells by Insulin via Transcriptional Inhibition of Forkhead Box Protein O1. *PLoS One*.2017;12(1):e0171004.

35. Craig LB, Ke RW, Kutteh WH. Increased prevalence of insulin resistance in women with a history of recurrent pregnancy loss. *Fertil Steril*.2002;78(3):487-490.
36. Tian L, Shen H, Lu Q, Norman RJ, Wang J. Insulin resistance increases the risk of spontaneous abortion after assisted reproduction technology treatment. *J Clin Endocrinol Metab*.2007;92(4):1430-1433.
37. Lee CH, Kim TH, Lee JH, Oh SJ, Yoo JY, Kwon HS, Kim YI, Ferguson SD, Ahn JY, Ku BJ, Fazleabas AT, Lim JM, Jeong JW. Extracellular signal-regulated kinase 1/2 signaling pathway is required for endometrial decidualization in mice and human. *PLoS One*.2013;8(9):e75282.
38. Toyofuku A, Hara T, Taguchi T, Katsura Y, Ohama K, Kudo Y. Cyclic and characteristic expression of phosphorylated Akt in human endometrium and decidual cells in vivo and in vitro. *Hum Reprod*.2006;25(5):1122-1128.
39. Yoshino O, Osuga Y, Hirota Y, Koga K, Yano T, Tsutsumi O, Taketani Y. Akt as a possible intracellular mediator for decidualization in human endometrial stromal cells. *Mol Hum Reprod*.2003;9(5):265-269.
40. Baek MO, Song HI, Han JS, Yoon MS. Differential regulation of mTORC1 and mTORC2 is critical for 8-Br-cAMP-induced decidualization. *Exp Mol Med*.2018;50(10):141.
41. Buzzio OL, Lu Z, Miller CD, Unterman TG, Kim JJ. FOXO1A differentially regulates genes of decidualization. *Endocrinology*.2006;147(8):3870-3876.
42. Boucher J, Kleinridders A, Kahn CR. Insulin receptor signaling in normal and insulin resistant states. *Cold Spring Harb Perspect Biol*.2014;6(1): doi: 10.1101/cshperspect.a009191.
43. Mueckler M, Thorens B. The SLC2 (GLUT) family of membrane transporters. *Mol Aspects Med*.2013;34(0):121-138.
44. Frolova AI, Moley KH. Quantitative analysis of glucose transporter mRNAs in endometrial stromal cells reveals critical role of GLUT1 in uterine receptivity. *Endocrinology*.2011;152(5):2123-2128.
45. von Wolff M, Ursel S, Hahn U, Steldinger R, Strowitzki T. Glucose transporter proteins (GLUT) in human endometrium: expression, regulation, and function throughout the menstrual cycle and in early pregnancy. *J Clin Endocrinol Metab*.2003;88(8):3885-3892.
46. Taha C, Mitsumoto Y, Liu Z, Skolnik EY, Klip A. The insulin-dependent biosynthesis of GLUT1 and GLUT3 glucose transporters in L6 muscle cells is mediated by distinct pathways. Roles of p21ras and pp70 S6 kinase. *J Biol Chem*.1995;270(42):24678-24681.
47. Taha C, Liu Z, Jin J, Al-Hasani H, Sonenberg N, Klip A. Opposite translational control of GLUT1 and GLUT4 glucose transporter mRNAs in response to insulin. Role of mammalian target of rapamycin, protein kinase b, and phosphatidylinositol 3-kinase in GLUT1 mRNA translation. *J Biol Chem.*1999;274(46):33085-33091.
48. Barthel A, Okino ST, Liao J, Nakatani K, Li J, Whitlock JP Jr, Roth RA. Regulation of GLUT1 gene transcription by the serine/threonine kinase AKT. *J Biol Chem.*1999;274(29):20281-20286.
49. Montessuit C, Thorburn A. Transcriptional activation of the glucose transporter GLUT1 in ventricular cardiac myocytes by hypertrophic agonists. *J Biol Chem*.1999;274(13):9006-9012.
50. Nose A, Mori Y, Uchiyama-Tanaka Y, Kishimoto N, Maruyama K, Matsubara H, Iwasaka T. Regulation of glucose transporter (GLUT1) gene expression by angiotensin II

in mesangial cells: involvement of HB-EGF and EGF receptor transactivation. *Hypertens Res*.2003;26(1):67-73.
51. Zhai J, Liu CX, Tian ZR, Jiang QH, Sun YP. Effects of metformin on the expression of GLUT4 in endometrium of obese women with polycystic ovary syndrome. *Biol Reprod*.2012;87(2):29.
52. Frolova AI, O'Neill K, Moley KH. Dehydroepiandrosterone Inhibits Glucose Flux Through the Pentose Phosphate Pathway in Human and Mouse Endometrial Stromal Cells, Preventing Decidualization and Implantation. *Mol Endocrinol*.2011;25(8):1444–1455.
53. Kommagani R, Szwarc MM, Kovanci E, Gibbons WE, Putluri N, Maity S, Creighton CJ, Sreekumar A, DeMayo FJ, Lydon JP, O'Malley BW. Acceleration of the Glycolytic Flux by Steroid Receptor Coactivator-2 Is Essential for Endometrial Decidualization. *PLoS Genet*.2015;11(9):e1005515.
54. Chakraborty P, Goswami SK, Rajani S, Sharma S, Kabir SN, Chakravarty B, Jana K. Recurrent pregnancy loss in polycystic ovary syndrome: role of hyperhomocysteinemia and insulin resistance. *PLoS One*.2013;8(5):e64446.
55. Jakubowicz DJ, Iuorno MJ, Jakubowicz S, Roberts KA, Nestler JE. Effects of metformin on early pregnancy loss in the polycystic ovary syndrome. *J Clin Endocrinol Metab*.2002;87(2):524-529.
56. Nawaz FH, Rizvi J. Continuation of metformin reduces early pregnancy loss in obese Pakistani women with polycystic ovarian syndrome. *Gynecol Obstet Invest*.2010;69(3):184-189.
57. Zhang B, Jin Z, Sun L, Zheng Y, Jiang J, Feng C, Wang Y. Expression and correlation of sex hormone-binding globulin and insulin signal transduction and glucose transporter proteins in gestational diabetes mellitus placental tissue. *Diabetes Res Clin Pract*.2016;119:106-117.
58. Ayaz L, Karakaş Çelik S, Cayan F. The G1057D polymorphism of insulin receptor substrate-2 associated with gestational diabetes mellitus. *Gynecol Endocrinol*.2014;30(2):165-168.
59. Bodhini D, Radha V, Deepa R, Ghosh S, Majumder PP, Rao MR, Mohan V. The G1057D polymorphism of IRS-2 gene and its relationship with obesity in conferring susceptibility to type 2 diabetes in Asian Indians. *Int J Obes*.2007;31(1):97-102.

CHAPTER 4: Future Studies

FUTURE STUDIES FOR CHAPTER 2

Analysis of differential methylation of uterine epigenome following BPA exposure of mice

The study in chapter 2 demonstrates that long term oral exposure to the environmental toxicant BPA at a concentration deemed by the EPA to be safe for human exposure is linked to physiological changes conducive to the development of endometrial hyperplasia and cancer. This included suppression of the anti-proliferative factor HAND2, leading to excessive proliferation. Our study reveals BPA induced expression of DNA methyltransferases (DNMT) and methylated DNA binding protein (MBD) and increased methylation at the *Hand2* promoter. We chose to focus on HAND2 specifically because of its anti-proliferative function; however, it is likely that multiple genes are differentially methylated following BPA exposure. Other groups have demonstrated differential methylation at other target genes, including *Esr1, Gck*, and *Pgc1α* following BPA exposure (1,2,3,4). However, these previous studies were performed in rodents exposed to BPA during critical windows of development and analysis was often restricted to male subjects. It would be interesting in a future study to take a comprehensive look at factors that are differentially methylated in the uterus following adult exposure to BPA. To do this, we would like to perform methylated DNA immunoprecipitation (MeDIP) on uterine tissue from vehicle and BPA treated mice using an antibody against 5-methylcytosine, followed by high throughput sequencing. This would provide us with an unbiased report of differentially methylated genes. We can then use RNA-seq to identify targets that are differentially expressed in response to BPA. We can also confirm transcriptional repression due to hypermethylation by observing MBD2 occupancy at hypermethylated sites. We can then use programs like DAVID to

classify these targets by biological categories to observe what cellular functions are promoted or suppressed by BPA exposure.

Effects of combined toxicant exposure on uterine health

Another aspect we would like to explore is the effect of combined toxicant exposure on the uterus. Humans are exposed to multiple endocrine disrupting chemicals throughout the day via food packaging, personal care products and occupational exposure. It is possible that simultaneous or sequential exposures to these chemicals may have a greater physiological affect than an individual chemical (5). Several chemicals have been shown to differentially affect uterine weight, including parabens, phthalates, and Bisphenol-A replacements like Bisphenol-B, -S, and –AF (6). We propose a series of dosing experiments using combinations of these chemicals to observe their net effect on uterine weight and epithelial proliferation. A dosing scheme using multiple endocrine disrupting chemicals would be more representative of daily human exposure.

FUTURE STUDIES FOR CHAPTER 3

Mechanisms of Regulation of GLUT expression by IRS2 during decidualization

Chapter 3 focuses on the role of IRS2 during stromal decidualization. We report that loss of IRS2 reduced *GLUT1* and *GLUT4* expression. However, since IRS2 is an adaptor molecule and does not have inherent transcriptional activity, we were curious how *GLUT* gene expression was regulated. Using pharmacological inhibitors to block downstream activation of MAPK or PI3K/AKT, we observed reduced *GLUT1* expression [Fig. 4.1]. The induction of *GLUT1* gene expression via MAPK and PI3K/AKT activation is well documented and could result from the activation of downstream transcription factors like CREB or NFκB (7,8,9,10,11). Further work is

needed to elucidate the exact method of *GLUT1* transcriptional regulation. Interestingly, *GLUT4* expression was maintained despite inhibitor treatment suggesting a mechanism distinct from *GLUT1*. Recently, we observed via microarray analysis of stromal cells isolated from *Hif2α* null mice that *Glut4* expression is dependent on functional HIF2α (data not shown). HIF2α is a transcription factor that is induced in uterine stromal cells undergoing decidualization under the control of estrogen (12). HIF2α functions predominantly during conditions of low oxygen, or hypoxia, where the protein is further stabilized and accumulates in the nucleus to transcriptionally regulate hypoxia inducible genes (13). In vitro, under normoxic conditions (20% O_2), we observed increased expression of *HIF2α* in HESC undergoing decidualization [Fig. 4.2(a)], while *HIF2α* expression was reduced with loss of IRS2 [Fig. 4.2(b)]. siRNA mediated knockdown of *HIF2α* reduced expression of *GLUT4*, but did not affect *IRS2* [Fig. 4.2(c)], suggesting it may act downstream of IRS2. HIF2α was detectable in the nucleus and cytoplasm of cells decidualized in normoxia, and its expression increased in hypoxia (3% O_2) [Fig. 4.3(a)]. We also observed greater induction of GLUT4 in hypoxia compared to normoxia [Fig. 4.3(b-c)]. With hypoxia, loss of IRS2 reduced both *HIF2α* and *GLUT4* expression [Fig. 4.4(a)], whereas, loss of HIF2α reduced *GLUT4* without affecting *IRS2* expression [Fig. 4.4(b)]. Together, these data suggest that in hypoxia HIF2α acts downstream of IRS2 to regulate GLUT4, similar to what we observe in normoxia. To explore this interaction further, we performed in silico analysis using the Contra V3 software and identified several putative HIF2α binding sites within the *GLUT4* proximal and distal promoter regions. We plan to perform ChIP-qPCR analysis using a HIF2α antibody to determine whether *GLUT4* is directly regulated by HIF2α. Additionally, we plan to explore the contribution of GLUT4 to decidualization by performing siRNA mediated knockdown in normoxic and hypoxic conditions to observe how expression of

decidual markers and glucose uptake is affected. Little is known about the role of GLUT4 during the secretory phase of the uterine cycle and the underlying molecular changes occurring in the uterine stromal cells. This work would help fill the gaps in our understanding of glucose utilization during early pregnancy.

FIGURES

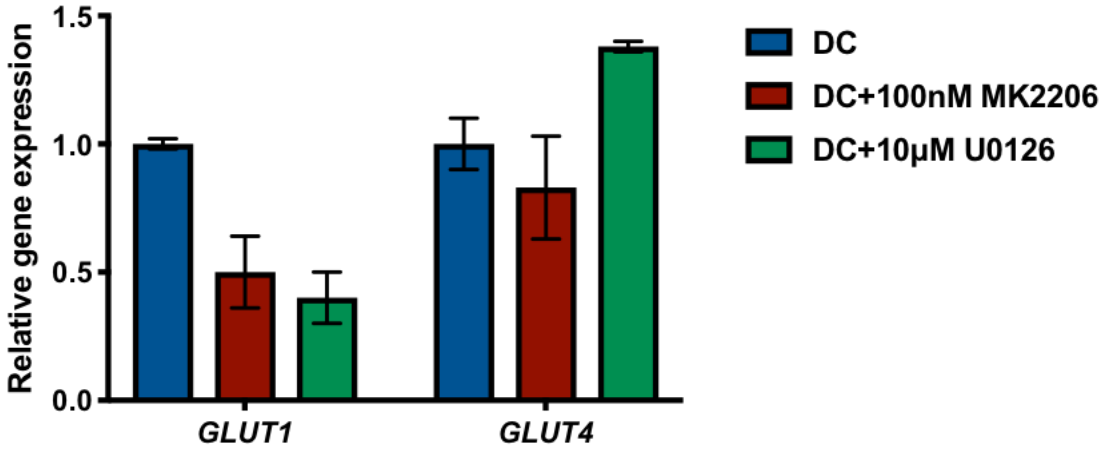

Figure 4.1 MAPK and PI3K/AKT activation are required for *GLUT1* but not *GLUT4* expression
Gene expression analysis was performed with RNA isolated from HESC treated with DC and DMSO or either 10μM U0126 or 100nM MK2206 for 72h using primers specific for *GLUT1* and *GLUT4*. *36B4* was used for normalization. Data are represented as the mean fold induction relative to DC+DMSO.

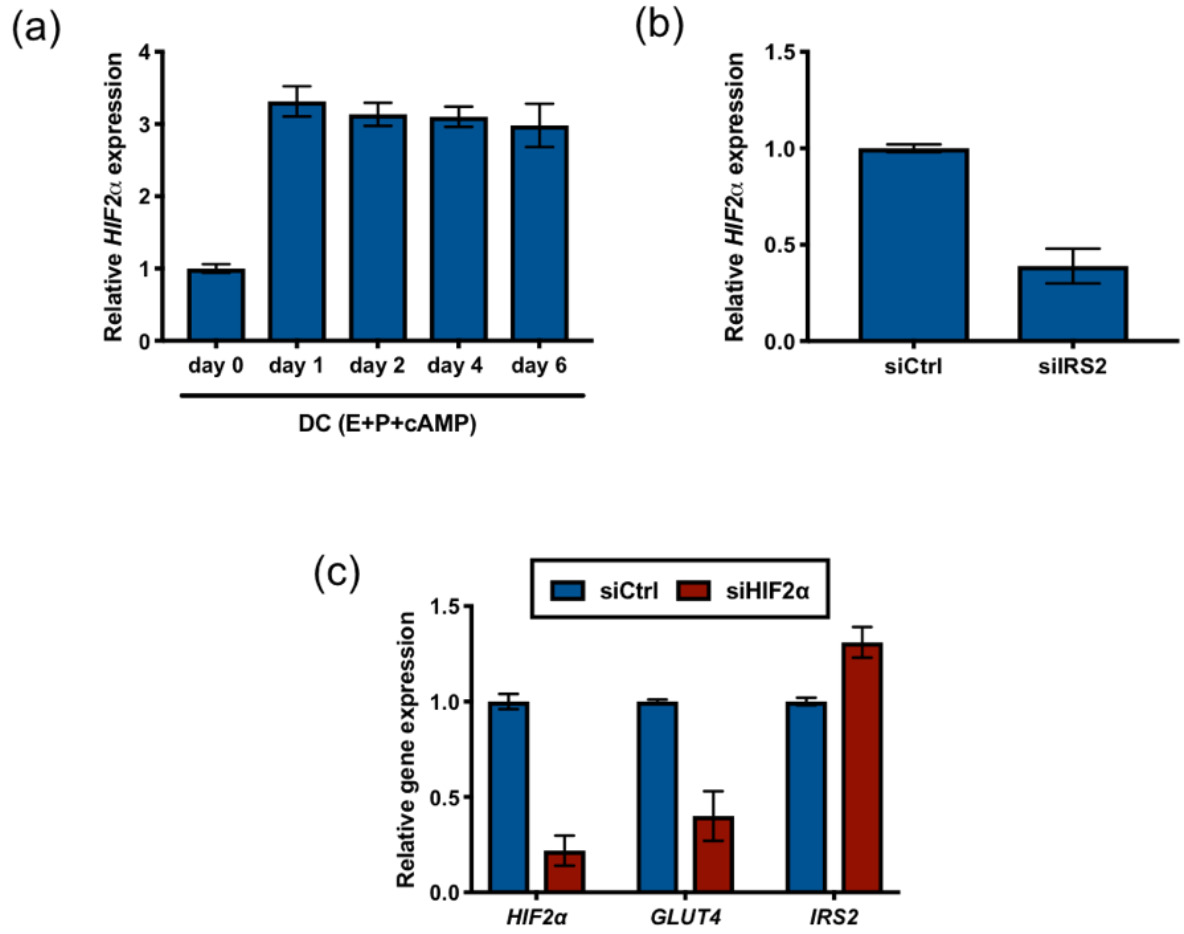

Figure 4.2 *HIF2α* is induced during decidualization and regulates *GLUT4* under normoxia
HESC were treated with DC (E+P+cAMP) for 0-6 days and gene expression analysis was performed using primers specific for *HIF2α. 36B4* was used for normalization. Data are represented as the mean fold induction relative to d0. Following siRNA mediated knockdown of *IRS2* (**b**) or *HIF2α* (**c**)and stimulation with DC for 72h, gene expression analysis was performed using primers specific to *IRS2*, *HIF2α*, and *GLUT4. 36B4* was used for normalization. Data are represented as the mean fold induction relative to siCtrl.

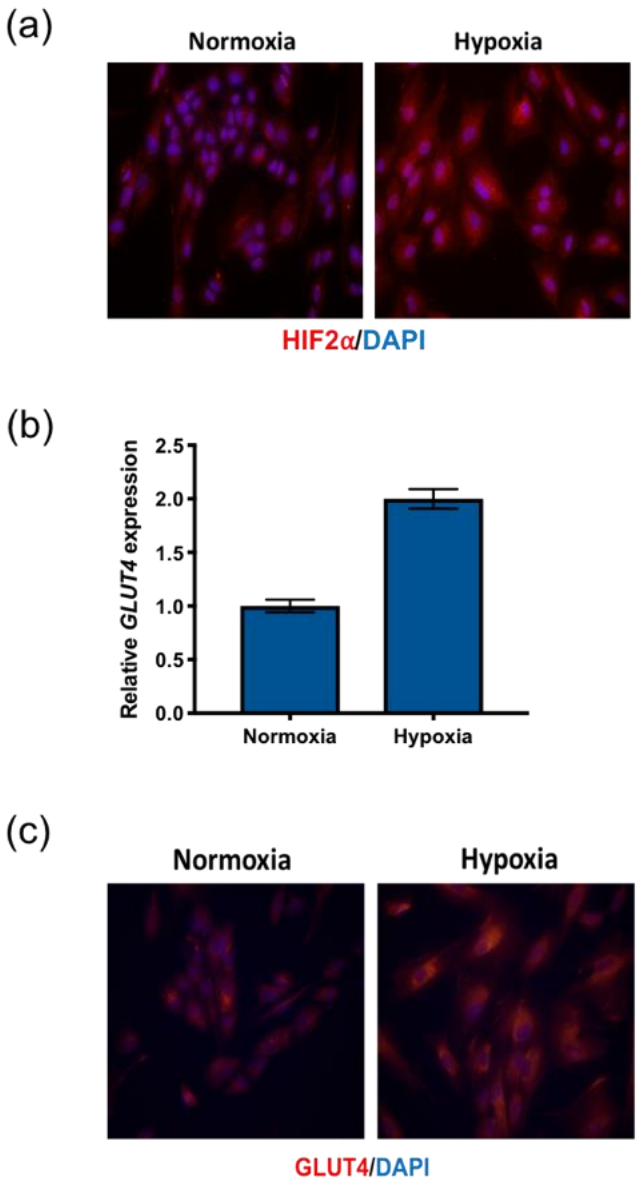

Figure 4.3 Hypoxia causes HIF2α accumulation and increased expression of GLUT4
HESCS were stimulated with DC under normoxia (20% O_2) or hypoxia (3% O_2) for 72h. (**a**) Immunofluorescent staining was performed using antibody specific for HIF2α. DAPI was used as a nuclear stain. Images provided are x40 magnification. (**b**) Gene expression analysis was performed using primers specific for *GLUT4*. *36B4* was used for normalization. (**c**) Immunofluorescent staining was performed using antibody specific for GLUT4. DAPI was used as a nuclear stain. Images provided are x40 magnification.

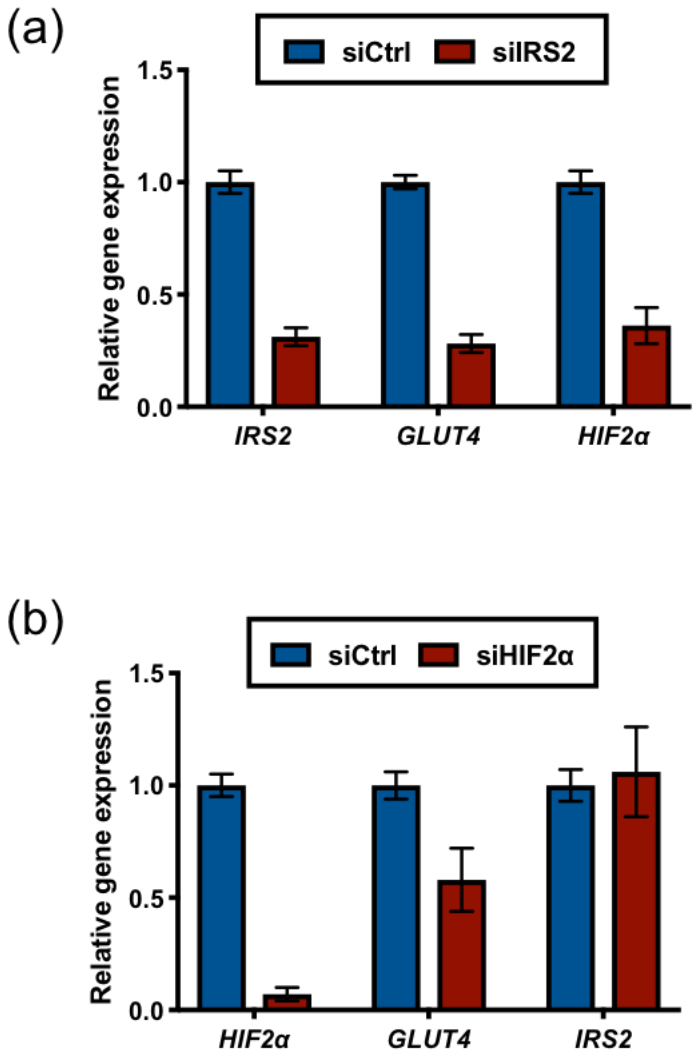

Figure 4.4 *HIF2α* regulates *GLUT4* under hypoxia
Following knockdown of either *IRS2* (**a**) or *HIF2α* (**b**), HESCS were stimulated with DC under hypoxia (3% O_2) for 72h. Gene expression analysis was performed using primers specific to *IRS2*, *HIF2α*, and *GLUT4*. *36B4* was used for normalization. Data are represented as the mean fold induction relative to siCtrl.

REFERENCES

1. Doshi T, Mehta SS, Dighe V, Balasinor N, Vanage G. Hypermethylation of estrogen receptor promoter region in adult testis of rats exposed neonatally to bisphenol A. *Toxicology*. 2011; 289(3):74-82.
2. Patel BB, Raad M, Sebag IA, Chalifour LE. Lifelong Exposure to Bisphenol A Alters Cardiac Structure/Function, Protein Expression, and DNA Methylation in Adult Mice. *Toxicol Sci*. 2013;133(1):174–185.
3. Ma Y, Xia W, Wang DQ, Wan YJ, Xu B, Chen X, Li YY, Xu SQ. Hepatic DNA methylation modifications in early development of rats resulting from perinatal BPA exposure contribute to insulin resistance in adulthood. *Diabetologia.* 2013;56(9):2059-2067.
4. Jiang Y, Xia W, Yang J, Zhu Y, Chang H, Liu J, Huo W, Xu B, Chen X, Li Y, Xu S. BPA-induced DNA hypermethylation of the master mitochondrial gene PGC-1α contributes to cardiomyopathy in male rats. *Toxicology*. 2015;329:21-31.
5. Silins I, Hogberg J. Combined toxic exposures and human health: biomarkers of exposure and effect. *Int J Environ Res Public Health*.2011;8(3):629-647.
6. Kleinstreuer NC, Ceger PC, Allen DG, Strickland J, Chang X, Hamm JT, Casey WM. A curated database of rodent uterotrophic bioactivity. *Environ Health Perspect*.2015;124(5):556-562.
7. Taha C, Mitsumoto Y, Liu Z, Skolnik EY, Klip A. The insulin-dependent biosynthesis of GLUT1 and GLUT3 glucose transporters in L6 muscle cells is mediated by distinct pathways. Roles of p21ras and pp70 S6 kinase. *J Biol Chem*.1995;270(42):24678-24681.
8. Taha C, Liu Z, Jin J, Al-Hasani H, Sonenberg N, Klip A. Opposite translational control of GLUT1 and GLUT4 glucose transporter mRNAs in response to insulin. Role of mammalian target of rapamycin, protein kinase b, and phosphatidylinositol 3-kinase in GLUT1 mRNA translation. *J Biol Chem.*1999;274(46):33085-33091.
9. Barthel A, Okino ST, Liao J, Nakatani K, Li J, Whitlock JP Jr, Roth RA. Regulation of GLUT1 gene transcription by the serine/threonine kinase AKT. *J Biol Chem.*1999;274(29):20281-20286.
10. Montessuit C, Thorburn A. Transcriptional activation of the glucose transporter GLUT1 in ventricular cardiac myocytes by hypertrophic agonists. *J Biol Chem*.1999;274(13):9006-9012.
11. Nose A, Mori Y, Uchiyama-Tanaka Y, Kishimoto N, Maruyama K, Matsubara H, Iwasaka T. Regulation of glucose transporter (GLUT1) gene expression by angiotensin II in mesangial cells: involvement of HB-EGF and EGF receptor transactivation. *Hypertens Res*.2003;26(1):67-73.
12. Das A, Mantena SR, Kannan A, Evans DB, Bagchi MK, Bagchi IC. De novo synthesis of estrogen in pregnant uterus is critical for stromal decidualization and angiogenesis. *PNAS*.2009;106(30):12542-12547.
13. Majmundar AJ, Wong WJ, Simon MC. Hypoxia-inducible factors and the response to hypoxic stress. *Mol Cell*.2010;40(2):294-309.